الجمهورية الجزائرية الديمقراطية الشعبية
République Algérienne Démocratique et Populaire
وزارة التعليم العالي و البحث العلمي
Ministère de l'Enseignement Supérieur et de la Recherche Scientifique

المدرسة الوطنية المتعددة التقنيات
Ecole Nationale Polytechnique

المدرسة الوطنية المتعددة التقنيات
قسم الآلية
École Nationale Polytechnique
Département d'Automatique

Laboratoire de Commande des Processus

End of Studies Project Dissertation

For obtaining the state engineer's degree in Automation and Control

Study of Standalone Photovoltaic System

Realized by :

RACHED Isra and **AMMAR Afaf**

Under the supervision of **Pr. BERKOUK El-Madjid**
and **Pr. SMAILI Arezki**

Publicly presented and defended on the 4th of July, 2024, in front of the jury composed of :

President	Pr. NEZLI Lazhari	ENP
Examiner	Dr. BELKACEMI Rabie	ENP
Promoter	Pr. BERKOUK El-Madjid	ENP

ENP 2024

الجمهورية الجزائرية الديمقراطية الشعبية
République Algérienne Démocratique et Populaire
وزارة التعليم العالي و البحث العلمي
Ministère de l'Enseignement Supérieur et de la Recherche Scientifique

المدرسة الوطنية المتعددة التقنيات
Ecole Nationale Polytechnique

المدرسة الوطنية المتعددة التقنيات
قسم الآلية
École Nationale Polytechnique
Département d'Automatique

Laboratoire de Commande des Processus

End of Studies Project Dissertation

For obtaining the state engineer's degree in Automation and Control

Study of Standalone Photovoltaic System

Realized by :

RACHED Isra and **AMMAR Afaf**

Under the supervision of **Pr. BERKOUK El-Madjid**
and **Pr. SMAILI Arezki**

Publicly presented and defended on the 4th of July, 2024, in front of the jury composed of :

President	Pr. NEZLI Lazhari	ENP
Examiner	Dr. BELKACEMI Rabie	ENP
Promoter	Pr. BERKOUK El-Madjid	ENP

ENP 2024

الجمهورية الجزائرية الديمقراطية الشعبية
République Algérienne Démocratique et Populaire
وزارة التعليم العالي و البحث العلمي
Ministère de l'Enseignement Supérieur et de la Recherche Scientifique

المدرسة الوطنية المتعددة التقنيات
Ecole Nationale Polytechnique

المدرسة الوطنية المتعددة التقنيات

قسم الآلية

École Nationale Polytechnique

Département d'Automatique

Laboratoire de Commande des Processus

Mémoire de Projet de Fin d'Études

Pour l'obtention du diplôme d'Ingénieur d'État en Automatique

Étude d'un Système Photovoltaïque Autonome

Réalisé par :

RACHED Isra et **AMMAR Afaf**

Sous la supervision de **Pr. BERKOUK El-Madjid**
et **Pr. SMAILI Arezki**

Présenté et soutenu publiquement le 4 Juillet 2024, devant le jury composé de :

Président	Pr. NEZLI Lazhari	ENP
Examinateur	Dr. BELKACEMI Rabie	ENP
Promoteur	Pr. BERKOUK El-Madjid	ENP

ENP 2024

Dedication

“

To my dear mother,
To my dear father,
To my grandmother,
To my sisters Hana and Manel,
To all my family and friends,
To my partner in this work Isra

”

- Afaf

“

To my dear mother,
To my dear father,
To my dear grandmother,
To my dear brother Raid,
To my dear sisters Amira and Anfel,
To my dear sister in law Fazia,
To all my family and friends,
To my partner in this work Afaf

”

- Isra

Acknowledgement

We would like to express our deepest appreciation to all those who helped us, in one way or another, to complete this thesis. First and foremost, we thank ALLAH Almighty who provided us with strength and direction and showered us with blessings throughout.

Our sincerest gratitude to our supervisors **Pr. El Madjid BERKOUK** and **Pr. Arezki SMAILI** for their continuous guidance and support. With their expert guidance and immense knowledge, we were able to overcome all the obstacles that we encountered during our final project journey. We could not have imagined having better advisors and mentors, who have been more like fatherly figures to us.
We would also like to express our sincere gratitude to the PhD student **Rania OMAR AMRANI** for her invaluable assistance and support throughout this project.

We also would like to sincerely thank the members of our thesis committee, **Pr. Lazhari NEZLI** and **Dr. Rabie BELKACEMI** for accepting to be members of the committee and for their constructive analysis of the present work.

Our deepest appreciation goes to our families and friends for their unconditional love and support, and to all the people who have been by our side throughout this thesis journey.

ملخص

تقدم هذه المذكرة دراسة شاملة حول تصميم وتحجيم و التحكم في أنظمة الطاقة الشمسية الذاتية. تبدأ الدراسة بنمذجة مولد شمسي يتم إدارته بواسطة محول تصعيد لتتبع نقطة الطاقة القصوى (MPP) باستخدام تقنيات مختلفة مثل خوارزميات الاضطراب والمراقبة (PO)، المنطق الضبابي، و تقنية تحسين سرب الجسيمات (PSO). يتم إدخال نظام تخزين يعتمد على البطاريات، يتم التحكم فيه عبر محول DC/DC ذو اتجاهين بواسطة منظم PI، مع نظام إدارة الطاقة (EMS) المتكامل. كما تبرز المذكرة أهمية التحجيم الدقيق لأنظمة الطاقة الشمسية من خلال تحجيم نظام شمسي ذاتي حقيقي، وتقدم التصميم والمحاكاة لنظام كامل يغذي حمولة AC.

كلمات مفتاحية : الأنظمة الكهروضوئية المستقلة، المولدات الكهروضوئية، محول التصعيد، نقطة الطاقة القصوى (MPP)، خوارزمية الاضطراب والمراقبة (PO)، المنطق الضبابي، خوارومية تحسين سرب الجسيمات (PSO)، محول ثنائي الاتجاه، نظام إدارة الطاقة (EMS)، حمولة AC

Résumé

Cette thèse présente une étude approfondie sur la conception, le dimensionnement et le contrôle des systèmes photovoltaïques autonomes. Elle inclut la modélisation d'un générateur photovoltaïque (GPV) géré par un convertisseur élévateur pour suivre le point de puissance maximale (MPP) utilisant des techniques comme les algorithmes de perturbation et d'observation (P&O), la logique floue et l'optimisation par essaim de particules (PSO). Un système de stockage par batteries est intégré, contrôlé par un convertisseur DC/DC bidirectionnel avec régulation PI, accompagné d'un système de gestion de l'énergie (EMS). La thèse souligne également l'importance du dimensionnement précis des systèmes photovoltaïques à travers l'étude d'un système réel, et propose la conception et la simulation d'un système complet alimentant une charge AC.

Mots clés : Systèmes photovoltaïques autonomes, GPV, convertisseur élévateur, MPP, P&O, logique floue, PSO, convertisseur DC/DC bidirectionnel, système de gestion de l'énergie (EMS), charge AC

Abstract

This thesis presents a comprehensive study on the design, sizing, and control of standalone systems. It begins with the modeling of a photovoltaic generator (PVG) managed by a boost converter to track the Maximum Power Point (MPP) using various techniques such as perturb and observe (P&O) algorithms, fuzzy logic (FL), and Particle Swarm Optimization (PSO). A battery-based storage system is introduced, controlled by a bidirectional DC/DC converter with a PI regulator, along with an integrated Energy Management System (EMS). The thesis also underscores the importance of precise system sizing through the study of a real autonomous solar system, and provides the design and simulation of a complete system powering an AC load.

Keywords : Standalone systems, PVG, boost converter, MPP, P&O, fuzzy logic, PSO, bidirectional DC/DC converter, EMS, AC load

Contents

List of Figures

List of Tables

List of Abbreviations

PV	*Photovoltaic*
MPPT	*Maximum Power Point Tracking*
FL	*Fuzzy Logic*
PSO	*Particle Swarm Optimization*
GA	*Genetic Algorithm*
ACO	*Ant Colony Optimization*
FOCV	*Fractional Open Circuit Voltage*
CV	*Constant Voltage*
ANN	*Artificial Neural Networks*
ANFIS	*Adaptive Neuro Fuzzy Inference System*
DC	*Direct Current*
AC	*Alternating Current*
BMS	*Battery Management System*
EMS	*Energy Management System*
PI	*Proportinal Intergral*
SOC	*State of Charge*

General Introduction

There is a significant perception of future high global energy consumption. In recent years, declining fossil-fuel reserves and climate change have encouraged the development of renewable energy sources in order to reduce global warming. One of the candidates to replace pollutant fossil-fuel energy sources is Photovoltaic (PV) energy [1]. Its advantages include cheap repair costs, the absence of moving or rotating elements, and little worldwide impact. The entire amount of incident solar energy on Earth exceeds the world's current and expected energy needs. Solar energy has the ability to provide all of the world's energy needs if properly harnessed. During operating, it emits no greenhouse gases or hazardous substances. Its use serves to minimize reliance on fossil fuels, which contributes to a reduction in environmental impact. Due to all its advantages, it is expected that in the 21st century solar energy will become the most important renewable source during the energy transition towards a sustainable development. These reasons justify why solar energy is a focus of such research interest [2].

The control of solar photovoltaic (PV) systems has recently gained a lot of interest. In recent years, there have been numerous reports on control objectives and controllers. Two main aims can be identified. The primary goal is to obtain the maximum available PV power with maximum power point tracking (MPPT) management, while the second goal is to maximize PV power utilization. PV panels provide power that can be used to meet load demands or injected into the electrical grid. PV systems fall into two types based on their application: Standalone systems and grid-connected systems [2].

Many photovoltaic systems function independently. Such systems include a photovoltaic generator, energy storage (such as a battery), AC and DC consumers, and power conditioning components. A stand-alone system, by definition, does not interface with the electric grid. A PV generator can comprise many arrays. Each array is made up of multiple modules, each of which contains multiple sun cells. When the PV modules' power exceeds the load demand, the battery bank stores it and releases it when the PV supply is insufficient. A stand-alone PV system can have a variety of loads, including both DC (television, lighting) and AC (electric motors, heaters, and so on). The power conditioning system connects all of the PV system's components, providing protection and control. The most common components of a power conditioning system are blocking diodes, charge regulators, and DC-AC converters [3].

Problem Statement

The rise in global energy demand along with the lowering reserves of fossil fuel and immediate requirement to solve the problems of climate change, new sustainable and renewable energy sources are needed. Solar energy, particularly photovoltaic (PV) technology, stands out as a great option due to its potential to meet the world's energy needs without emitting greenhouse gases.

However, there are still some challenges we need to overcome to exploit the most of solar energy in stand-alone PV systems. These challenges include variation of meteorological conditions, effective energy storage, and optimizing the control and conversion of the energy. Addressing these issues is important for making solar energy a dependable and mainstay power source for the future.

Objectives and Challenges

In this work, our objective is to design the various components of a standalone photovoltaic power system to supply an AC load. We will consider the energy requirements for laboratory equipment at the national polytechnic school as a practical case study, providing a detailed step-by-step design procedure. The design of a stand-alone PV system will be developed using the MATLAB/Simulink software including the components : a photovoltaic generator, DC-DC converters, battery-based storage, a DC-AC inverter, and a single-phase transformer.

The main challenges in designing a photovoltaic system center around modeling the PV array, extracting maximum power from the PV panels, managing energy storage, and converting energy efficiently. Through this work, we focus on modeling a photovoltaic array using the single-diode model. We aim to develop and implement efficient control techniques to track the maximum power point, including Perturb & Observe (P&O), fuzzy logic (FL), and Particle Swarm Optimization (PSO) methods. Additionally, the implementation of PI controllers to manage energy flow within the PV system components via a bidirectional DC-DC converter. Finally, we will design a DC-AC inverter with a single-phase transformer to meet the load requirements.

Organization of the thesis

This work is organized into several chapters to provide a systematic and comprehensive exploration of standalone photovoltaic systems. This is how the thesis is organized :

This chapter serves as an introduction to the topic, offering an overview of the objectives and challenges of this work. It also defines the scope of the study and gives the structure of the following chapters.

The first chapter presents an overview of photovoltaic systems with a focus on their general structure and main elements, as well as their importance. It includes a state-

of-the-art review, highlighting the motivations behind using photovoltaic system for a sustainable renewable energy.

The second chapter will focus on modeling photovoltaic systems managed by boost converters and provide a comprehensive understanding of their mathematical and electrical representations. It also provides details about the dynamics and characteristics of PV modules and boost converters.

The third chapter will present various control techniques to optimize the extraction of maximum power from PV panels using a boost converter. It compares classical and advanced methods such as Perturb and Observe (P&O), Fuzzy Logic (FL), and Particle Swarm Optimization (PSO), discussing their design, implementation and performance evaluation.

The fourth chapter will address the integration of battery-based storage into PV systems, which is an essential component, particularly in standalone systems. An energy management system will be designed and implemented to enhance the system performance.

The fifth chapter will cover a real-world case study, demonstrating the practical application of the concepts discussed in previous chapters. It includes the sizing of the system to determine the energy requirements, followed by the design of an overall standalone PV system. This chapter provides a step-by-step approach to design a PV system to meet specific energy requirements.

The thesis concludes with a summary of our research findings and explores potential future investigations and advancements in the field of photovoltaic systems.

Chapter 1

Background and State-of-the-art of Photovoltaic Systems

1.1 Introduction

Renewable energy sources are considered alternative energy sources because of rising environmental concerns and depleting conventional energy resources. Solar energy has a significant role in meeting the increased requirement for electricity with a reduced environmental impact.

In the first chapter of our study, we provide a simple overview of photovoltaic systems, focusing on how they connect to loads, the use of static converters to improve efficiency, the importance of energy storage for reliable power supply, and the latest advancements in MPPT control techniques. This chapter aims to lay a solid foundation for understanding photovoltaic systems in today's energy context.

1.2 Renewable Energies

As the world population grows and places more demand on limited fossil fuels, renewable energy becomes more relevant as part of the solution to the impending energy dilemma. Renewable energy is now included in national policies, with goals for it to be a significant percentage of generated energy within the coming decades [4].

At the end of 2022, global renewable generation capacity amounted to 3372 GW. Renewable hydropower accounted for the largest share of the global total, with a capacity of 1256 GW. Solar and wind energy accounted for most of the remainder, with total capacities of 1 053 GW and 899 GW respectively. Other renewable capacities included 149 GW of bioenergy and 15 GW of geothermal, plus 524 MW of marine energy [5].

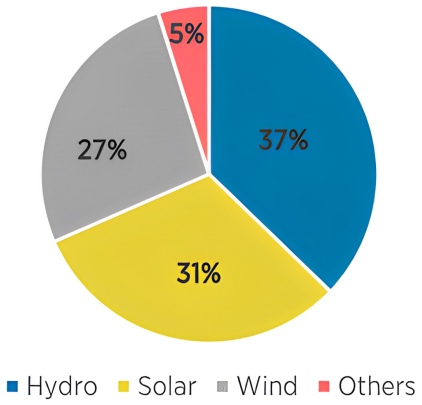

Figure 1.1 : Renewable Generation Capacity by Energy Source .

Renewable generation capacity increased by 295 GW (+9.6%) in 2022. Solar energy continued to lead capacity expansion, with a massive increase of 192 GW (+22%), followed by wind energy with 75 GW (+9%). Renewable hydropower capacity increased by 21 GW (+2%) and bioenergy by 8 GW (+5%). Geothermal energy increased by a very modest 181 MW. Solar and wind energy continued to dominate renewable capacity expansion,

jointly accounting for 90% of all net renewable additions in 2022. This growth in wind and solar led to the highest annual increase in renewable generating capacity and the second highest growth on record in percentage terms [5].

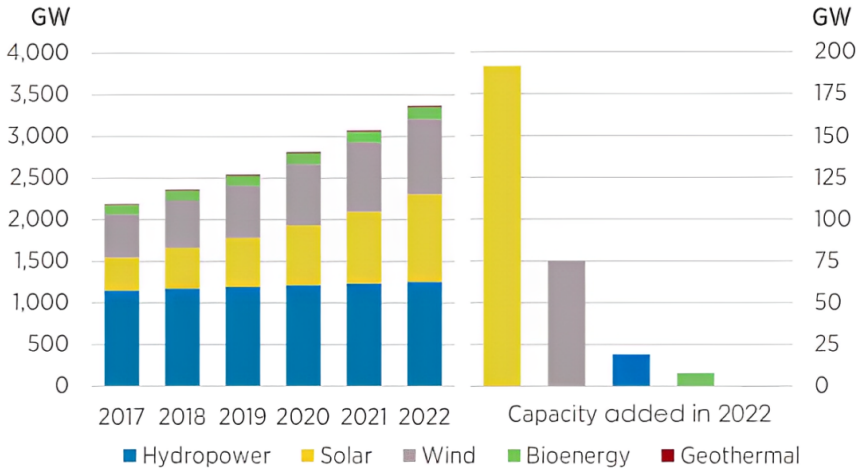

Figure 1.2 : Renewable Power Capacity Growth.

1.2.1 What is Renewable Energy ?

Renewable energies are energy sources that naturally regenerate over time and do not run out. They are the most important part of the transition to an energy system that moves away from fossil fuels, thus countering global warming. And they are clean energies that safeguard human health and the environment [6].

All countries in the world share the same need to produce increasingly more renewable energy and to abandon conventional sources. According to data from the latest International Renewable Energy Agency (IRENA)[1] report, in 2022 as much as 83 percent of all electricity capacity added lo was from renewable sources. While in 2021, according to a report published by the independent climate think tank Ember, renewables generated 38 percent of the world's electricity [6].

1.2.2 Types of Renewable Energy Sources

There area range of renewable sources that have been developed, with each offering their own advantages and challenges depending on factors such as geographical location, requirements for use and even the time of year [7]. The mostly used renewable energy sources are :

[1]**IRENA :** The International Renewable Energy Agency (IRENA) is an intergovernmental organisation that supports countries in their transition to a sustainable energy future, and serves as the principal platform for international co-operation, a centre of excellence, and a repository of policy, technology, resource and financial knowledge on renewable energy.

1.2.2.1 Solar Energy

Solar energy is the most abundant of all energy resources and can even be harnessed in cloudy weather. The rate at which solar energy is intercepted by the Earth is about 10,000 times greater than the rate at which humankind consumes energy.

Solar technologies convert sunlight into electrical energy either through photovoltaic panels or through mirrors that concentrate solar radiation. The cost of manufacturing solar panels has plummeted dramatically in the last decade, making them not only affordable but often the cheapest form of electricity. Solar panels have a lifespan of roughly 30 years, and come in variety of shades depending on the type of material used in manufacturing [7].

1.2.2.2 Wind Energy

Wind energy harnesses the kinetic energy of moving air by using large wind turbines located on land (onshore) or in sea- or freshwater (offshore). Wind energy has been used for millennia, but onshore and offshore wind energy technologies have evolved over the last few years to maximize the electricity produced - with taller turbines and larger rotor diameters.

Though average wind speeds vary considerably by location, the world's technical potential for wind energy exceeds global electricity production, and ample potential exists in most regions of the world to enable significant wind energy deployment.

Many parts of the world have strong wind speeds, but the best locations for generating wind power are sometimes remote ones. Offshore wind power offers tremendous potential [7].

1.2.3 Renewable Energy in Algeria

Within the framework of the dynamics of energy transition, Algeria, like many other countries in the world, seeks to use renewable energy sources to enhance its energy security by diversifying its energy mix and reducing its dependence on fossil fuels. The country enjoys great potential for renewable energy, especially solar and wind energy, due to abundant sunlight and strong winds in certain areas [8].

- **Solar Energy :** On account of its geographical location, Algeria holds one of the highest solar potentials in the world which is estimated at 13.9 TWh per year. The country receives annual sunshine exposure equivalent to 2,500 KWh/m^2. Daily solar energy potential varies from 4.66 kWh/m^2 in the north to 7.26 kWh/m^2 in the south. The high solar potentials make people's life easier with lots of environmentally-friendly products and services such as LED lighting, electricity production and car title loans [9].
- **Wind Energy :** Algeria has promising wind energy potential of about 35 TWh/year. Almost half of the country experience significant wind speed. The country's first wind farm is being built at Adrar with installed capacity of 10MW with substantial

funding from state-utlity Sonelgaz. Two more wind farms, each of 20 MW, are to be developed during 2014- 2013. Studies will be led to detect suitable sites to realize the other projects during the period 2016-2030 for a power of about 1700 MW [9].

1.3 Photovoltaic Systems

Solar energy is environmentally friendly technology, a great energy supply and one of the most significant renewable and green energy sources. It plays a substantial role in achieving sustainable development energy solutions. Therefore, the massive amount of solar energy attainable daily makes it a very attractive resource for generating electricity. Both technologies, applications of concentrated solar power or solar photovoltaic, are always under continuous development to fulfil our energy needs [10]. Photovoltaics (PV) are probably the most elegant way to convert solar energy into electricity.

1.3.1 Photovoltaic Cell

A photovoltaic (PV) cell is an energy harvesting technology, that converts solar energy into useful electricity through a process called the photovoltaic effect. There are several different types of PV cells which all use semiconductors[2] to interact with incoming photons from the sun in order to generate an electric current.

1.3.1.1 Types of PV Cells

Photovoltaic cells are made of semiconductors based on silicon (Si), germanium (Ge), selenium (Se), cadmium sulfide (CdS), cadmium telluride (CdTe) or gallium arsenide (GaAs). Silicon is currently the most widely used material for photovoltaic cells, because it is so abundant in nature. It is found in nature in the form of silica stone. Silica is a chemical compound (silicon dioxide) and a mineral with the formula SiO2[11]. The different types of PV cells available are:

- Monocrystalline silicon cells are bluish-gray or black with a uniform appearance, with an efficiency of 13 to 17%, (a)
- Polycrystalline silicon cells are blue with a mosaic appearance, yield 11-15%, (b)
- Thin-Film Solar Cells (TFSC) are 6 to 10 % efficient, (c)

[2]**Semiconductor :** Semiconductors offer variable conductivity, making them useful for regulating electrical current. Their conductivity can be altered by factors such as applied voltage, current or exposure to specific wavelengths of light, hence their application in photovoltaic systems.

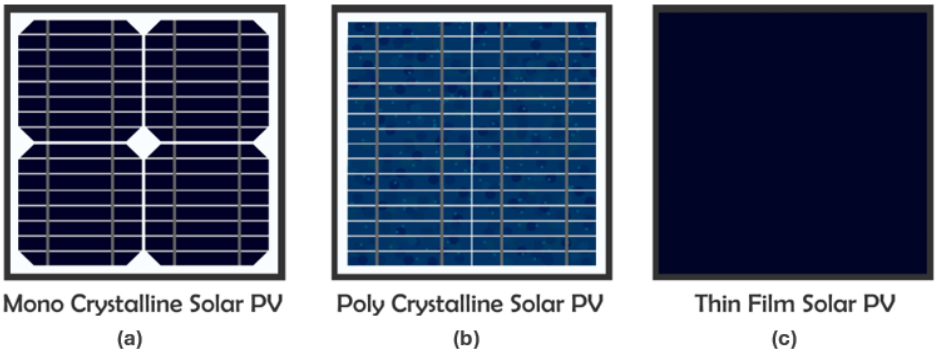

Figure 1.3 : Types of PV Cells

1.3.1.2 Photovoltaic Effect

The photovoltaic effect is a process that generates voltage or electric current in a photovoltaic cell when it is exposed to sunlight. These solar cells are composed of two different types of semiconductors a p-type and an n-type that are joined together to create a p-n junction as shown in figure (1.4) [12].

By joining these two types of semiconductors, an electric field is formed in the region of the junction as electrons move to the positive p-side and holes move to the negative n-side. This field causes negatively charged particles to move in one direction and positively charged particles in the other direction [12].

Light consists of photons, which are small bundles of electromagnetic energy. When photons of suitable wavelengths hit solar cells, their energy is transferred to electrons in the semiconductor material, causing the electrons to jump to the conduction band. In this excited state, electrons are free to move, generating an electric current in the cell.

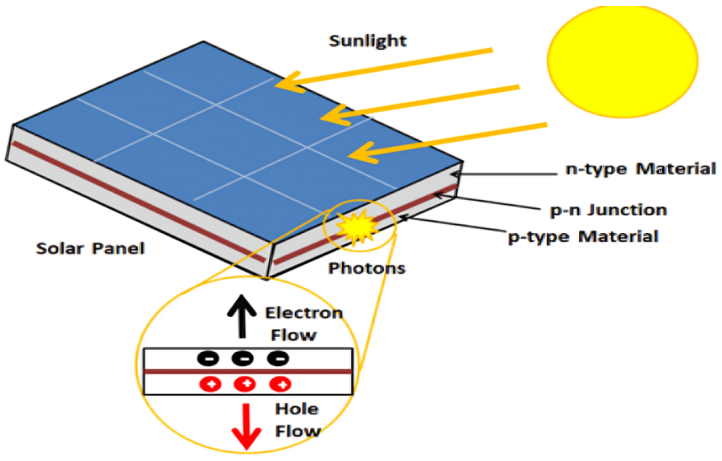

Figure 1.4 : A diagram showing the photovoltaic effect

1.3.1.3 Photovoltaic Cell Characteristics

The photovoltaic cell is characterized by :

- **Open-circuit voltage (V_{oc}):**
  A solar cell is placed under a constant light source, with no receiver at its terminals, and will produce a DC voltage of between 0.3 and 0.7, depending on the semiconductor material used, the cell temperature and its state of aging.

- **Short-circuit current I_{sc} :**
  If a solar cell is short-circuited, it will deliver a maximum current at zero voltage is known as the short-circuit current.

- **Current-voltage characteristic**
  The $I = f(V)$ characteristic of a solar cell represents the variation in current it produces at its terminals.

- **Power-voltage characteristic**
  The $P = f(V)$ characteristic of a solar cell represents the product of current and voltage delivered by a solar cell $P = V.I$

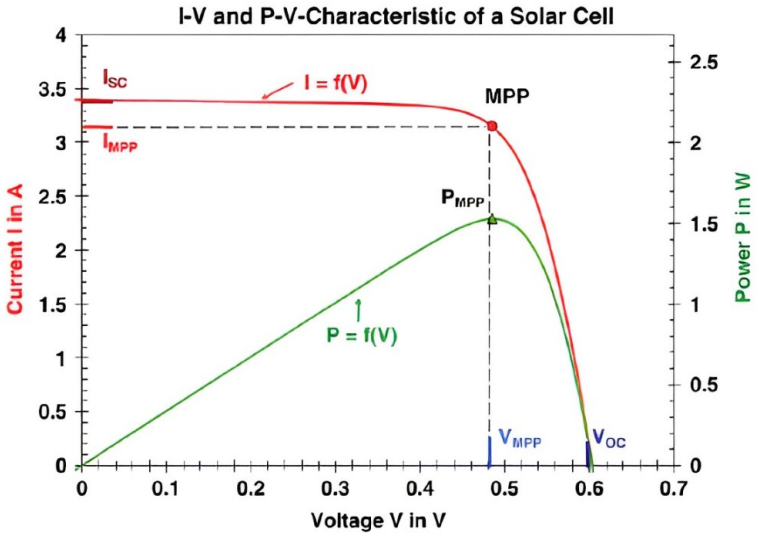

Figure 1.5 : I-V and P-V characteristic curves

1.3.2 Photovoltaic Module

Photovoltaic modules, commonly known as solar panels, are a web that captures solar power to transform it into sustainable energy. Photovoltaic modules are made up of many individual, interconnected photovoltaic cells. To ensure the modules are tilted correctly and facing the sun, they are housed in support structures. Every module has two output terminals that collect the generated current and transfer it to the management systems at a solar power station [13].

PV cells are wired in parallel to increase current and in series to produce a higher voltage. 36 cell modules are the industry standard for large power production.

1.3.2.1 Association of Photovoltaic Cells

Modules can also be connected in series and parallel to increase voltage and current. However, it is important to take a few precautions, as the existence of less efficient cells or the occlusion of one or more cells (due to shade, dust, etc.) can permanently damage the cells.

- **In Series :**
  The voltage delivered by a photovoltaic cell is limited to the gap voltage of the semiconductor used, so several cells are connected in series to increase the output voltage. The same current flows through these cells, and the generator voltage is proportional to their number[14].
  In terms of equations, we have :

$$\begin{cases} V_{oc_{ns}} = N_s V_{oc} \\ I_{sc} = I_{sc_{ns}} \end{cases} \tag{1.1}$$

  With
  $V_{OC_{ns}}$: Voltage across N_s cells in series ; V_{OC} : Voltage across a single cell
  $I_{SC_{ns}}$: Current through N_s cells in series ; I_{SC} : Current through a single cell
  N_s : Number of cells in series The I-V characteristic of series grouping shown in figure is therefore obtained by adding voltages to a given current.

- **In parallel**
  For parallel connection, we need to check that the voltages of the photovoltaic cells are identical, and the current obtained represents the product of the current of the elementary cell and the number of these cells for a voltage that remains the same .[14]

$$\begin{cases} I_{SC_{np}} = N_p I_{SC} \\ V_{OC} = V_{OC_{np}} \end{cases} \tag{1.2}$$

  With :
  $I_{SC_{np}}$: Current flowing through N_p cells in parallel
  $V_{OC_{np}}$: Voltage across N_p cells in parallel
  N_p : Number of cells in parallel

- **Mixed Association (series and parallel)**
  Increasing the power output of photovoltaic generators requires group photovoltaic cells in series and in parallel to obtain an equivalent mixed generator.[14]

1.3.3 Photovoltaic Array

1.3.3.1 What is a Photovoltaic Array ?

If photovoltaic solar panels are made up of individual photovoltaic cells connected together, then the Solar Photovoltaic Array, also known simply as a Solar Array is a system made up of a group of solar panels connected together as shown in figure 1.6.

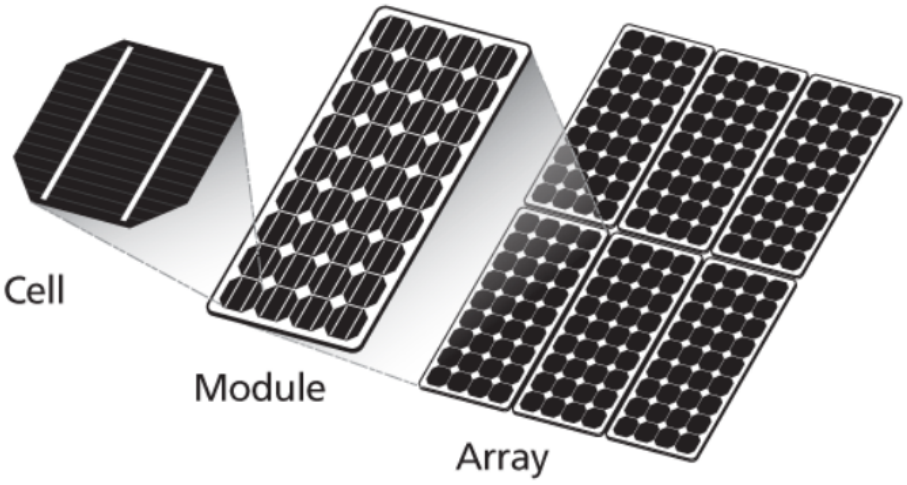

Figure 1.6 : Photovoltaic cell, module and array

A photovoltaic array is therefore multiple solar panels electrically wired together to form a much larger PV installation (PV system) called an array, and in general the larger the total surface area of the array, the more solar electricity it will produce [15].

1.3.3.2 Association of Solar Panels

PV modules can be associated in three primary configurations: series, parallel and mixed.

- **Series Connection :** In a series connection, the positive terminal of one module is connected to the negative terminal of another module, and so on. This configuration increases the voltage output while keeping the current constant [16].
- **Parallel Connection :** In a parallel connection, the positive terminals of all modules are connected together, and the negative terminals are connected together. This configuration increases the current output while keeping the voltage constant [16].
- **Mixed Connection :** A mixed connection combines series and parallel connections to achieve a desired voltage and current output. This configuration is often used in large-scale solar installations to optimize energy production and system design [16].

1.3.4 Influence of External Parameters on PV System Characteristics

1.3.4.1 Influence of Irradiance

The value of the short-circuit current is directly proportional to the radiation intensity. The open-circuit voltage, on the other hand, does not vary to the same extent, remaining virtually unchanged even at low irradiance as shown in figure (1.7) [17]

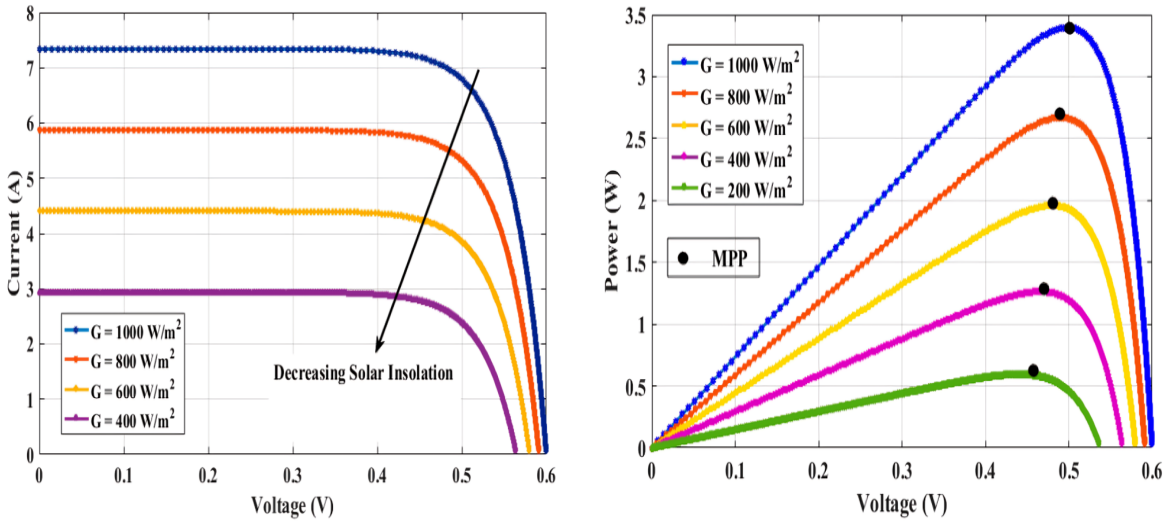

Figure 1.7 : Influence of irradiance on I-V and P-V characteristics

1.3.4.2 Influence of Temperature

The temperature has a negligible influence on the value of the short-circuit current. On the other hand, the open-circuit voltage drops quite sharply with increasing temperature, and consequently the extractable power decreases as shown in figure (1.8) [17].

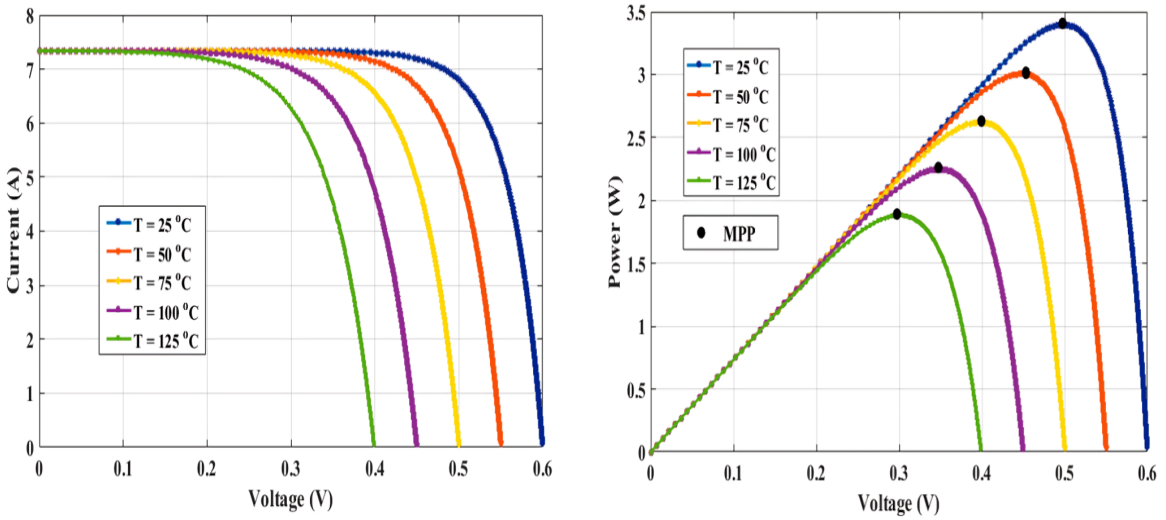

Figure 1.8 : Influence of temperature on I-V and P-V characteristics

1.4 PV-Load Connection

1.4.1 Direct Connection

The simplest type of PV system one could ever design is by connecting single or multiple PV modules directly to the DC load as shown in figure (1.9) below [18].

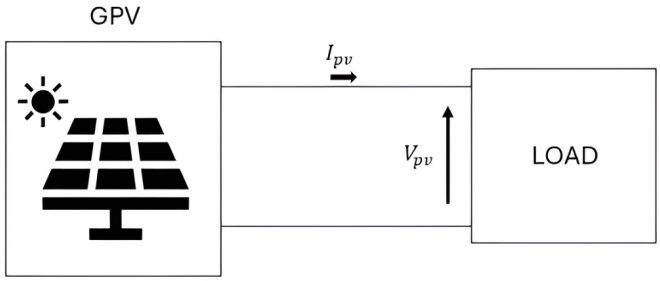

Figure 1.9 : Direct connected PV module with DC load

The overall capacity of the modules is such that it can supply power only during the sunshine hours. No special arrangement is made to have the maximum utilization of the modules by tracking the maximum power point of the modules with a charge controller throughout the day.

1.4.2 Indirect Connection via DC-DC Adaptation

In order to address the issue raised, it was necessary to add an adaptation stage, as indicated in figure (1.11). This stage ensures the transfer of energy under optimal operating conditions for the PV generator and the load.

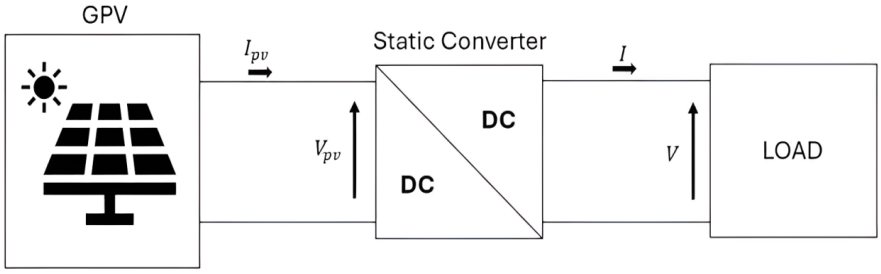

Figure 1.10 : PV-load connection through a DC/DC converter

For the system to function ideally, various control loops are required at the input and output of the adaptation stage :

- At the input, they ensure the extraction of the available PPM (Peak Power Maximum) at the terminals of the PV generator at each moment.
- At the output, they allow optimal operation of each application in its most suitable mode.

The techniques used for the input control loops involve associating with the adaptation stage a control called MPPT (Maximum Power Point Tracking) "1.7", which continuously searches for the maximum power point (PPM).

1.5 DC-DC Static Converters

1.5.1 Overview on DC-DC Converters

A DC-DC converter is an electrical system (device) which converts direct current (DC) sources from one voltage level to another. In other words, a DC-DC converter takes as input a DC input voltage and outputs a different DC voltage. The output DC voltage can be higher or lower than the DC input voltage. As the name implies, a DC-DC converter only works with direct current (DC) sources and not with alternative current (AC) sources [19].
A DC-DC converter is also called a DC-DC power converter or voltage regulator.

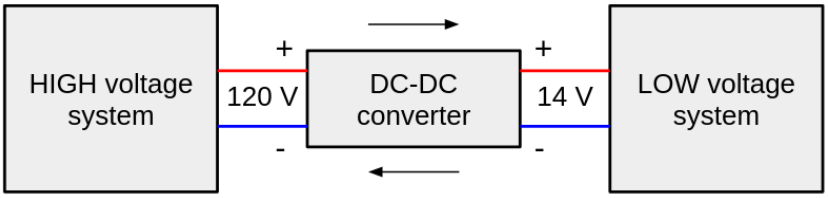

Figure 1.11 : Operational principle of DC-DC converters

1.5.2 Types of DC-DC Converters

1.5.2.1 Buck Converter

This steps down the input voltage to a lower output voltage while increasing the output current. It employs a series of switches, an inductor, and a capacitor to regulate the output voltage by adjusting the duty cycle of the switches. Buck converters are commonly used in applications that require a lower voltage level than the input supply, such as battery-powered devices and voltage regulation in computer systems [19].

1.5.2.2 Boost Converter

This steps up the input voltage to a higher output voltage while decreasing the output current. It utilizes switches, an inductor, and a capacitor to manage energy transfer, resulting in an increased output voltage. Boost converters are commonly used in applications requiring a higher output voltage than the input supply, such as power LED drivers or voltage boosting for portable devices [19].

1.5.2.3 Buck–Boost Converter

This is a versatile topology that can step up or step down the input voltage, depending on the duty cycle of the switches. This topology combines elements of both buck and

boost converters, making it suitable for applications with varying input voltages or when both step-up and step-down conversions are needed. Buck-boost converters are used in applications such as solar power systems and battery-powered devices with fluctuating voltage levels [19].

In the figure (1.13) [20] below, the electrical representations of different DC-DC converter configurations are illustrated, highlighting the fundamental components and connections of Buck, Boost, and Buck-Boost converters :

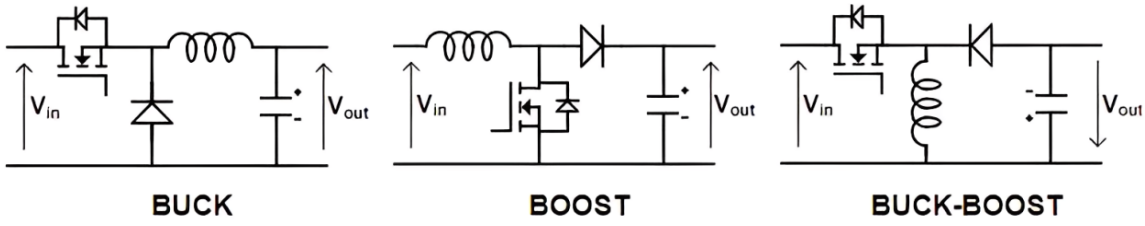

Figure 1.12 : Electrical circuits of most common DC-DC converters

1.6 Energy Storage in Photovoltaic Systems

In stand-alone photovoltaic (PV) systems, energy storage is important for providing continuous power to the load when sunlight is not available. The most common form of storage is batteries, which store the electrical energy generated by the PV panels during sunshine hours [21].

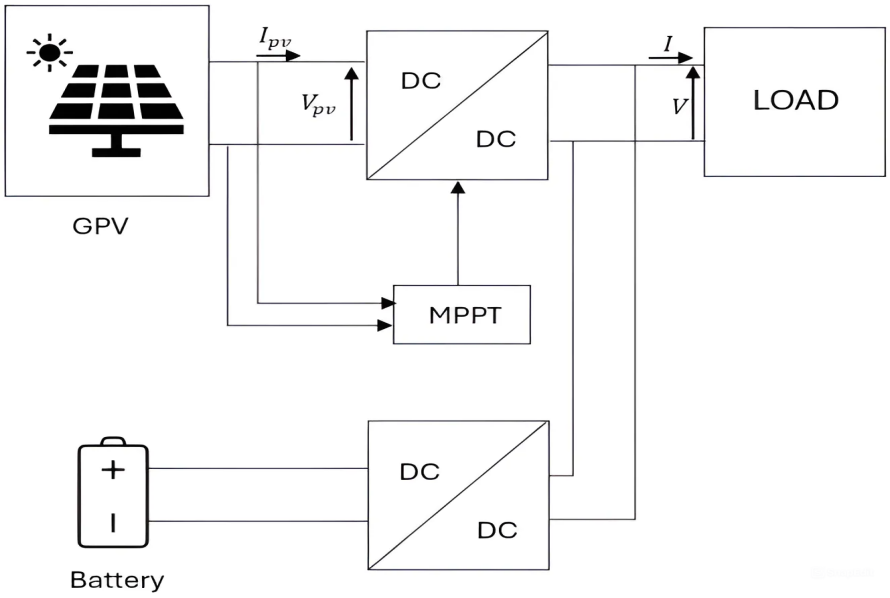

Figure 1.13 : Photovoltaic system with energy storage

1.6.1 Solar Batteries

Batteries are essential components in off-grid solar systems as they store excess energy generated by the solar panels. This stored energy can be used when the sun isn't shining,

ensuring a consistent power supply. The type and size of the batteries depend on the user's energy needs and consumption patterns. Choosing the best battery for any solar system depends on various factors, including cost, maintenance requirements, and lifespan [22].

A bidirectional DC-DC (buck-boost) converter is an important part of standalone solar Photovoltaic systems for interfacing the battery storage system. It provides the required bidirectional power flow for battery charging and discharging mode. The duty cycle of the converter controls charging and discharging based on the state of charge of the battery and direction of the current [23] .

1.6.2 Characteristics of Solar Batteries

A solar battery also called stationary battery is characterized by a certain number of parameters:

- **Battery Voltage :** The terminal voltage during operating condition is known as nominal voltage or working voltage. This voltage will be specified by manufactures. It may be 3V, 6V, 12V, 24V etc... [21]
- **Battery Capacity :** The storage capacity of the battery is represented in Ampere hour or Ah. If V is the battery voltage then the energy storage capacity of the battery can be Ah x V = Watt-hour. Usually battery capacity will be specified for a given discharge/charge rating or C rating. The actual capacity depends on operating conditions such as load, temperature, etc... [21]
- **Battery Life Cycle :** It is the number of complete charge – discharge cycles a battery can work before the nominal capacity decreases less than 80% of its rated initial capacity. After the specified life cycle, the battery will work with reduced capacity. It can be used but the capacity will be lower [21].
- **Depth of discharge (DOD) :** The depth of discharge is the specified amount of energy that can be safely drawn from the battery before it needs to be recharged. It is also known as the solar battery discharge limit. Batteries used in solar PV systems need to have a high DoD to maximize the usable energy stored [24].
- **The State of Charge (SOC) :** The state of charge of a battery is the difference between the full charge and the depth of discharge of the battery in percentage. If the DOD is 25% then the state of charge is (100 - 25) = 75% [21].

1.7 Principle of Maximum Power Point Tracking (MPPT)

Photovoltaic generation systems have two major problems: the conversion efficiency of electric power generation is very low (9%-17%), especially under low irradiation conditions, and the amount of electric power generated by solar arrays changes continuously with weather conditions.

Moreover, the solar cell V-I characteristic is nonlinear and varies with irradiation and temperature. As a general rule, the photovoltaic system as a whole (array, inverter, etc.) operates most efficiently and generates the greatest power output at a single point on the V-I or V-P curve, known as the Maximum Power Point (MPP). Although the position of the MPP is unknown, it can be found using search algorithms or calculation models. The operating point of the photovoltaic generator must therefore be maintained at its maximum power point (MPP) using maximum power point tracking (MPPT) procedures [25].

1.7.1 MPPT Basic Concept

1.7.1.1 MPPT Controller

MPPT (Maximum Power Point Tracking), maximum efficiency tracker, also known as solar controller. The MPPT controller can flexibly adjust the output voltage and output current of the PV photovoltaic cell array, allowing the photovoltaic cells to work near the maximum power point to maximize the solar output conversion efficiency.

1.7.1.2 MPPT Working Principle

MPPT control is generally accomplished through DC/DC conversion circuits. Its schematic block diagram is shown in the figure (1.17). The photovoltaic cell array and the load are connected through a DC/DC circuit, and the maximum power tracking device continuously detects the current and voltage changes of the photovoltaic array. And adjust the duty cycle of the PWM drive signal of the DC/DC converter according to its changes.

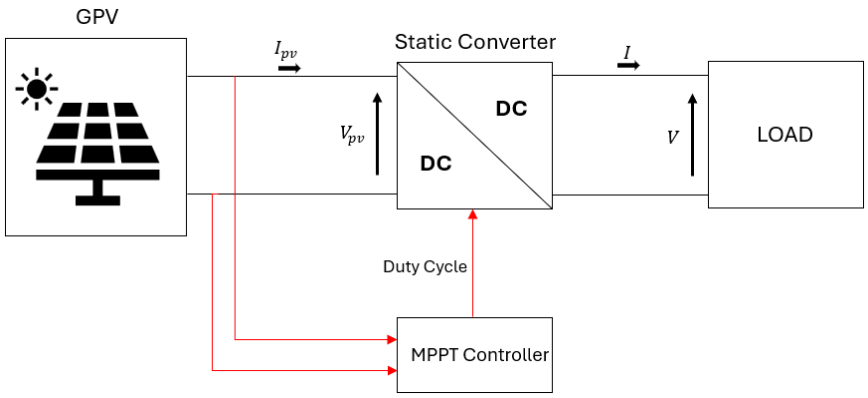

Figure 1.14 : Structure of a PV system with MPPT controller

In summary, the MPPT controller will continuously track the maximum power point in the solar panel to bring out the maximum efficiency of the solar panel. The higher the

voltage, the more electricity can be outputted through maximum power tracking, thus improving the charging efficiency. In this sense, the MPPT solar charge and discharge controller is bound to eventually replace traditional solar controllers [26].

1.7.2 State-of-the-Art in MPPT Control Techniques

In the realm of photovoltaic systems, the need for efficient energy conversion has led to the development of various MPPT techniques. These techniques play a pivotal role in optimizing the power output of solar panels by continuously adjusting the operating conditions to extract the maximum available power. Some of the key control applied to MPPT in PV systems can be classified as follows :

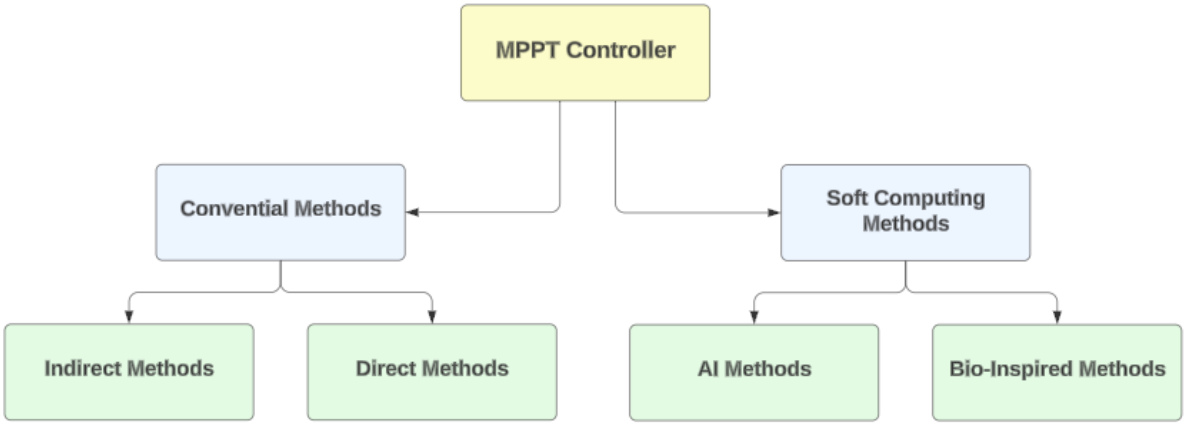

Figure 1.15 : Classification of MPPT Control Techniques

1.7.2.1 Convential Methods

- **Indirect Methods**
  Indirect methods used to control MPPT (Maximum Power Point Tracking) systems are techniques that estimate the maximum power point (MPP) using external sensors or parameters such as temperature, irradiance, or open-circuit voltage. These methods indirectly estimate the MPP without directly measuring the voltage and current of the photovoltaic (PV) array. The most applied indirect methods are:

  - Fractional Open Circuit Voltage (FOCV) method [27].
  - Constant Voltage (CV) method [28].

- **Direct Methods**
  Direct methods of MPPT (Maximum Power Point Tracking) in PV systems involve measuring the actual instantaneous values of PV voltage and currents to track the MPP. These methods directly track the MPP by scanning through the I-V curve of the solar cell. The most applied direct methods are :

  - Incremental Conductance method (InCon) [29, 30, 31, 32].
  - Perturb & Observe method (P&O) [33, 34, 35, 36].

1.7.2.2 Soft Computing Methods

- **AI Methods**
  Artificial Intelligence (AI) methods are increasingly being used for Maximum Power Point Tracking (MPPT) control in photovoltaic (PV) systems to improve their efficiency and performance. AI-based MPPT techniques can adapt to changing environmental conditions and improve the tracking speed and output DC power, thereby enhancing the overall efficiency of PV systems. The AI methods used in controlling photovoltaic (PV) systems include :

  - Artificial Neural Network based MPPT (ANN)[37, 38].
  - Fuzzy Logic based MPPT [39, 40, 41].
  - Genetic Algorithms Optimized Fuzzy Logic based MPPT [42, 43, 44].
  - Adaptive Neuro Fuzzy Inference System (ANFIS) based MPPT [45, 46, 47, 48, 49].
  - Deep Reinforcement Learning based MPPT [50, 51, 52].

- **Bio-Inspired Methods**
  Bio-inspired methods are a class of Maximum Power Point Tracking (MPPT) techniques that are based on the behavior of living organisms or natural phenomena. These methods are used to optimize the energy output of photovoltaic (PV) systems by tracking the maximum power point (MPP) under various environmental conditions. The Bio-Inspired methods used in controlling photovoltaic (PV) systems include :

  - Genetic Algorithms based MPPT (GA) [53, 54, 55].
  - Particle Swarm Optimization (PSO) based MPPT [56, 57, 58].
  - Ant Colony Optimization (ACO) [59, 60, 61].

1.8 Photovoltaic Systems Applications

Photovoltaic systems can be divided into two broad categories: Stand-alone systems, i.e. those not connected to an electricity grid, and systems connected to the public electricity distribution network.

1.8.1 Stand-Alone Systems

Autonomous or ”stand-alone”, these isolated installations are dedicated to domestic, rural or other off-grid use, but must ensure that load demand is covered at all times. The power output of the photovoltaic array is not sufficient to meet the load demand. The system’s autonomy is therefore ensured by an energy storage system, an inverter and a control system.

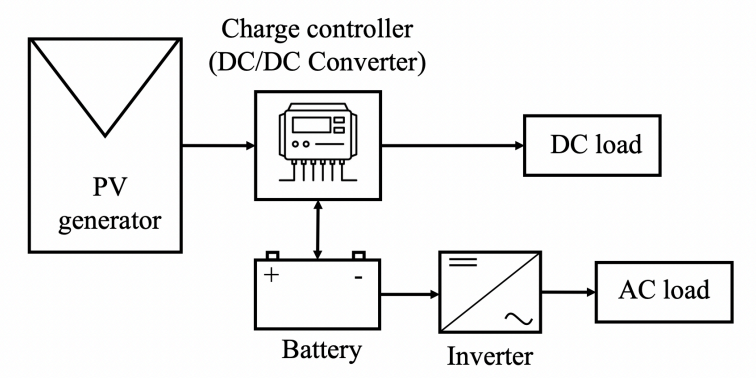

Figure 1.16 : Stand-alone photovoltaic system

1.8.2 Grid-Connected Systems

Grid-connected PV systems are the most frequent because they are easier to construct and often less expensive than off-grid PV systems that rely on batteries. Grid-connected PV systems enable homes to use less energy from the grid while also supplying unused or excess energy to the utility grid. The system's structure and size are determined by its intended use.

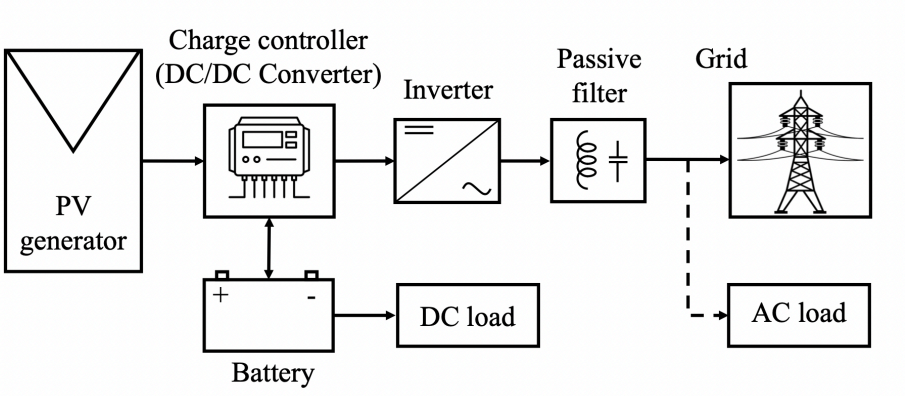

Figure 1.17 : Grid-connected system

1.9 Conclusion

In conclusion, this chapter has provided a comprehensive overview of photovoltaic systems and their key components. We've discussed how these systems connect to loads, the role of static converters in improving efficiency, the importance of energy storage for a reliable power supply, and the latest advancements in MPPT control techniques. By understanding these basics, we can better harness the potential of photovoltaic systems to meet our energy needs while reducing environmental impact. In the following chapters, we'll introduce deeper aspects such as system modeling, control strategies, energy management and systems sizing.

Chapter 2

Photovoltaic Systems Modeling

2.1 Introduction

Modeling is a very important part of any engineering practice. Today it is possible to model incredibly complicated systems, predict their performance and monitor them using computers and powerful software. A typical photovoltaic system may consist of the solar generator itself and other components that maybe any one of the following: The utility grid, storage components (particularly in standalone systems), power converters (DC/DC or inverters), and related control circuitry [62].

It is important for system sizing, cost analysis, and monitoring to have models of each of these parts available at every step of system development, particularly for the solar generator itself. Moreover, such models may be tested together with other distributed system models in order to evaluate and predict the overall system performance [62].

In the following chapter on modeling, we will explore the specific techniques used in our project, particularly focusing on the single diode model used to accurately represent the photovoltaic generator. Additionally, we will elaborate the modeling and sizing of the boost converter, highlighting how these modeling approaches contribute to the efficient design and optimization of photovoltaic systems.

2.2 Photovoltaic Panel Modeling

A standard PV panel datasheet provides the following parameters: open circuit voltage V_{oc}, short-circuit current I_{sc}, maximum power point (MPP) voltage V_{mp}, maximum power point current I_{mp} and maximum power P_m, at standard test condition (STC) which is defined as the solar irradiation of 1000 W/m² equivalent to one sun at 25°C. In addition tothese parameters, the temperature coefficients at V_{oc} and I_{sc} are provided by these datasheets [63].

2.2.1 Mathematical Modeling of PV Module

Various methods of modelling photovoltaic panels exist. In this case, a single exponential model has been selected, which is also known as one diode model. The equivalent circuit of a PV cell is shown in Figure 2.1 [64].

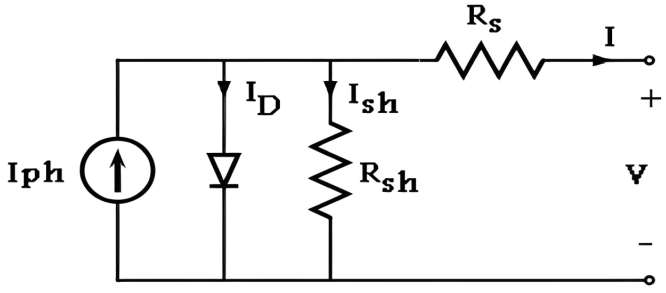

Figure 2.1 : Equivalent circuit of one-diode model of a PV cell

The current source I_{ph} represents the cell photocurrent. R_{sh} and R_s are the intrinsic shunt

and series resistances of the cell, respectively. Usually the value of Rsh is very large and that of Rs is very small, hence they may be neglected to simplify the analysis [64].

The voltage–current characteristic equation of a solar cell is provided as :

- **Module photo-current I_{ph} :**

$$I_{\mathrm{ph}} = [I_{\mathrm{sc}} + K_{\mathrm{i}}(T - 298)] \times \frac{I_{\mathrm{r}}}{1000} \tag{2.1}$$

I_{ph} : photo-current (A); I_{sc} : short circuit current (A) ;
K_{i} : short-circuit current of cell at 25 °C and 1000 W/m^2 ;
T : operating temperature (K); I_{r} : solar irradiation (W/m^2) ;

- **Module reverse saturation current I_{rs} :**

$$I_{\mathrm{rs}} = \frac{I_{\mathrm{sc}}}{\left[\exp\left(\frac{qV_{\mathrm{OC}}}{N_{\mathrm{S}}k_{\mathrm{n}}T}\right) - 1\right]} \tag{2.2}$$

q : Electron charge, $q = 1.6 \times 10^{-19}\,\mathrm{C}$;
V_{OC} : Open circuit voltage (V) ;
N_{S} : Number of cells connected in series
n : Ideality factor of the diode
k : Boltzmann's constant, $k = 1.3805 \times 10^{-23}\,\mathrm{J/K}$.

- **The module saturation current I_0 :**
It varies with the cell temperature and it is given by :

$$I_0 = I_{rs}\left[\frac{T}{T_r}\right]^3 \exp\left[\frac{q \times E_{g0}}{nk}\left(\frac{1}{T} - \frac{1}{T_r}\right)\right] \tag{2.3}$$

T_{r} : Nominal temperature, $T_{\mathrm{r}} = 298.15\,\mathrm{K}$
E_{g0} : Band gap energy of the semiconductor, $E_{g0} = 1.1\,\mathrm{eV}$

- **The diode current I_d :**

$$I_d = I_0\left[\left(\exp\left(\frac{q(V + IRs)}{nKNsT}\right) - 1\right)\right] \tag{2.4}$$

V_{T} : Volt equivalent temperature

$$V_{\mathrm{T}} = \frac{k \cdot T}{q} \tag{2.5}$$

- **Shunt current I_{sh} :**

$$I_{\mathrm{sh}} = \frac{V + IR_{\mathrm{s}}}{R_{\mathrm{sh}}} \tag{2.6}$$

- **The current output of pv cell :**

$$I = I_{\mathrm{ph}} - I_{\mathrm{d}} - I_{\mathrm{sh}} \tag{2.7}$$

$$I = I_{\mathrm{ph}} - I_0\left[\exp\left(\frac{q(V + IR_s)}{nkN_sT}\right) - 1\right] - \frac{V + IR_s}{R_{sh}} \tag{2.8}$$

2.2.2 Mathematical Modeling of PV Array

The equivalent circuit for PV array is shown in Figure 2.1 [64]. C

- **The current output of PV array :**

$$I = N_P \times I_{ph} - N_P \times I_0 \times \left[\exp\left(\frac{V/n_S N_S + I \times R_s/N_P}{n \times V_t}\right) - 1\right] - I_{sh} \tag{2.9}$$

With :

$$I_{sh} = \frac{V \times N_P/n_S N_S + I \times R_S}{R_{sh}} \tag{2.10}$$

N_P : Parallel connected modules ; N_S : Series connected cells in module
n_s : Series connected modules

The formulas of I_{ph}, I_0 and V_t are sated in equations 2.1, 2.3 and 2.5 respectively.

2.2.3 Characteristics of The PV Panel

To verify the authenticity of our modeled system, we utilized the 1 Soltech 1STH-250-WH photovoltaic module as a reference for comparison and validation. The 1Soltech 1STH-250-WH PV panel is a high-efficiency solar module designed for optimal performance in various environmental conditions.

Table 5.3 provides a detailed overview of the characteristics of the 1Soltech 1STH-250-WH PV panel at standard test conditions (STC) :

I_{sc}[A]	Short-circuit current	8.66
V_{oc}[V]	Open circuit voltage	37.3
I_{mp}[A]	Current at maximum power point	8.15
V_{mp}[V]	Voltage at maximum power point	30.7
$P_{\max}$[W]	Maximum power	250.205
$R_s[\Omega]$	Series resistance	0.23724
$R_{sh}[\Omega]$	Shunt resistance	224.1886
α[A/C]	Temperature coefficient of I_{sc}	0.086998
β[V/C]	Temperature coefficient of V_{oc}	-0.36901

Table 2.1 : Characteristics of the PV panel 1SolTech 1-STH-250-WH at standard test conditions

2.2.3.1 I-V and P-V Characteristics at 25°C with Varying Irradiances

Irradiance [W/m^2]	1000	700	500
I_{mp}[A]	8.091	9.15	8.163
V_{mp}[V]	32.106	30.7	29.32
$P_{\max}$[W]	259.793	250.205	239.35

Table 2.2 : Characteristics of the PV panel 1Soltech 1STH-250-WH at 25°C and varying irradiances

2.2.3.2 I-V and P-V Characteristics at 1000 W/m² with Varying Temperatures

Temperature [°C]	15	25	35
I_{mp}[A]	8.091	9.15	8.163
V_{mp}[V]	32.106	30.7	29.32
$P_{\max}$[W]	259.793	250.205	239.35

Table 2.3 : Characteristics of the PV panel 1Soltech 1STH-250-WH at 1000 W/m² and varying temperatures

2.2.4 Photovoltaic Panel Model

To model the 1Soltech 1STH-250-WH photovoltaic module, we employed a widely used one-diode model that integrates the shunt resistance, as illustrated in Figure (2.1) in section (2.2.1). This model offers a good compromise between simplicity and accuracy. Many power electronic designers prefer this model for the simulation of PV devices with power converters. Its characteristic equation is given in eqaution (2.8) in section (2.2.1).

To simulate the I(V) and P(V) characteristics of the 1Soltech STH-250-WH PV panel, we required the data mentioned in table 2.4 :

I_{sc}[A]	Short-circuit current	8.66
V_{oc}[V]	Open circuit voltage	37.3
$R_s[\Omega]$	Series resistance	0.23724
$R_{sh}[\Omega]$	Shunt resistance	224.1886
$R_{sh}[\Omega]$	Shunt resistance	224.1886
α[A/C]	Temperature coefficient of I_{sc}	0.086998
n	Diode ideality factor	1.019
N_p	Parallel connected modules	1
N_s	Series connected modules	1

Table 2.4 : Characteristics of the PV panel 1Soltech 1STH-250-WH used in simulation

2.2.5 Simulation Setup

We implemented the equations (2.1), (2.3) and (2.10) using MATLAB functions and Simulink blocks, as illustrated in the figure (2.2) below :

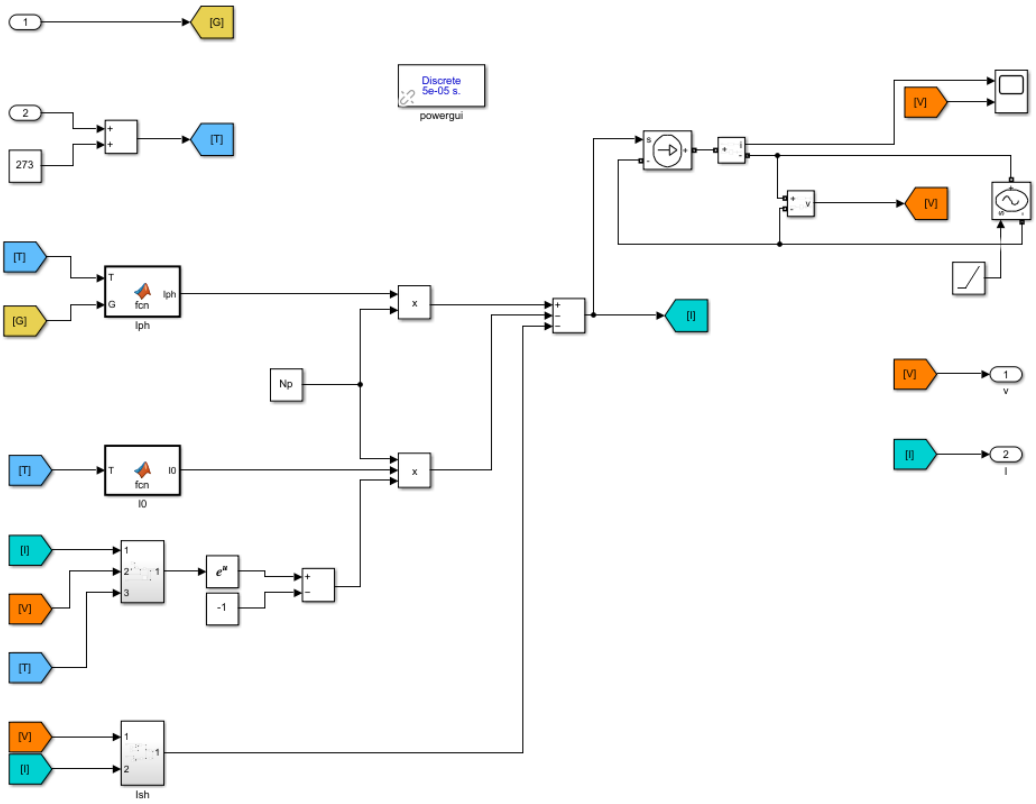

Figure 2.2 : Simulink Model of the PV Panel

2.2.6 Simulation Results

2.2.6.1 I-V and P-V Characteristics at Standard Test Conditions (STC)

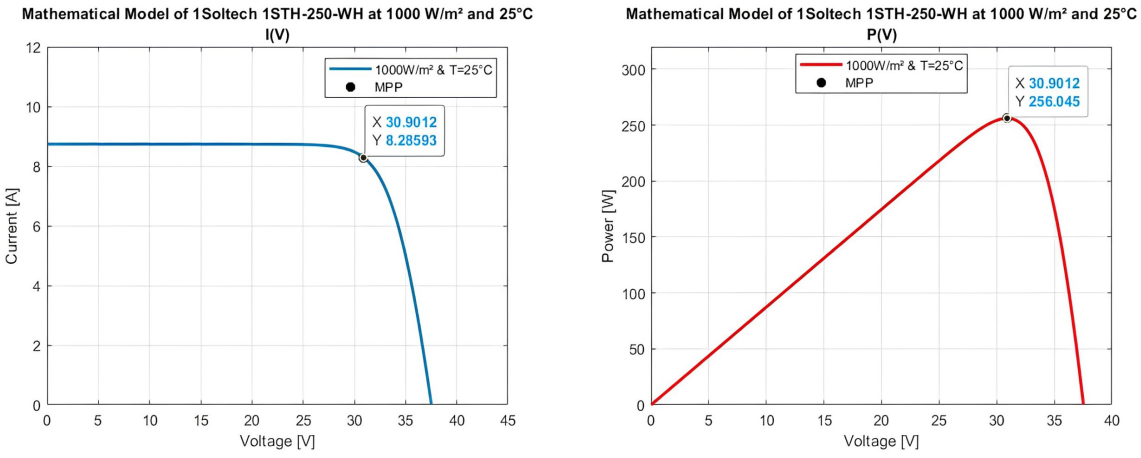

Figure 2.3 : Simulation of I-V and P-V characteristics of the PV model at STC

2.2.6.2 I-V and P-V Characteristics at 1000 W/m² with Varying Temperatures

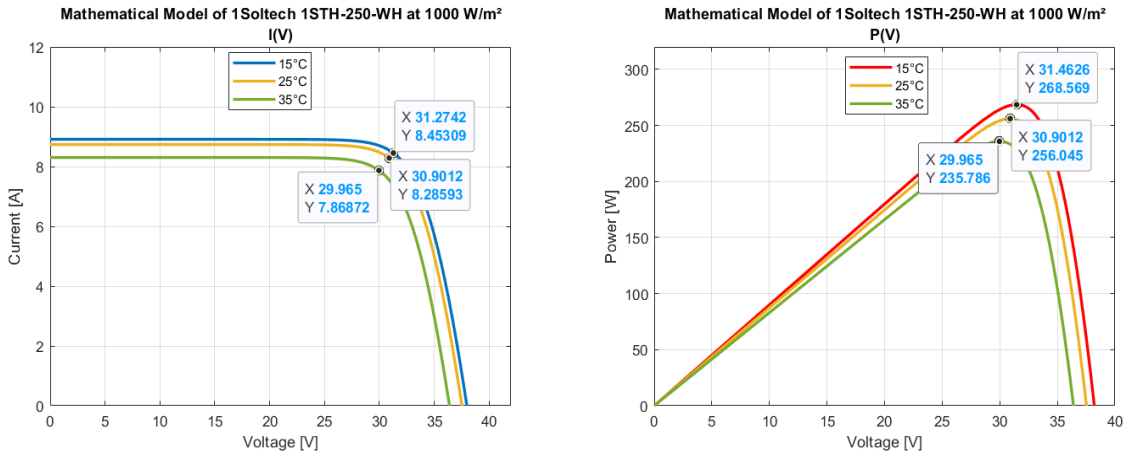

Figure 2.4 : Simulation of I-V and P-V characteristics of the PV model at 1000W/m² and varying temperatures

2.2.6.3 I-V and P-V Characteristics at 25°C with Varying Irradiances

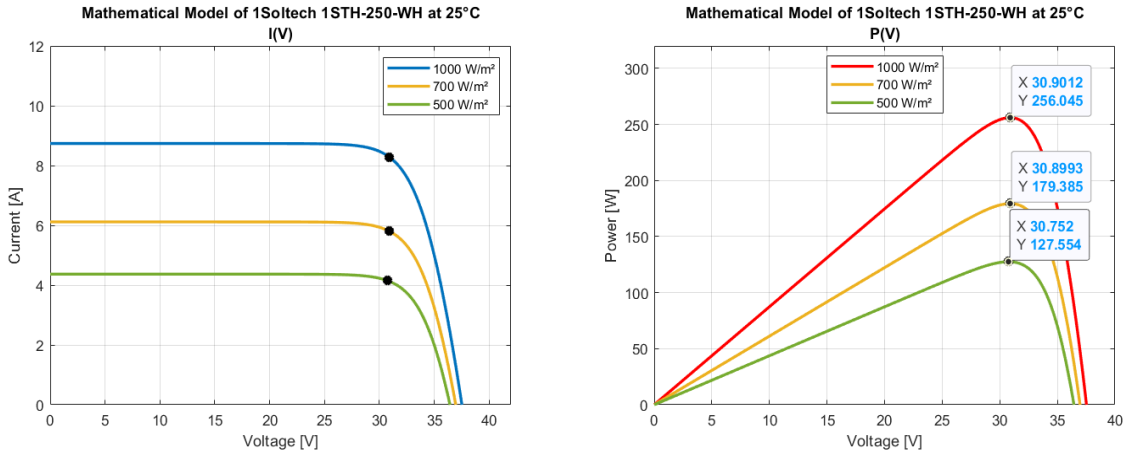

Figure 2.5 : Simulation of I-V and P-V characteristics of the PV model at 25°C and varying irradiances

2.2.7 Results Analysis

- Figure (2.3) shows the model's performance, closely aligning with the actual characteristics of the 1-Soltech 1STH-250-WH. The PV model achieves a maximum power output of 256 Watts, compared to the real-world value of 250 Watts, resulting in a small difference of just 6 Watts. Additionally, the maximum voltage provided by the model, at 30.9 Volts, nearly matches the real V_{mp} of the PV panel, which is 30.7 Volts. Furthermore, there is only a small error of 0.1 Amperes between the maximum current generated by the model and the real I_{mp} value, proving the model's accuracy.

- When analyzing temperature variations, Figure (2.4) shows a decrease in both the maximum output voltage and output power as temperature increases with its values

for voltage, current, and power closely matching the characteristics of the real PV panel.

- When varying irradiance, Figure (2.5) illustrates an expected increase in PV power and current as irradiance increases with its values for power and current are closely equal the real PV panel's characteristics under varying irradiance.

2.3 Boost Converter Modeling

A boost converter in a solar system effectively raises the low voltage output from photovoltaic arrays to a higher level. This enables effective power transfer and consumption, especially in different weather conditions. Boost Converters optimize power extraction from solar panels, maintain high efficiency, minimize current ripple, and use MPPT algorithms to operate around the maximum power point. [65].

2.3.1 Boost Converter Working Principle

Boost converters are a type of DC-DC switching converter that efficiently increases (steps up) the input voltage to produce a greater output voltage. This voltage conversion is made feasible by storing energy in an inductor during the switch-on phase and transferring it to the load during the switch-off phase. Boost converters are particularly useful in power electronics applications that require a higher output voltage than the input source. Boost converter equivalent circuit is illustrated in the figure (2.6) below [66] :

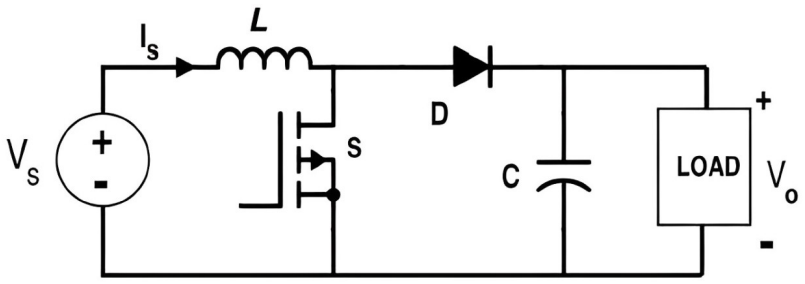

Figure 2.6 : Basic boost converter circuit diagram

The boost converter works by storing energy in an inductor's magnetic field and then transferring it to the output capacitor, increasing the voltage. This is how it works :

- **Switch-On State :** When the switch is turned on, the input voltage is applied across the inductor, causing current to increase and store energy in the magnetic field. During this time, the output capacitor delivers energy to the load [67].

- **Switch-Off State :** When the switch is turned off, the inductor attempts to continue the current flow. This causes the voltage across the inductor to invert, so forward-biasing the diode. The inductor then discharges its stored energy via the diode to the output capacitor and load [67].

The output voltage is always higher than the input voltage. The voltage conversion ratio is determined by the duty cycle of the switch :

$$V_{\text{out}} = \frac{V_{\text{in}}}{(1 - D)} \tag{2.11}$$

Where D is the duty cycle, defined as the ratio of switch-on time to the total switching period [67].

The inductor limits the input current ripple, while the output capacitor filters the output voltage ripple [67].

The boost converter can efficiently increase the input voltage to a higher controlled output voltage by managing the switch duty cycle. This makes it suitable for applications that require a greater voltage than the input source [67].

2.3.2 Components Sizing

When building boost converters, a variety of factors must be addressed, including component selection, input/output voltage and current requirements, switching frequency, and target efficiency. The primary design elements and calculations for developing a boost converter are discussed below : [68] :

2.3.2.1 Duty Cycle

$$D = 1 - \frac{V_{\text{in}}}{V_{\text{out}}} \tag{2.12}$$

V_{in} : Input voltage
V_{out} : Output voltage

2.3.2.2 Inductance L

$$L = \frac{V_{\text{in}} \cdot (V_{\text{out}} - V_{\text{in}})}{\Delta I_L \cdot fs \cdot V_{\text{out}}} \tag{2.13}$$

V_{out} : Output voltage
V_{in} : Input voltage
f_{s} : Switching frequency
ΔI_L : Estimated inductor ripple current [69]

$$\Delta \text{I}_{\text{L}} = \Delta I_{\%} \times \text{I}_{\text{out}} \times \frac{V_{\text{out}}}{\text{V}_{\text{in}}} \tag{2.14}$$

$\Delta I_{\%}$: The ripple factor ; typically between 20% and 40%

2.3.2.3 Capacitor C

$$C = \frac{I_{\text{out}} \cdot D}{fs \cdot \Delta V_{\text{out}}} \tag{2.15}$$

D : Duty cycle
I_{out} : Output current
f_s : Switching frequency
ΔV_{out} : Estimated output ripple voltage, it's typically lower than 1% of the average output voltage [69].

2.3.3 Boost Converter Model

In the initial stage of design, the calculation of the parameters for the boost converter circuit must be performed based on the characteristics of the 1Soltech 1STH-250-WH PV panel, as detailed in table 5.3.

The purpose of this simulation is to step up the voltage from the 1Soltech 1STH 250 WH PV panel, which has a maximum power point voltage V_{mp} of 30.7 V to an output voltage of 60 V.

Based on the equations provided in section (2.3.2) ; the parameters of the designed boost converter are written in the table 2.5 below :

D	Duty cycle	0.488
L[mH]	Inductance	7.97
C[μF]	Capacitor	339

Table 2.5 : Boost converter parameters

2.3.4 Simulation Setup

The schematic diagram of the DC–DC boost converter is shown in Figure 2.7, where the PV source is connected to the load through a converter to meet the requirements of the load. Efficient converters will determine the performance of the PV panel.

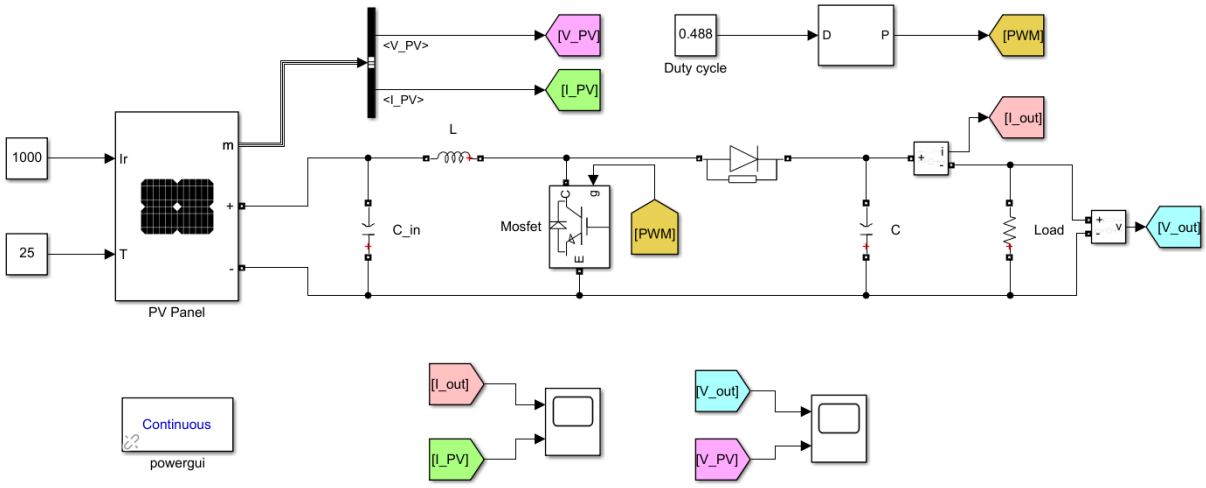

Figure 2.7 : Simulink model for a PV panel connected to the load via boost converter

- **Input Capacitor Characteristics**
  A capacitor is attached between the PV panel and power converter to filter voltage and current ripple, ensuring that ripple content does not influence the PV panel [70]. The minimum value for the input capacitor is usually specified in the datasheet. A minimum value is required to stabilize the input voltage due to the peak current requirement of a switching power supply [69].

- **Load Characteristics**
  For the simulation of the Boost Converter, a resistive load was selected to evaluate the performance of the system. The resistive load was chosen based on the following parameters :

  – Nominal voltage : 60 Volts.

  – Nominal power : 250 Watts.

- **PWM Generator**
  It generates a pulse-width modulation (PWM) signal with a duty cycle of 48.8% and a frequency of 5000 Hz. The PWM signal controls the MOSFET, which in turn controls the energy transfer from the inductor to the capacitor and load.

2.3.5 Simulation Results

The simulation results obtained from the designed boost converter system are illustrated below. The simulations were performed using the Simulink model described in the previous section. The primary objectives of these simulations were to evaluate the performance of the boost converter in terms of voltage, current, and power outputs when connected to the 1Soltech 250 WH PV panel at STC.

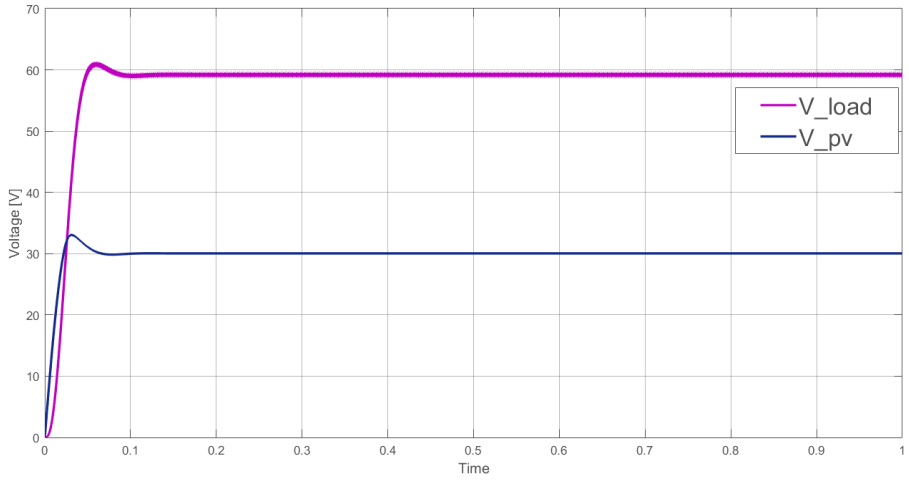

Figure 2.8 : Load and PV output voltage.

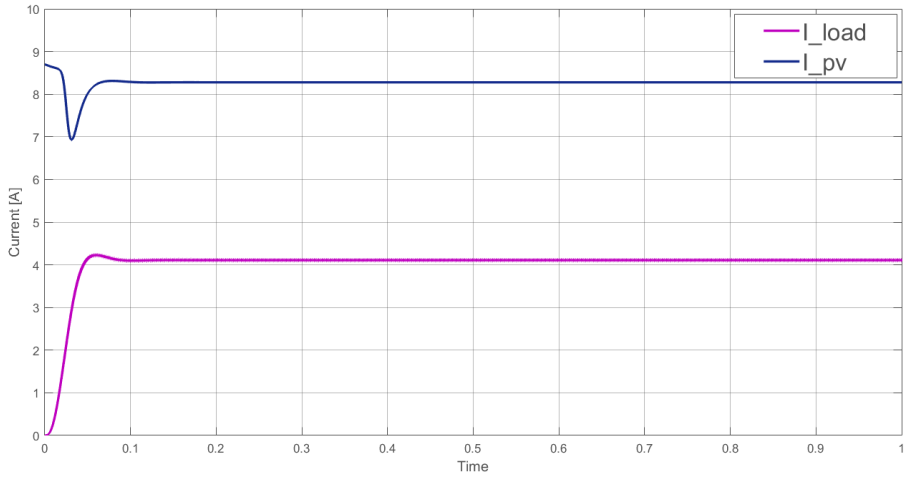

Figure 2.9 : Load and PV output current.

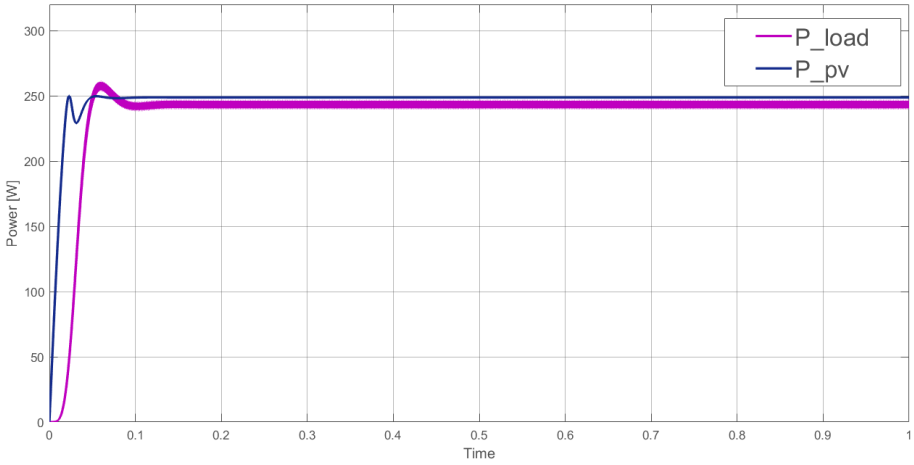

Figure 2.10 : Load and PV output power.

2.4 Results Analysis

- The boost converter, as designed, doubles the voltage output from the photovoltaic (PV) panel, giving in an output voltage of approximately 60 Volts as seen in figure (2.8). This significant voltage increase is important for meeting the requirements of the load.
- We can observe a decrease in the PV current from 8.5 to 4 Amperes as shown in figure (2.9). This decrease in current is an expected outcome of the boost converter's operation, as it prioritizes voltage amplification to meet the load's voltage requirements while conserving overall power.
- We notice that the boost converter effectively tracks the maximum power point of the PV panel, ensuring that the system operates at its peak efficiency and delivers maximum power to the load as illustrated in figure (2.10).

2.5 Conclusion

In conclusion, the modeling and simulation of the photovoltaic (PV) panel and boost converter have validated our system design. The PV panel model accurately reflects real-world characteristics with effective maximum power point tracking (MPPT) under varying environmental conditions.

Additionally, the boost converter's performance in increasing the PV output voltage, while simultaneously conserving overall power through a controlled decrease in current, has been successfully validated through simulation. These results affirm the performance of our modeling approach and highlight the system's efficiency in meeting load requirements while maximizing energy extraction.

Chapter 3

Photovoltaic Systems Control

3.1 Introduction

The significance of photovoltaic (PV) systems is on the rise, as they tap into solar radiation, a sustainable, abundant, and eco-friendly energy source. Nonetheless, PV systems encounter two main issues: limited energy conversion efficiency and energy loss due to changing weather conditions [71]. To address these challenges, Maximum Power Point Tracking (MPPT) control techniques are crucial for maximizing the energy captured by PV modules. MPPT systems enable the automatic tracking of the Maximum Power Point (MPP), ensuring optimal energy extraction [71].

The PV systems efficiency is widely enhanced by a continuous operation at the MPP despite variations in climate conditions; the implementation of MPPT methods ensures extraction of maximum power from the PV array for all weather conditions. To do so, it is necessary to automatically track the MPP in terms of voltage and current. In general, MPPT techniques use values of current and voltage of the PV panel to ccalculate the MPP and manipulate the duty cycle of the power converter and, in this way, extract the maximum power available [71].

In this chapter, we provide a comprehensive study of three different MPPT control techniques: the conventional Perturb and Observe (P&O) method, the AI-based fuzzy logic MPPT, and the bio-inspired PSO-based MPPT method. Following this, we present a comparative analysis of the performance of these three methods.

3.2 Perturb and Observe (P&O) Controller

To maximize the available power from a PV system and improve installation efficiency, various MPPT control techniques are employed. The most popular conventional MPPT method is perturb and observe (P&O). It is widely used in commercial products and serves as the foundation for many of the more advanced algorithms discussed in the literature. P&O is commonly utilized in practice due to its low cost, simplicity, and ease of implementation [72].

3.2.1 P&O Control Principle

The perturb and observe (P&O) algorithm is a conventional and one of the most widely used Maximum Power Point Tracking (MPPT) techniques in photovoltaic (PV) systems. The main objective of the P&O algorithm is to continuously adjust the operating point of the PV system to maximize power output. [72].

The *P&O* algorithm works by periodically perturbing (adjusting) the voltage or current of the PV system and observing the resulting change in power as shown in figure (**3.1**) [73]. Based on this observation, the algorithm decides whether to increase or decrease the voltage or current in the next step.

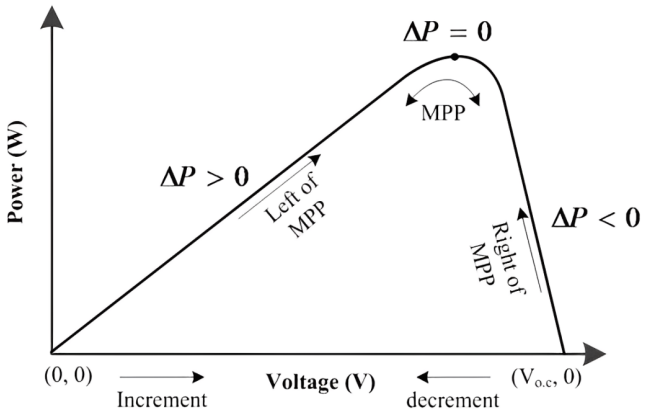

Figure 3.1 : Conventional *P&O* MPPT technique

3.2.2 P&O Algorithm for MPPT

In *P&O* method, the MPPT algorithm is based on the following steps [74] :

Step 1 : Initialization

- Measure the initial voltage and current of the PV module.
- Calculate the initial power based on these measurements.

Step 2 : Introduce perturbation

- Introduce a minor perturbation to cause the power variation of the PV module.

Step 3 : Measure and Compare Power

- Periodically measure the PV output power.
- Compare the measured power with the previous power.

Step 4 : Decision Making

- If the output power increases : Continue the same process.
- If the output power decreases : Reverse the perturbation direction.

Step 5 : Voltage Adjustment

- If an increase in voltage leads to an increase in power, the operating point of the PV module is on the left of the MPP. Hence, further perturbation is required towards the right to reach the MPP.
- If an increase in voltage leads to a decrease in power, the operating point of the PV module is on the right of the MPP. Hence, further perturbation towards the left is required to reach the MPP.

Step 6 : Repeat Process

- Continuously repeat the process to track the maximum power point.

The flow chart of the adopted *P&O* algorithm for the charge controller is given in figure (3.2) below :

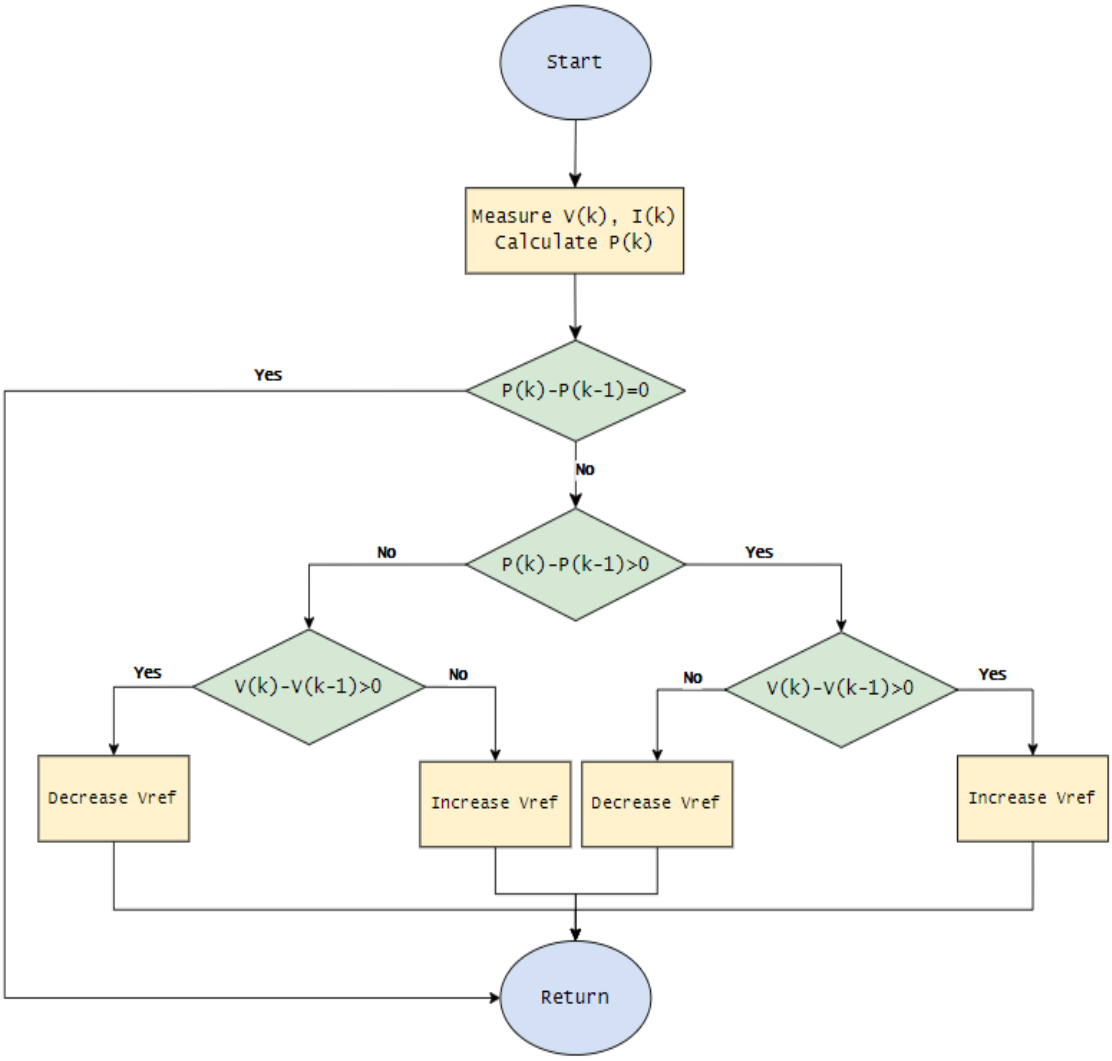

Figure 3.2 : Flowchart of the conventional *P&O* MPPT algorithm.

3.2.3 Simulation Setup

To validate the proposed MPPT algorithm model, a simulation of the PV module together with a boost converter is performed, as illustrated in figure (3.3) The concept involves controlling the switching operation of the boost converter through the proposed MPPT algorithm. The duty cycle value varies based on the perturbations in current and voltage from the PV cells. This dynamic adjustment ensures the system consistently operates at or near the maximum power point (MPP).

The boost converter is designed to step up the output voltage to meet the load requirements. Detailed information on the design of the boost converter can be found in chapter **2**, section **2.3**.

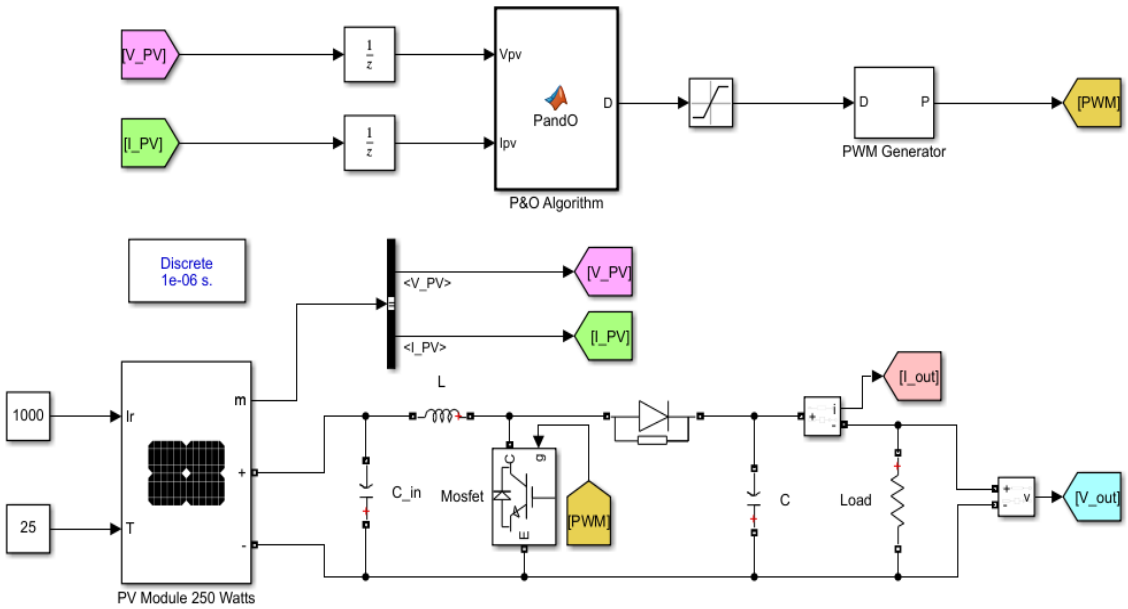

Figure 3.3 : Simulation setup of the PV module using P&O controller.

3.2.4 Simulation Results

The simulation results obtained from the Perturb and Observe (P&O) method for tracking maximum voltage (3.4), current (3.5), and power (3.6) of the PV module are represented below. These simulations were conducted using the Simulink model detailed in the previous section. The primary objective of these simulations is to test the performance of the P&O method in accurately tracking and maintaining maximum power output, current, and voltage levels when connected to the 1Soltech 250 WH PV panel at STC (Standard Test Conditions).

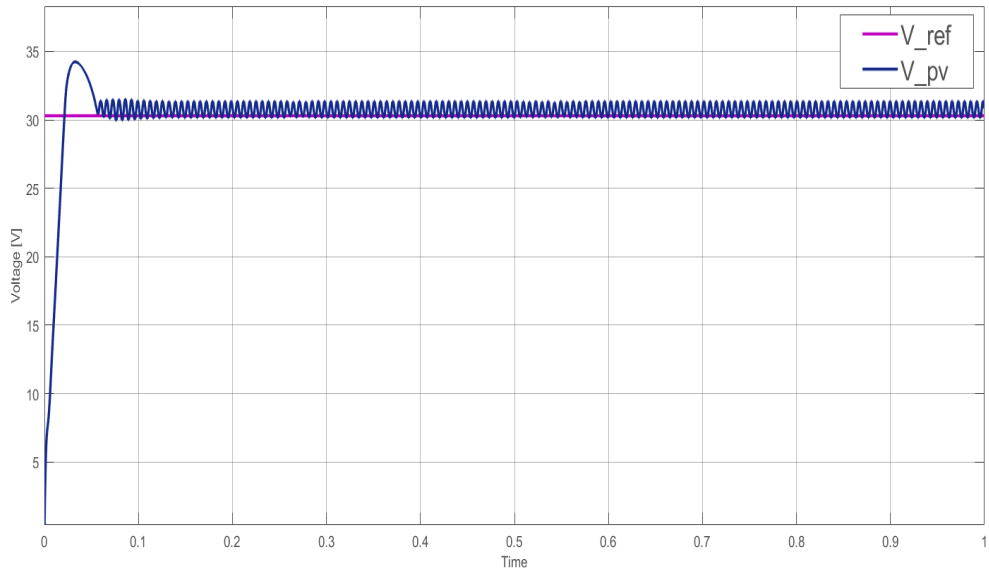

Figure 3.4 : Maximum voltage tracking using P&O.

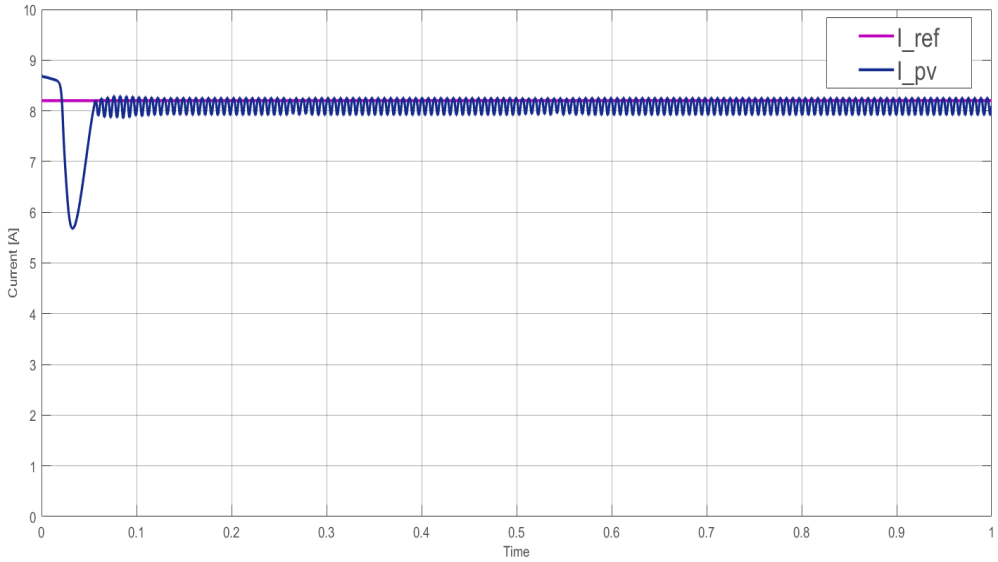

Figure 3.5 : Maximum current tracking using P&O.

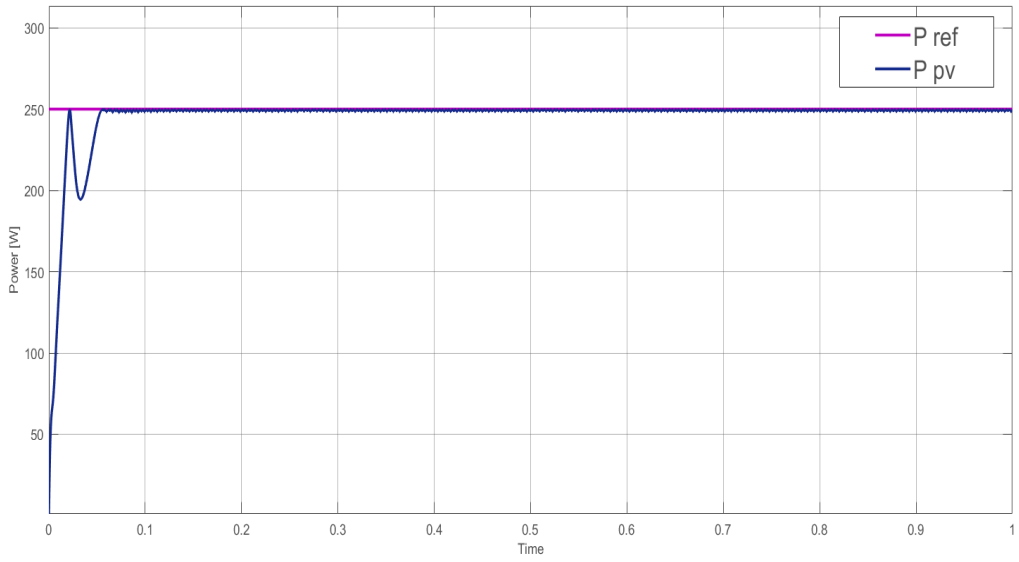

Figure 3.6 : Maximum power tracking using P&O.

3.2.5 Results Analysis

- We observe a consistent tracking of power, voltage, and current references as illustrated in figures (3.6), (3.4) and (3.5).

- We can notice a considerable perturbations around the MPP. These continuous oscillations caused by the method's algorithm cause energy losses.

- The efficiency of the P&O method was evaluated by considering its ability to accurately track the MPP and the energy losses caused by perturbations. While the method achieved good MPP tracking, the energy losses from perturbations decreases the overall efficiency.

3.3 Fuzzy Logic Controller

Conventional methods of tracking the optimal operating point, such as Perturb and Observe (P&O), have shown limitations, particularly in managing oscillations around the Maximum Power Point (MPP). These oscillations result in power loss and reduced efficiency, especially under rapidly changing environmental conditions.

To overcome these limitations, a Fuzzy Logic-based MPPT controller provides a robust and adaptive solution. Utilizing Artificial Intelligence through fuzzy logic improves control performance and enables the controller to effectively track the maximum power point by designing a fuzzy logic-based model [75].

Unlike convential approaches, Fuzzy Logic controllers do not require a precise mathematical model and may successfully handle PV systems' nonlinear features. Fuzzy Logic MPPT, which uses linguistic variables and a rule-based approach, can reduce oscillations while improving the overall performance and stability of the PV system under shifting irradiance and temperature circumstances.

3.3.1 Fuzzy Logic Control Principle

Fuzzy control is an approach that enables the development of nonlinear controllers using heuristic information derived from expert knowledge.

Figure (3.7) [76] shows the block diagram of a fuzzy controller. The fuzzification block processes input signals and assigns them a fuzzy value. The collection of rules is based on process knowledge and allows for the control of variables using a linguistic description. The inference mechanism interprets the data based on the rules and their membership functions. The defuzzification block converts fuzzy information from the inference method into non-fuzzy information, enabling the control process [76].

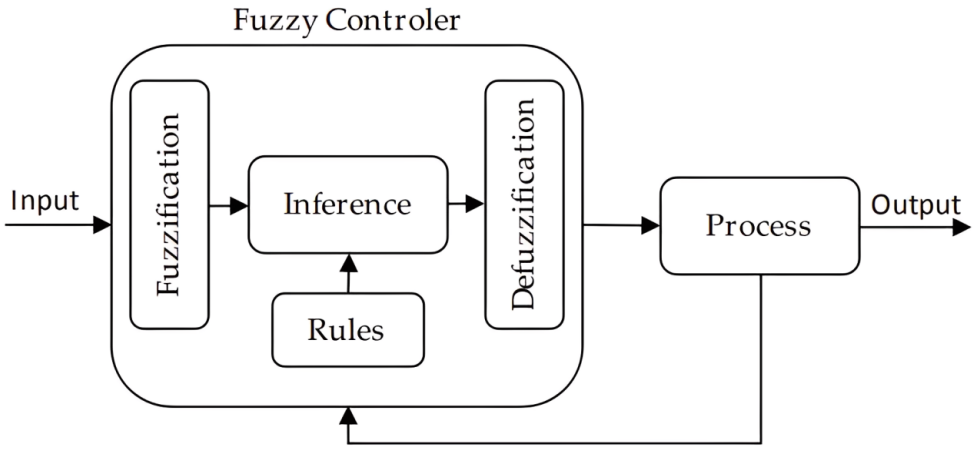

Figure 3.7 : Block diagram for a fuzzy controller

3.3.2 Fuzzy Logic Controller Design

Based on the fuzzy diagram above, a fuzzy controller with two inputs and one output was designed. The two input variables are Error (E) and Change of Error (CE), which are shown in Equations 3.1 and 3.2 for sample times k [76].

$$E(k) = \frac{P(k) - P(k-1)}{V(k) - V(k-1)} = \frac{\Delta P}{\Delta V} \tag{3.1}$$

$$CE(k) = E(k) - E(k-1) = \Delta E \tag{3.2}$$

The input E(k) represents the slope of the $P-V$ curve and determines the position of the MPP in the PV module. The CE(k) input indicates whether the operating point moves in the MPP direction or not. The output variable is the increment in duty cycle (ΔD), which might be positive or negative depending on the location of the operating point. This output is supplied to the dc-dc converter, which drives the load. The controller's value of ΔD was used to create an accumulator and calculate the duty cycle. [76]. See Equation 3.3.

$$D(k) = D(k-1) + \Delta D(k) \tag{3.3}$$

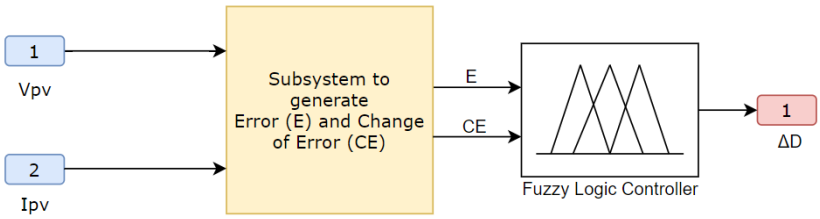

Figure 3.8 : Input processing for fuzzy logic controller

The internal functioning of a fuzzy controller is based on the structure presented in Figure **3.9** which includes three main blocks : Fuzzification, Fuzzy Inference and Defuzzification.

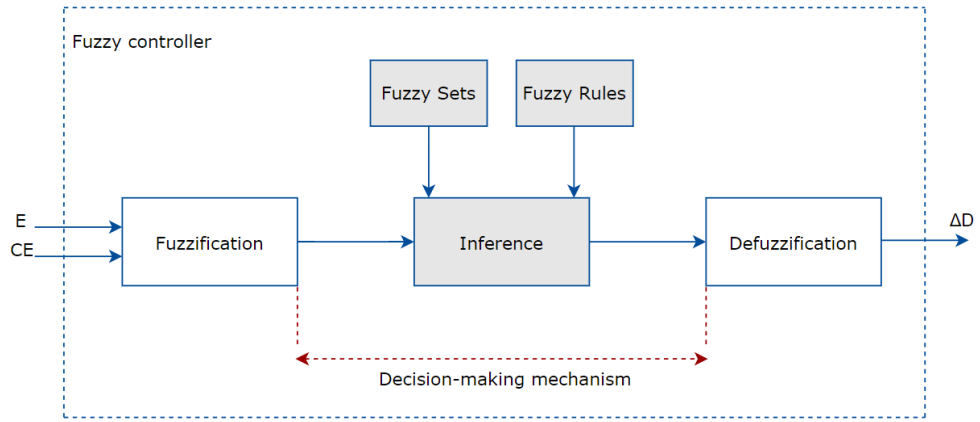

Figure 3.9 : The synoptic diagram of a fuzzy controller

3.3.2.1 Fuzzification

FLC works as a black box, hence the initialization of correct input and output variables with the suitable membership function is a must [77].

Triangular membership functions for the fuzzification process were used. For the inputs E, CE and for the output ΔD, 7 membership functions were defined in terms of the following linguistic variables: Negative Big (NB), Negative Medium (NM), Negative Small (NS), Zero (ZE), Positive Small (PS), Positive Medium (PM) and Positive Big (PB) [78]. The range for the error is (-50 to 50), for the change of error is (-10 to 10) and for the increment in duty cycle is (-0.1 to 0.1).

This MPPT approach uses Mamdani[1] Fuzzy Inference System (FIS) toolbox of fuzzy logic. [76]. Figure **3.10** shows the membership functions for the inputs and outputs of the controller :

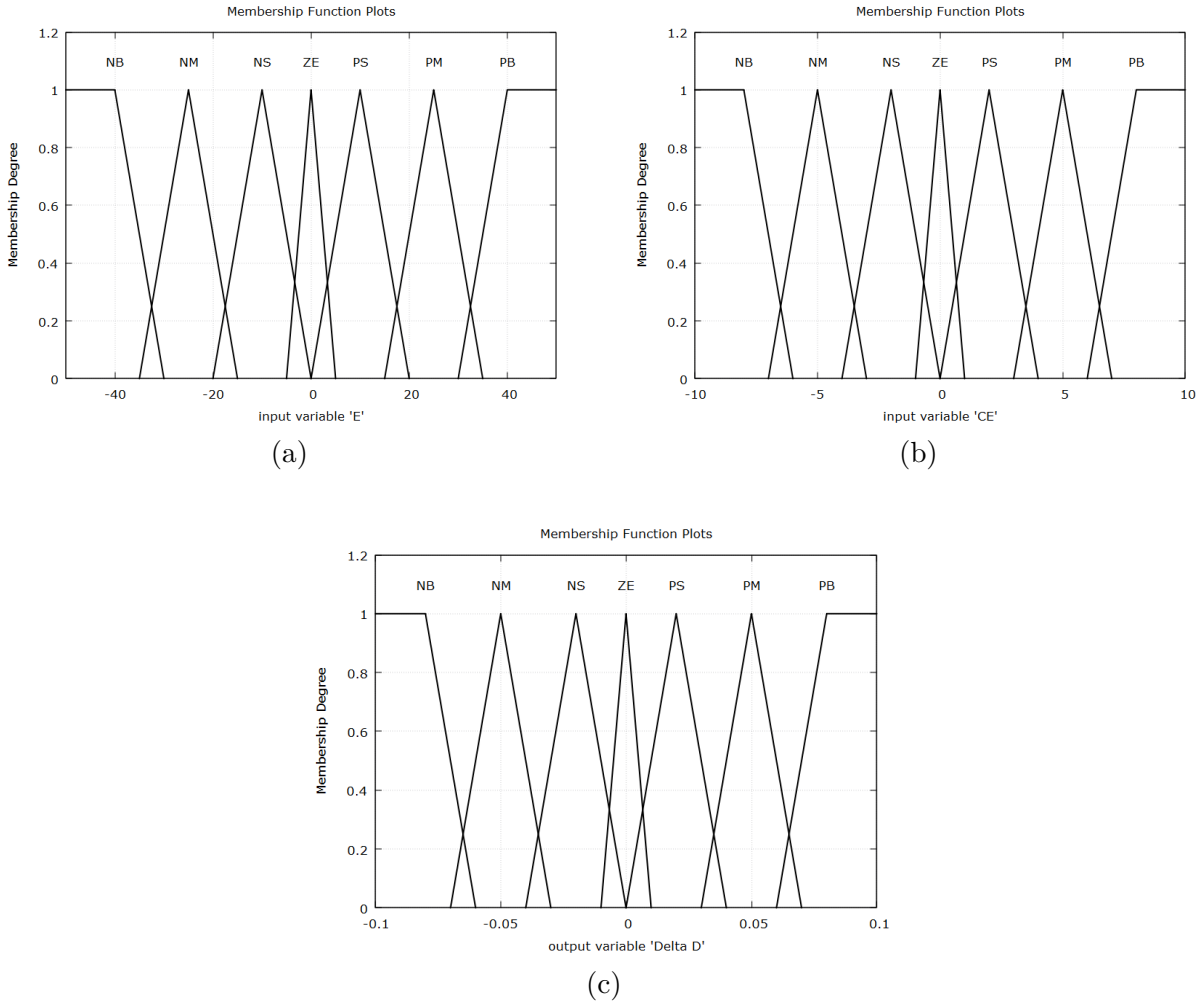

Figure 3.10 : Membership functions of the fuzzy controller : (a) : input variable E , (b) : iput variable CE , (c) : output variable Delta D

[1]**Mamdani FIS :** Mamdani fuzzy inference was first introduced as a method to create a control system by synthesizing a set of linguistic control rules obtained from experienced human operators. In a Mamdani system, the output of each rule is a fuzzy set.

3.3.2.2 Fuzzy Inference System

For the rule settings of fuzzy logic MPPT, different number of subset has been used. But for this work, seven subset based forty-nine rules have been used. Tuning forty-nine rules takes a long time, but it results in higher accuracy and dynamic reaction [78]. Table **3.1** represents the fuzzy rules.

E				CE			
	NB	NM	NS	ZE	PS	PM	PB
NB	ZE	ZE	ZE	NB	NB	NB	NB
NM	ZE	ZE	ZE	NM	NM	NM	NM
NS	NS	ZE	ZE	NS	NS	NS	NS
ZE	NM	NS	ZE	ZE	ZE	PS	PM
PS	PM	PS	PS	PS	ZE	ZE	ZE
PM	PM	PM	PM	ZE	ZE	ZE	ZE
PB	PB	PB	PB	ZE	ZE	ZE	ZE

Table 3.1 : The forty-nine fuzzy rules of the fuzzy system

3.3.2.3 Defuzzification

The defuzzification process involves converting fuzzy sets of inputs (E and CE) into a crisp output value (ΔD). In the Mamdani Fuzzy Inference System (FIS) used for maximum power point tracking (MPPT) in photovoltaic systems, the centroid method is commonly employed to calculate this crisp output, represented as ΔD, which determines the adjustment to the duty cycle.
The centroid is computed using the formula **3.4** :

$$\Delta D = \frac{\int \mu(x) \cdot x dx}{\int \mu(x) dx} \tag{3.4}$$

ΔD : The defuzzified output value, representing the change in duty cycle.
x : The variable corresponding to the duty cycle
$\mu(x)$: The membership function of the output fuzzy set.

3.3.3 Simulation Setup

The controller was modeled with the Matlab Fuzzy Logic Toolbox. A Mamdani controller with the centroid defuzzification method was used. This procedure was carried out using the fuzzy inference system editor (FIS editor).

Figure (3.11) shows the controller modeled in Simulink, for which a subsystem was performed to calculate the inputs E and CE.

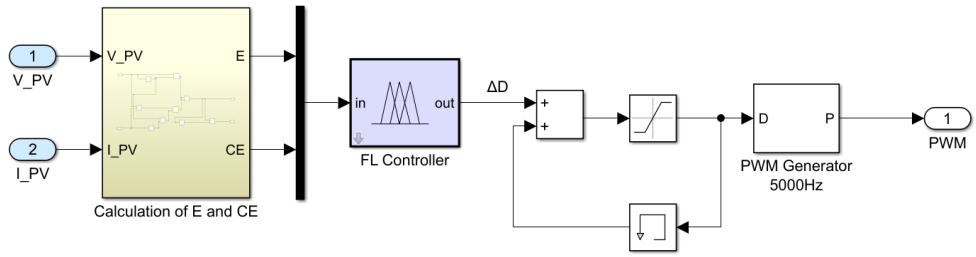

Figure 3.11 : Implementation of fuzzy logic controller in Simulink

3.3.4 Simulation Results

The simulation results obtained from the Fuzzy Logic Control (FLC) method for tracking maximum voltage 3.12, current 3.13, and power 3.14 of the PV module are illustrated below. These simulations were performed using the Simulink model described earlier. The primary focus of these simulations was to evaluate the performance of the FLC method in effectively tracking and regulating maximum power output, current, and voltage levels when connected to the 1Soltech 250 WH PV panel under STC.

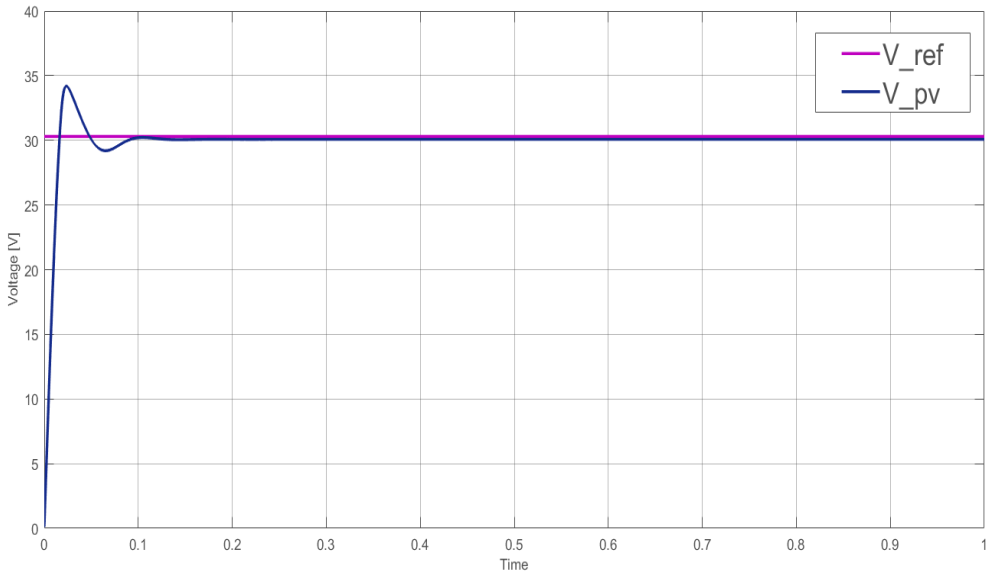

Figure 3.12 : Maximum voltage tracking using FLC.

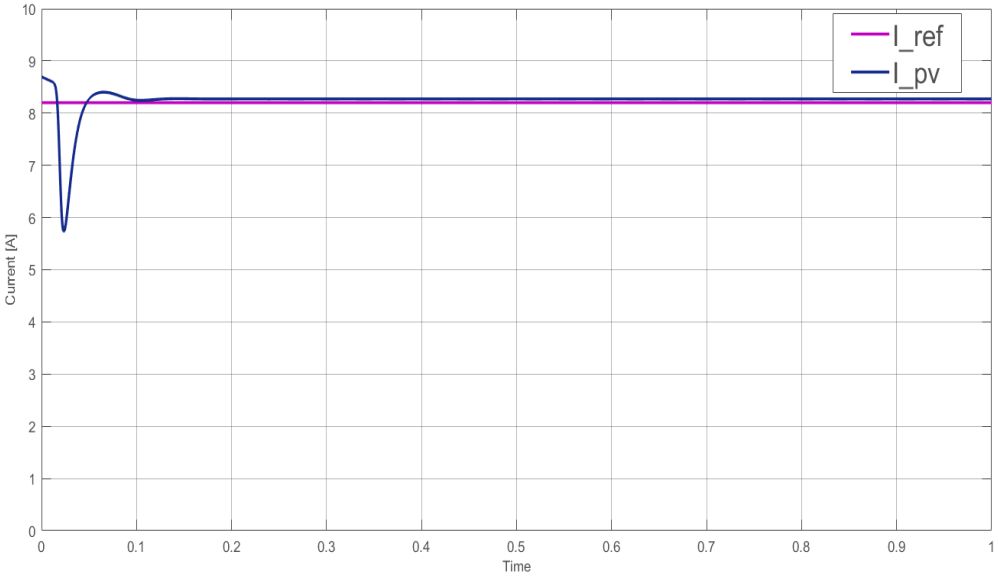

Figure 3.13 : Maximum current tracking using FLC.

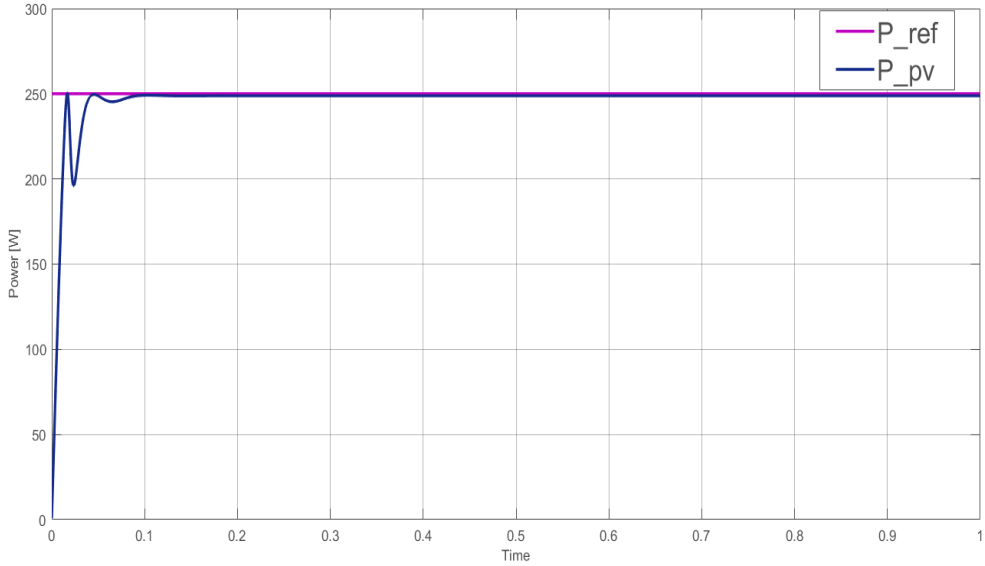

Figure 3.14 : Maximum power tracking using FLC.

3.4 Results Analysis

- We notice that the FLC-based MPPT system has faster tracking speed compared to the classical P&O method. It achieves high tracking accuracy, minimizes tracking error and ensures the PV system operates close to its optimal power output as shown in figure (3.14).

- It can be seen that the tracking results provided by the FLC are stable without considerable oscillations around the MPP. It conducts to a decrease in energy losses.

- The accuracy in tracking the MPP and stability around the MPP of the FLC prove its high performance.

3.5 Particle Swarm Optimization (PSO) Controller

Kennedy and Eberhart introduced the PSO method in 1995, which optimizes multivariable functions with many local optimal points. The PSO algorithm was developed based on observations of natural social behavior, including bird flocking and fish schooling. The PSO stands out from other global optimization approaches due to its ease of implementation and fast convergence. Researchers are increasingly exploring the usage of PSO in PV systems alongside MPPT [79].

3.5.1 PSO Control Principle

The PSO consists of a swarm of particles, each of which provides a possible solution to the optimization issue. The goal behind it is to emulate the success of other particles. In other words, the location of a particle is modified by the agent's position recommending the best solution through the current particle, $P_{best,i}$, and the best solution recommended through the entire population, G_{best}.

Particle position x_i is adjusted using equation (3.5) [80] :

$$x_i^{k+1} = x_i^k + v_i^{k+1} \tag{3.5}$$

Where the velocity component v_i represents the step size and is calculated using equation (3.6) [80] :

$$v_i^{k+1} = \omega v_i^k + c_1 r_1 \left(P_{best,i} - x_i^k\right) + c_2 r_2 \left(G_{best} - x_i^k\right) \tag{3.6}$$

ω : The inertial weight.
c_1 : Cognitive acceleration coefficient.
c_2 : Social acceleration coefficient.
r_1, r_2 : Random values uniformly distributed within the interval $[0, 1]$.
$P_{best,i}$: Individual best position of particle i.
G_{best} : Global best position for the swarm.

If the initialization condition (3.8) is satisfied, the method is updated according to (3.7) :

$$P_{best,i} = x_i^k \tag{3.7}$$

$$f\left(x_i^k\right) > f\left(P_{best,i}\right) \tag{3.8}$$

Where f represents the objective function that should be maximized [79].

The operating principles of a basic PSO method can be described as follows:

Step 1 (PSO Initialization) : Particles are often initialized randomly across the search space, or on grid nodes with equidistant locations. The initial velocity is chosen randomly.

Step 2 (Fitness Evaluation) : Evaluate the fitness value of each particle. Fitness evaluation is conducted by supplying the candidate solution to the objective function.

Step 3 (Update Individual and Global Best Data) : The best fitness values (pbest, i, and gbest) and locations are updated by comparing new values to prior ones and replacing them as needed.

Step 4 (Update Velocity and Position of Each Particle) : The position and velocity of each particle in the swarm are updated using (3.5) and (3.6).

Step 5 (Convergence Determination) : Check the convergence criterion. If the convergence criterion is met, the process can be terminated; otherwise, the iteration number will increase by 1 and goto step 2.

3.5.2 PSO Algorithm for MPPT

In the proposed system, the particle position is defined as the duty cycle value d of the DC–DC converter, and the fitness value evaluation function is chosen as the generated power P_{pv}, as demonstrated in equation (3.12), (3.9) respectively.

The purpose of the optimisation process is the maximisation of power extracted from the PV panel, which is defined to be the objective function(P). The fitness value evaluation function is defined as :

$$P\left(d_i^k\right) > P\left(d_i^{k-1}\right) \tag{3.9}$$

Update Individual and Global Best Duty Cycle

For each duty cycle d_i, the corresponding PV output power $P(d_i^k)$ is calculated by multiplying the measured voltage (V_{PVi}) and current (I_{PVi}). Then, the algorithm proceeds to check whether this duty cycle value will result in a better individual fitness value (compared to old $P_{best,i}$) (3.10). In such case, the personal best position ($d_{best,i}$) (3.11), as well as its corresponding best individual fitness value $P_{best,i}$, are updated; otherwise, $P_{best,i}$ retains its present value. The global best duty cycle, d_{best}, is determined by comparing fitness values of the actual population with the global best PV power achieved, P_{best}.

$$P\left(d_i^k\right) > P\left(d_{best,i}\right) \tag{3.10}$$

If it's satisfied then :

$$d_{best,i} = d_i^k \tag{3.11}$$

Where $d_{best,i}$ is the personal best position of particle i.

Update Velocity and Position of Each Particle

After the evaluation process, velocity and position of each particle in the swarm are updated. The new duty cycles are then calculated for each iteration by the equations:

$$d_i^{k+1} = d_i^K + v_i^{k+1} \tag{3.12}$$

$$v_i^{k+1} = \omega v_i^k + c_1 r_1 \left(d_{best,i} - d_i^k\right) + c_2 r_2 \left(d_{best} - d_i^k\right) \tag{3.13}$$

Figure (3.15) shows the flowchart of the proposed PSO-based MPPT technique :

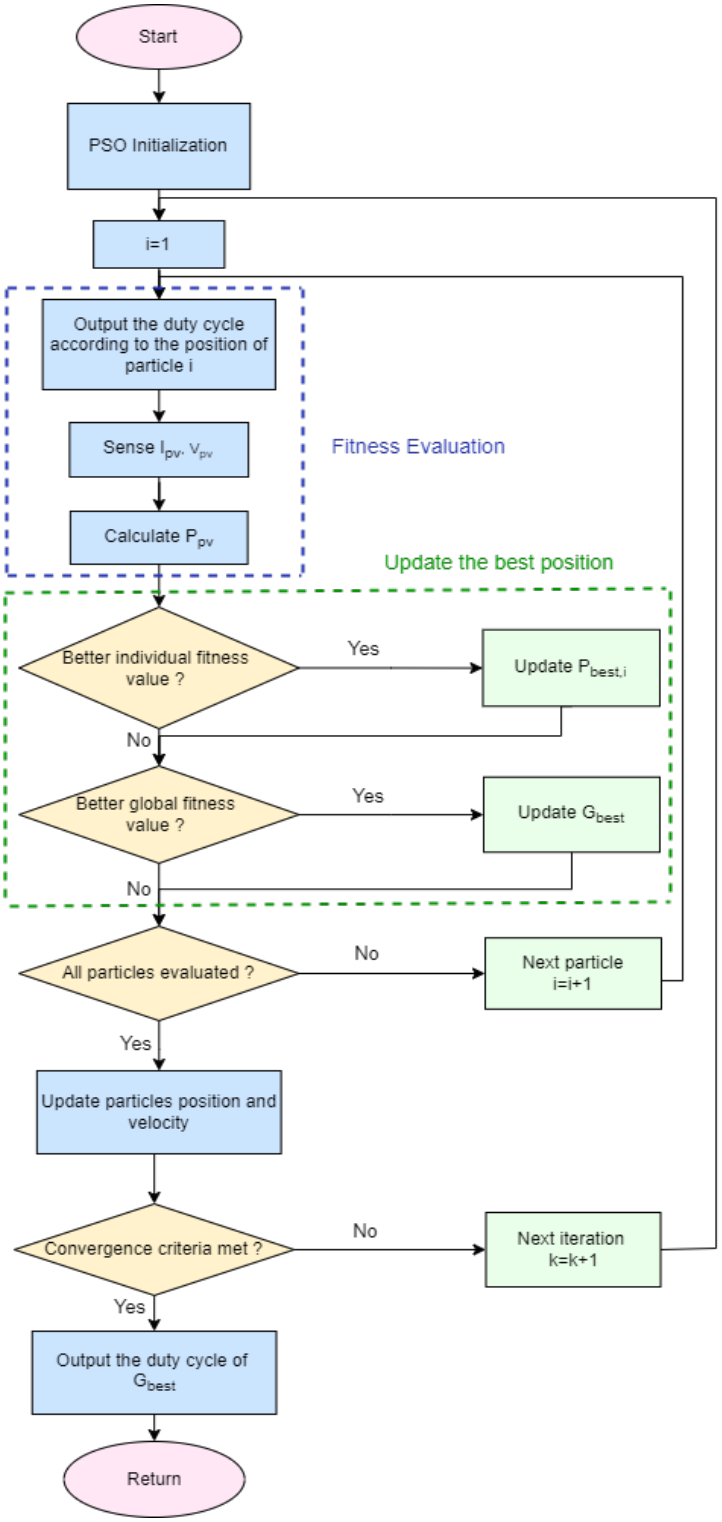

Figure 3.15 : Flowchart of the proposed PSO-based MPPT algorithm.

3.5.3 Simulation Setup

To validate the proposed MPPT algorithm model using PSO, a simulation of the PV module together with a boost converter is performed, as illustrated in figure (3.16). The concept involves controlling the switching operation of the boost converter through the proposed PSO-based MPPT algorithm. The duty cycle value is optimized based on the particle swarm optimization technique.

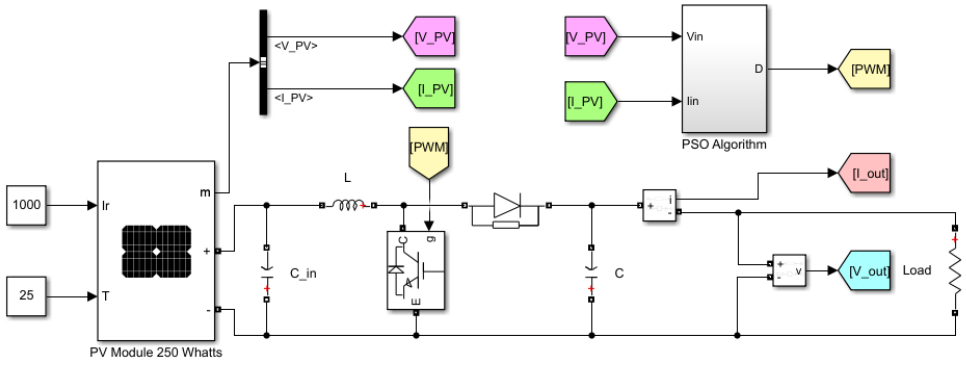

Figure 3.16 : Simulation setup of the PV module using PSO algorithm

3.5.4 Simulation Results

The simulation results obtained from the Particle Swarm Optimization (PSO) method for tracking maximum voltage (3.17), current (3.18), and power (3.19) of the PV module are presented below. These simulations were performed using the previous Simulink model. The main objective of these simulations was to assess the performance of the PSO method in accurately tracking and optimizing maximum power output, current, and voltage levels when connected to the 1Soltech 250 WH PV panel at STC conditions.

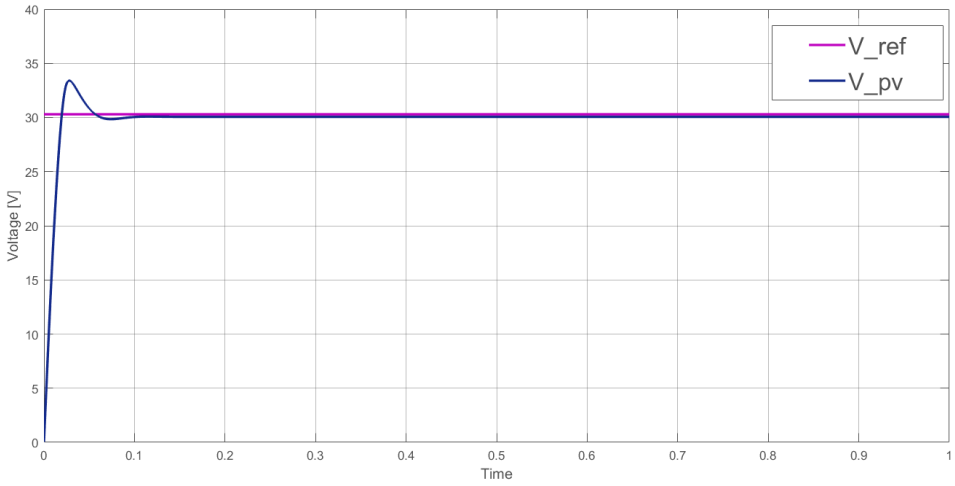

Figure 3.17 : Maximum voltage tracking using PSO.

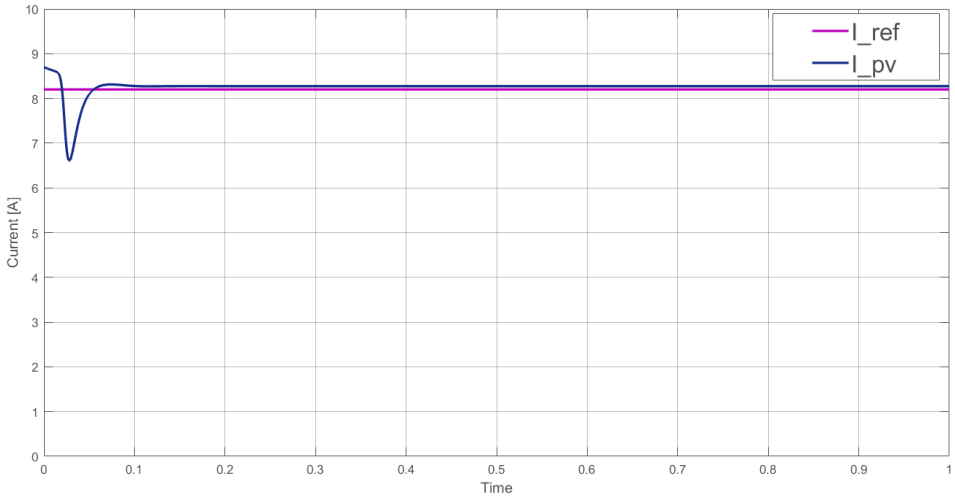

Figure 3.18 : Maximum current tracking using PSO.

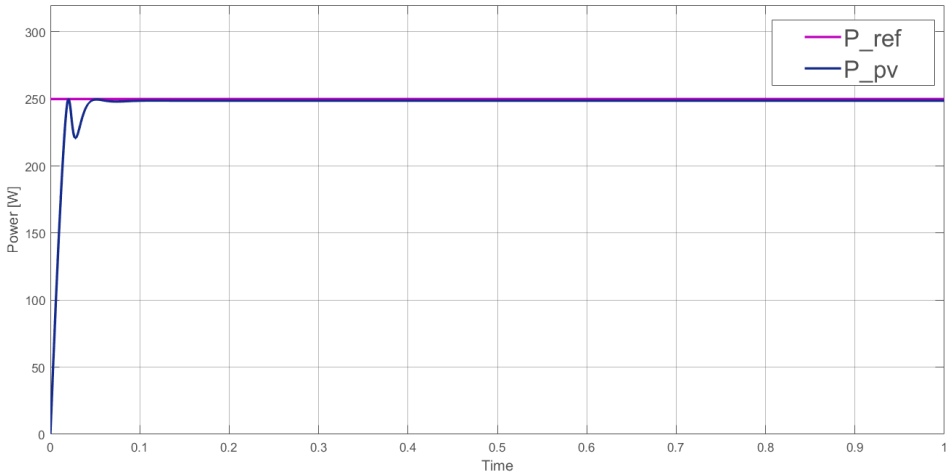

Figure 3.19 : Maximum power tracking using PSO.

3.5.5 Results Analysis

- We notice that the PSO algorithm has fast tracking speed. It achieves high tracking accuracy, minimizes tracking error and ensures the PV system operates consistently close to its optimal power output as shown in figure 3.19.
- The tracking voltage, current and power provided by the PSO controller show stability in tracking the MPP minimizing oscillations and perturbations around it, which reduce the energy losses.
- The PSO method's ability to track the MPP accurately without oscillations enhances overall energy efficiency.

3.6 Comparative Study of Control Methods

In photovoltaic (PV) systems, the efficiency of power conversion depends on the control methods used for Maximum Power Point Tracking (MPPT). This section provides a

comparison between three different MPPT control methods: the conventional Perturb and Observe (P&O) method, the Artificial Intelligence-based Fuzzy Logic (FL) method, and the bio-inspired Particle Swarm Optimization (PSO) method as illustrated in figure (3.20). By analyzing their convergence and stability, we aim to identify the most effective approach for optimizing PV system performance under varying environmental conditions.

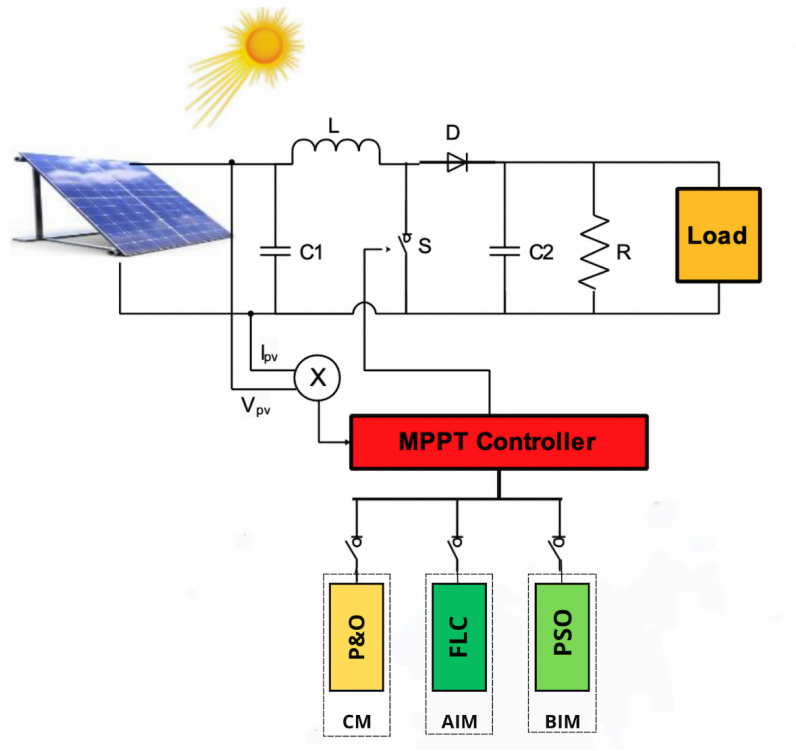

Figure 3.20 : Simulation setup with MPPT techniques P&O, FL and PSO

3.6.1 Performance Analysis

Based on the results obtained by P&O algorithm **(3.2)**, FL based MPPT **(3.3)** and PSO algorithm **(3.5)** ; we summarize their performances in Table **3.2** below :

MPPT Technique	Tracking Time (seconds)	Efficiency (%)
P&O	0.06	98.34
FL	0.05	99.05
PSO	0.05	99.03

Table 3.2 : Performance Comparison between P&O, FL, and PSO Based MPPT Techniques

$$Efficiency(\%) = \frac{\int P_{pv}}{\int P_{ref}} \times 100 \tag{3.14}$$

3.6.2 Robustness to Parameters Changes

Figures (3.22), (3.23) and (3.24) show the simulation results for the response of three methods under varying irradiance :

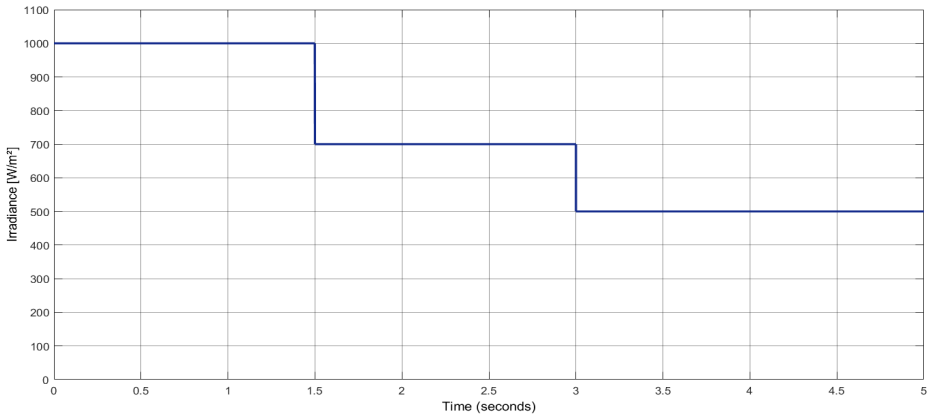

Figure 3.21 : Variation of irradiance

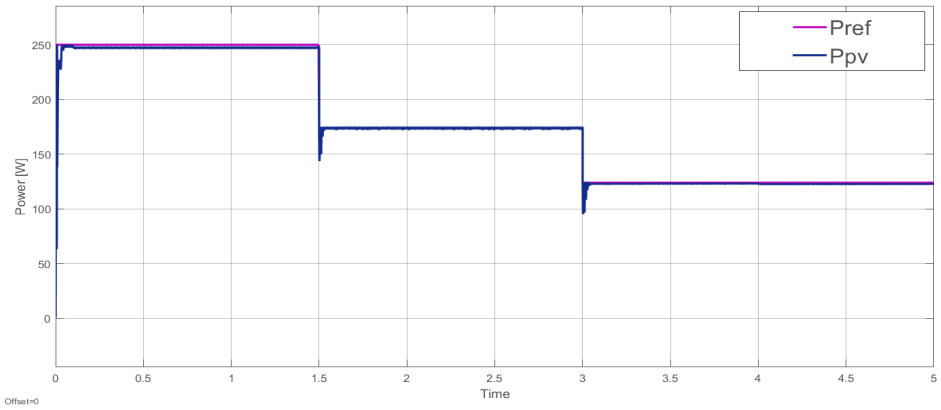

Figure 3.22 : MPP tracking using P&O under varying irradiance

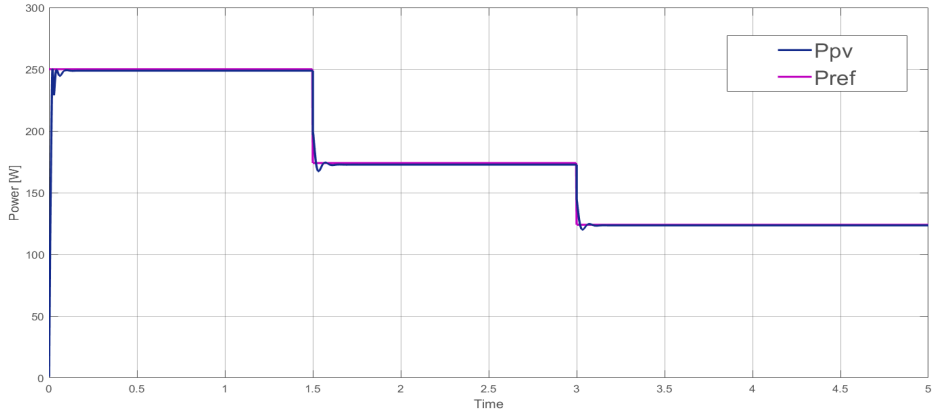

Figure 3.23 : MPP tracking using FLC under varying irradiance

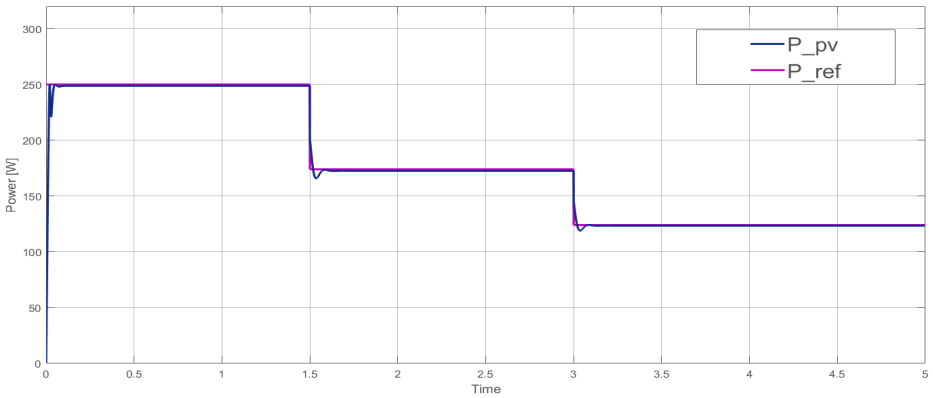

Figure 3.24 : MPP tracking using PSO under varying irradiance

3.6.3 Results Discussion

- We notice that both FLC and PSO track the MPP faster and they are more efficient than P&O. This means they adjust quickly to changes and keep the power output at its maximum.

- FLC and PSO show better performance at varying irradiances compared to P&O. Their robustness in adapting to dynamic changes in solar irradiance levels contributes to stable and efficient operation across different environmental conditions.

- However, we can see that P&O can have big fluctuations, especially when environmental conditions change quickly, which can affect the system's stability and performance.

- P&O is simple and easy to use, making it a popular choice for basic MPPT tasks. Its simple algorithm and low computing needs make it cost-effective.

- FLC and PSO, while offering best performance in terms of tracking efficiency and robustness, may require more complex implementation procedures. FLC involves designing and tuning fuzzy logic rules and membership functions, while PSO involves parameter optimization and algorithmic adjustments.

3.7 Conclusion

To improve the performance of photovoltaic (PV) systems, various methods have been used to track the Maximum Power Point (MPP), including conventional, intelligent, and bio-inspired techniques. This chapter coveres the most used MPPT methods in PV systems, such as the Perturbation and Observation (P&O) method, the fuzzy logic (FL) based method, and the PSO-based method. The simulation results proved that fuzzy logic and PSO-based MPPT controllers perform better than conventional MPPT methods like P&O. In terms of stability, precision, and speed in tracking the MPP, both the fuzzy logic and PSO controllers demonstrate better performance. These results highlight the potential of intelligent and bio-inspired MPPT techniques to optimize the efficiency of PV systems under diverse environmental conditions.

Chapter 4

Storage and Energy Management in Standalone PV Systems

4.1 Introduction

Power and energy management are key issues in performance improvement and reliability enhancement of stand-alone photovoltaic (PV) systems. Solar power is intermittent based on the sunlight, but this does not eliminate the need to supplies constant energy when sun is not present; night or cannot shine though cloudy rainy days and winter when day has a shorter period. These systems also guarantee a good utilization of the energy stored and overall efficiency gain by using right energy management strategies in stand-alone PV system.

If energy storage and utilization are properly handled then these systems can generate power 24/7 in each corner of the world where grid is not available or during grid failure. Energy storage and management, meanwhile, can help protect batteries as well as other system components against faults like overcharging or deep discharging.

This chapter provides a detailed analysis of energy storage in standalone photovoltaic (PV) systems, specifically addressing the control mechanisms involved in charging and discharging batteries using bidirectional converters. It also details an application of an energy management system to properly balance between peak load demand fulfillment and battery safeguarding.

4.2 Energy Storage

Energy storage is an important component in many photovoltaic (PV) systems, particularly stand-alone systems that are not connected to the electrical grid also known as off-grid, PV systems. The most common form of storage in PV systems is chemical storage in the form of batteries.

The choice of battery technology will depend on the investment cost, the lifetime of the batteries under the operating conditions corresponding to the chosen application, and the storage capacity. There are three main types of battery technologies that pair with residential solar systems: Lead acid batteries. Lithium ion batteries. Nickel based batteries.

In stand solar power systems batteries are important in storing electricity generated from solar energy, for nighttime use or during emergencies when sunlight is not available. They are essential because the output, from PV panels or arrays can vary and they convert energy into energy for later use when solar power is not being generated.

A bi directional DC DC converter enables power to move in both directions to charge and discharge batteries. The converters duty cycle manages this process by determining whether to charge or discharge based on the battery's charge level and the current flow direction [81].

4.3 Design of Bidirectional Converter

This section introduces a non-isolated bidirectional buck-boost DC–DC converter design meant for battery charging and discharging. This design utilizes just one energy storage element, which is the inductor, and incorporates two bidirectional switches, such as MOSFETs or IGBTs, to enable the necessary bidirectional power flow [82].

Figure (4.1) shows the non-isolated bidirectional DC-DC converters selected in our project. When charging the battery, it functions as a buck converter. Conversely, during discharge, it operates as a boost converter.

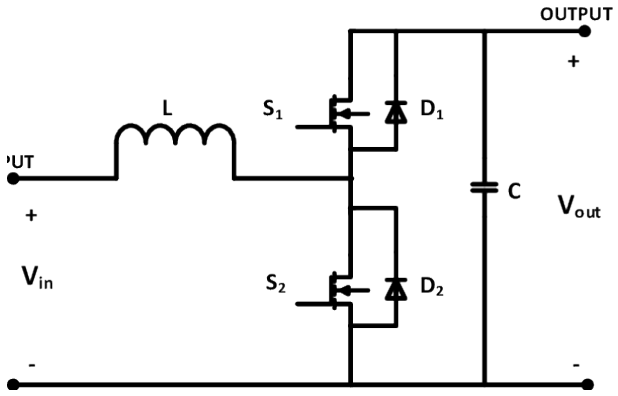

Figure 4.1 : Bidirectional buck-boost converter diagram

4.3.1 Buck Mode : Battery Charging

To charge the battery from the DC grid, switch S1 is triggered while switch S2 is kept off. When S1 is turned on, the input current rises and flows through S1 and inductor L. As S1 turns off, the current in the inductor decreases until the next cycle, supplying the energy stored in inductor L for charging the battery [82].

While battery's charging, the converter parameters are designed as follows[82] :

- **Duty Cycle**

$$D = \frac{V_{out}}{V_{in}} \tag{4.1}$$

- **Selection of Inductor**

$$L = \frac{D \cdot (V_{in} - Vout)}{f_s \Delta I_L} \tag{4.2}$$

- **Selection of Output Capacitor**

$$C = \frac{(1 - D) \cdot V_{out}}{8 \cdot L \cdot f_s^2 \cdot \Delta V_{out}} \tag{4.3}$$

V_{in} : DC bus voltage (input voltage)
V_{out} : Battery voltage (output voltage)
f_s : Switching frequency.
ΔI_L : The inductor ripple current is taken as 10% to 20% of the output current
ΔV_{out} : Output voltage ripple. It's generally taken as 10% of the output voltage.

4.3.2 Boost Mode : Battery Discharging

During Boost mode, the output voltage exceeds the input voltage. To discharge power to the load, switch S2 is activated while S1 is turned off. When S2 is on, the input current rises through inductor L and S2. As S2 turns off, the current in the inductor decreases until the next cycle, allowing the energy stored in inductor L to flow through the load [82].

While battery's discharging, the converter parameters are designed as follows[82] :

- **Duty Cycle**

$$D = 1 - \frac{V_{in}}{V_{out}} \tag{4.4}$$

- **Selection of Inductor**

$$L = \frac{D \cdot V_{in}}{f_s \Delta I_L} \tag{4.5}$$

- **Selection of Output Capacitor**

$$C = \frac{D \cdot I_{L_{max}}}{f_s \Delta V_{out}} \tag{4.6}$$

V_{in} : Battery voltage (input voltage)
V_{out} : DC bus voltage (output voltage)
f_s : Switching frequency.
ΔI_L : The inductor ripple current is taken as 10% to 20% of the output current
ΔV_{out} : Output voltage ripple. It's generally taken as 10% of the output voltage.

4.4 Battery Control

The main objective of this control system is to stabilize the DC bus voltage. To achieve this the bidirectional buck boost converter adjusts the DC bus voltage to maintain a power transfer, between the DC bus and the battery. As a result the converter is operated in a manner that keeps the DC bus voltage as solar conditions and load fluctuations occur.

Figure (4.2) shows the control strategy for the bidirectional buck-boost converter.

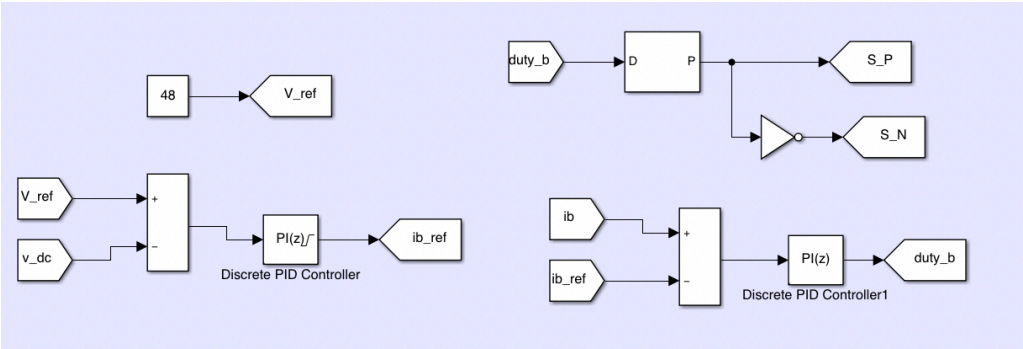

Figure 4.2 : Control strategy for bidirectional buck boost converter

The DC bus voltage (output voltage of boost converter) V_{dc} is compared to a desired reference voltage V_{ref} to get the error signal that is passed through the first PI controller

to produce the reference battery current, I_{bref}. Then, this reference current is compared with the sensed battery current, I_b to obtain an error signal that is passed through the second PI controller to obtain the control signal. The control signal is then compared with a carrier signal to obtain switching pulses. The control parameters that results to a constant DC bus voltage are listed in Table **4.1** :

Gain	K_p	K_i
Voltage loop	0.85	10
Current loop	1	1

Table 4.1 : Parameters of PI controller for the bidirectional converter

4.5 Energy Management System (EMS)

Management ensures correct operation and protection of the storage system. To accomplish this, we must examine the various potential cases, given the battery's state of charge and the power provided by the PV panel, and then propose the actions to be taken at each stage in order to optimize and ensure the chain's operation while also ensuring the storage system's maximum service life. This management system takes into account the battery state of charge (%) and PV power.

The main objectives of the energy management system are to :

- Ensure maximum power extraction from the PV arrays using maximum power point tracking (MPPT) techniques like incremental conductance or fuzzy control.

- Efficiently manage the charging and discharging of the battery bank to avoid overcharging or deep discharge.

- Control the power flow within the system components

4.5.1 The Proposed Energy Management Algorithm

The proposed algorithm proposed a robust battery management system designed to ensure that the battery's state of charge remains within the optimal limits of 20% to 80%. This management strategy prevents overcharging and deep discharging of the battery which might degrade battery life and enhance overall system performance. The different management modes are summarized in figure (4.3) below :

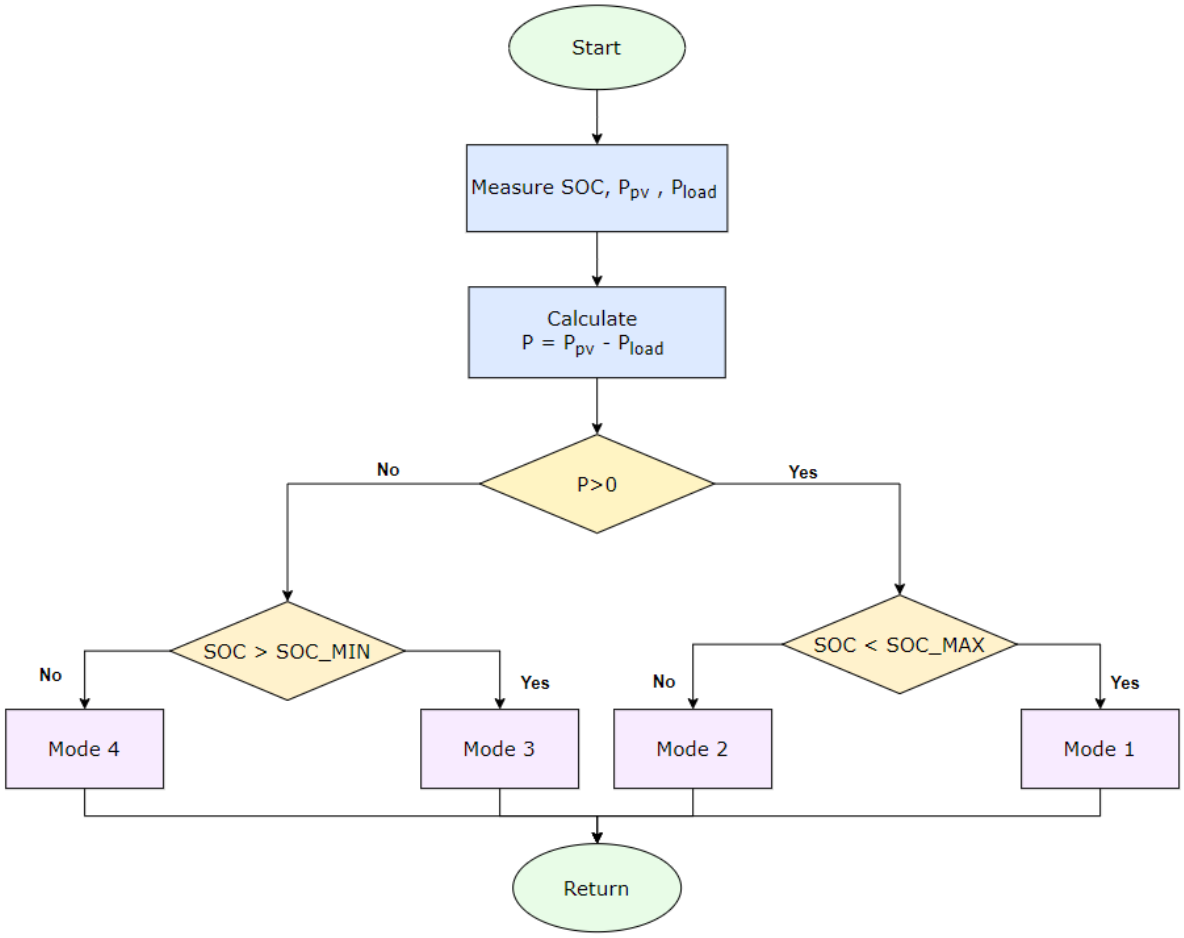

Figure 4.3 : Proposed energy management algorithm

The four management modes are described below :

- **Mode 1**
  The available power from PV source ($P_{av} \geq 0$) is sufficient to satisfy load demand and charge the batteries if $SOC < SOC_{max}$.

- **Mode 2**
  The power generated by PV source is sufficiently available and since batteries are charged to maximum level, they need to be disconnected to protect them. This is the power-limited operating mode.

- **Mode 3**
  The power supplied by the PV generator is insufficient ($0 < P_{pv} < P_{load}$) and ($SOC > SOC_{min}$); in this case, the power of batteries is added to satisfy the power demand. It's the compensation mode.

- **Mode 4**
  When the PV power is insufficient to supply the load and the batteries have been discharged to their minimum allowable level, the load must be disconnected.

4.5.2 Standalone System with Energy Management

Figure (5.4) shows the designed standalone system with energy management system. The different operating modes depend on the states of the three switches R1, R2 and R3.

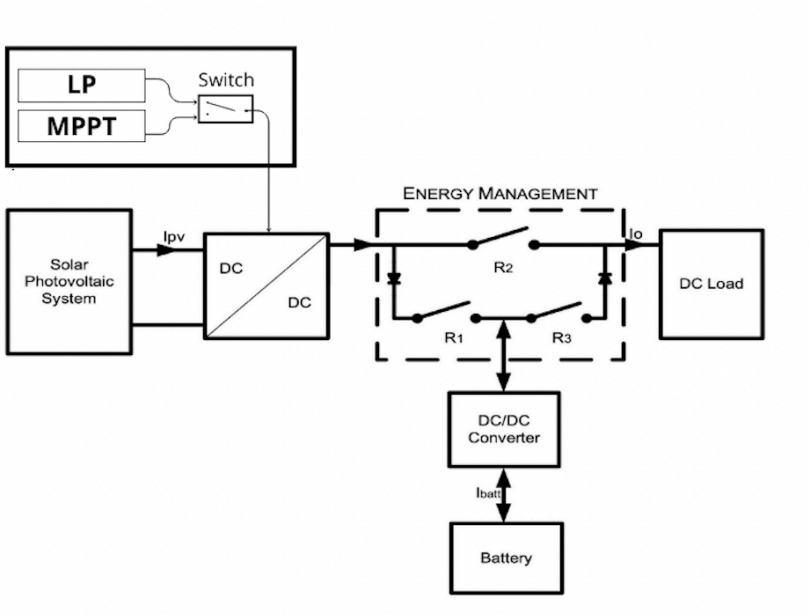

Figure 4.4 : Standalone PV system with energy management

Limited Power mode (LP)
By default, the PV operates in MPPT mode. However, if the power supplied by the PV exceeds the needed amount and the battery is completely charged (SOC greater than 80%), we need to limit the power generated by the PV by adding a PI controller for the DC bus voltage. This mode is called ”limited power mode”.

4.6 Simulation Setup

Our standalone PV system simulation features a 24V battery and a 48V, 500W resistive load. A bidirectional DC-DC converter manages battery charge/discharge, maintaining a 20-80% state of charge range to prevent over/undercharging. An Energy Management System (EMS) oversees power flow between PV array, battery, and load in real-time, adapting to varying meteorological conditions. The control algorithm ensures reliable load supply while safeguarding the battery.

4.7 Results and Analysis

4.7.1 Case 1 : $SOC_{min} < SOC_i$=50% $< SOC_{max}$

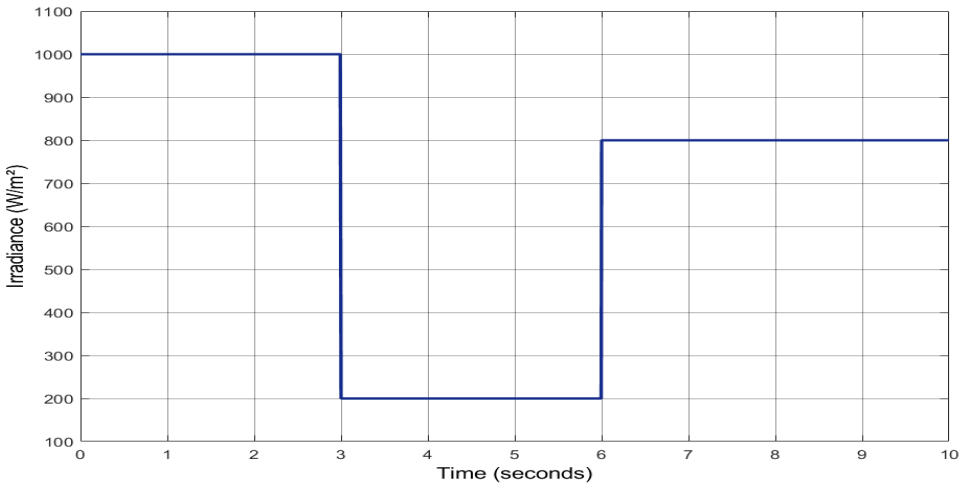

Figure 4.5 : Variation of irradiance

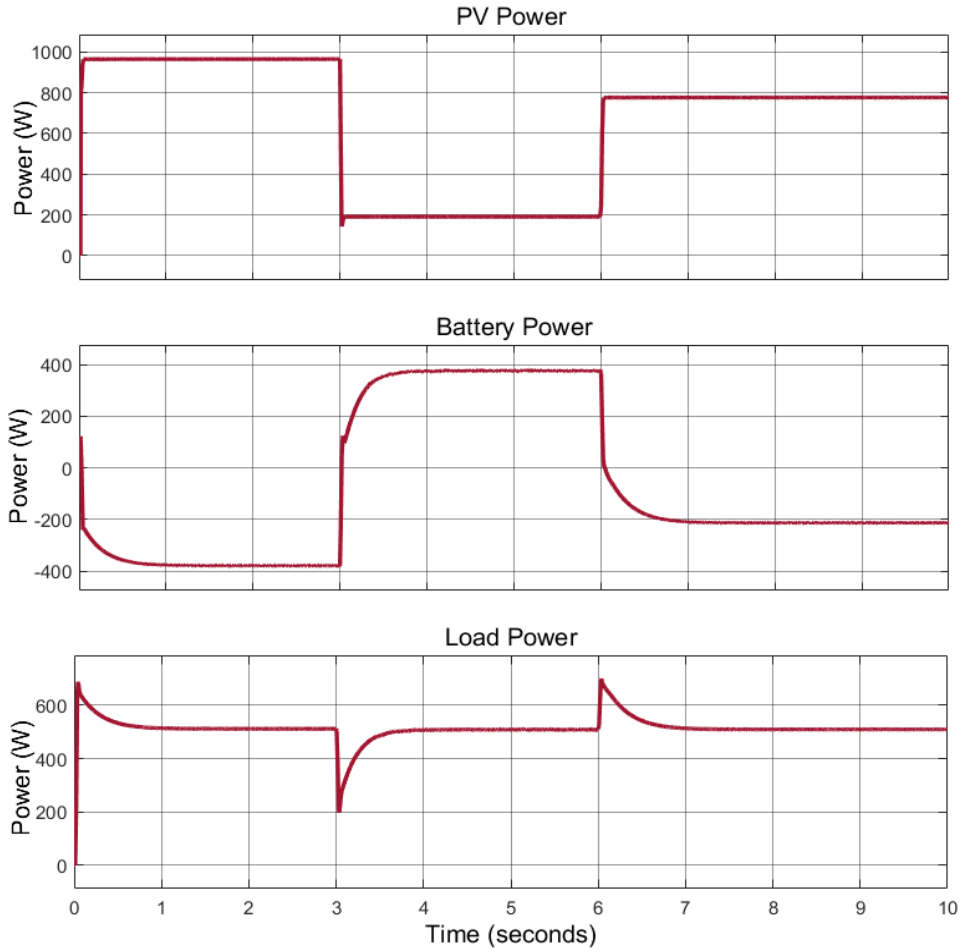

Figure 4.6 : PV power and load power,battery power

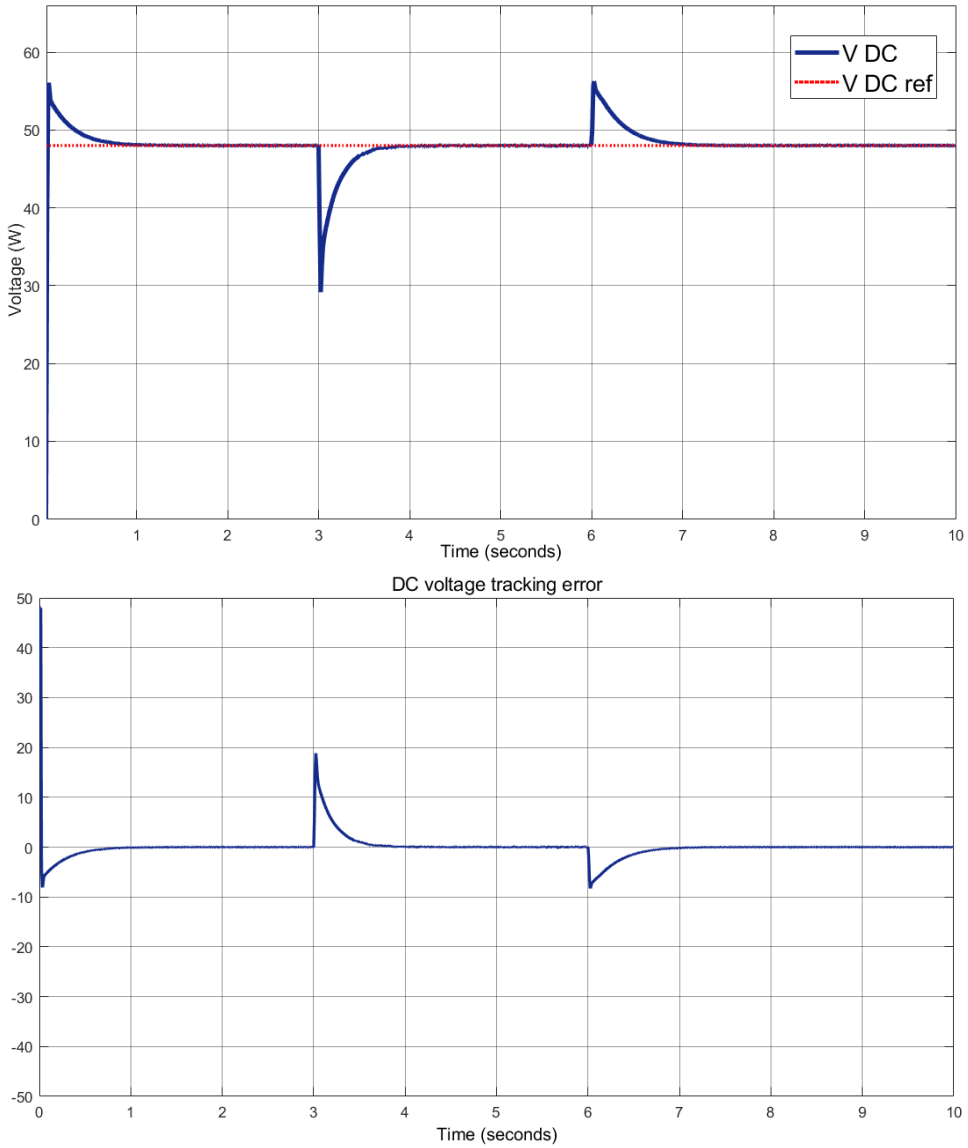

Figure 4.7 : DC bus voltage, Vdc error

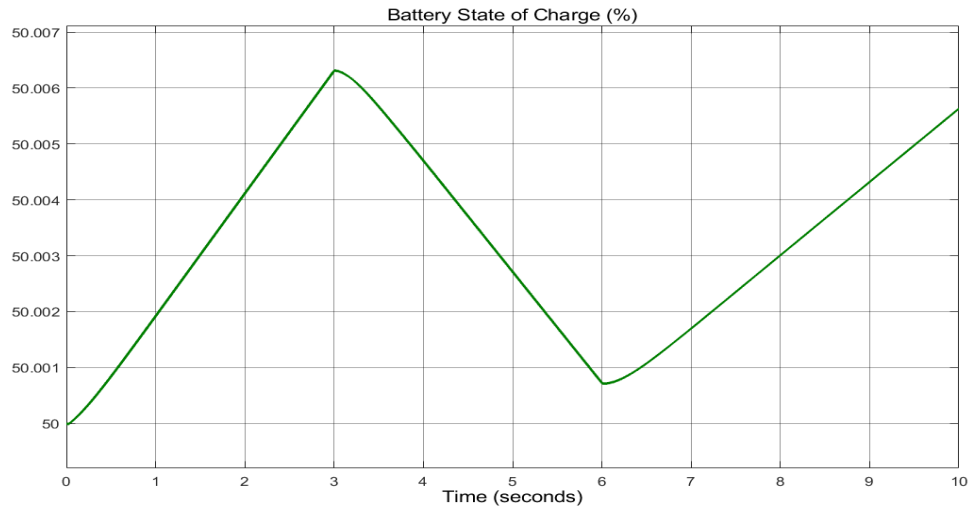

Figure 4.8 : battery state of charge

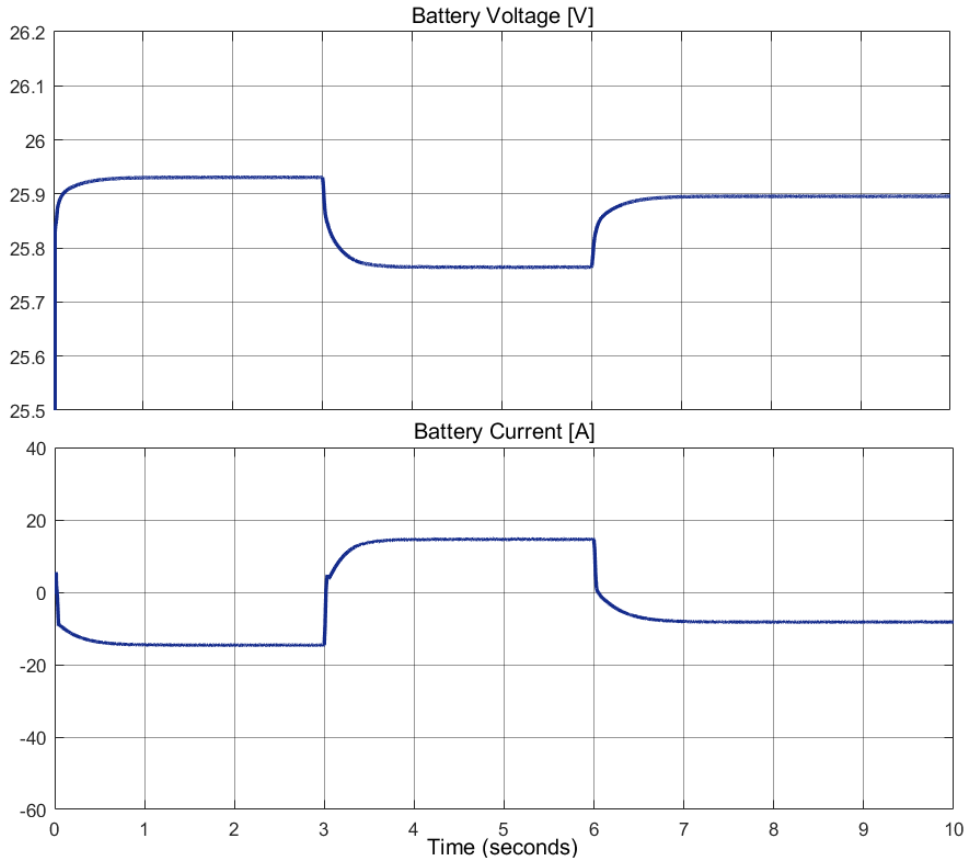

Figure 4.9 : Battery voltage,battery current

- At the beginning, the solar irradiance was constant at 1000 W/m^2 the photovoltaic power output (P_{pv}) provided power more than the load needs as shown in figure (4.6) .During this mode, the DC bus voltage increases steadily to reach the desired reference, as illustrated in Figure (4.7). At the same time the battery starts charging, as seen in Figure (4.8). This represents the 1st mode.

- Between 3 seconds and 6 seconds, the irradiance decreases from 1000 W/m^2 to 200 W/m^2. Consequently, the output power from the photovoltaic system decreases, as shown in Figure (4.6), leading to an insufficient supply of power to meet the load requirements. This provokes an initial drop in the DC bus voltage. However, as the battery begins to compensate for the lack in power to the load, the DC bus voltage follows its reference trajectory. The battery is observed discharging, as illustrated in Figure (4.8). This represents the 3rd operational mode.

- Finally, when the irradiance increased from 200W/m^2 to 800W/m^2 at 6s, we observed that the P_{pv} was sufficient to satisfy the load requirements, and then the battery controller maintained the desired DC bus voltage by charging it, as seen in Figure (4.8).

- Overall, we can see that the error between the reference DC voltage and the tracking voltage in Figure (4.7) is negligible. There are only minor perturbations that occur when the irradiance changes.

4.7.2 Case 2 : $SOC_i = 80\% = SOC_{max}$

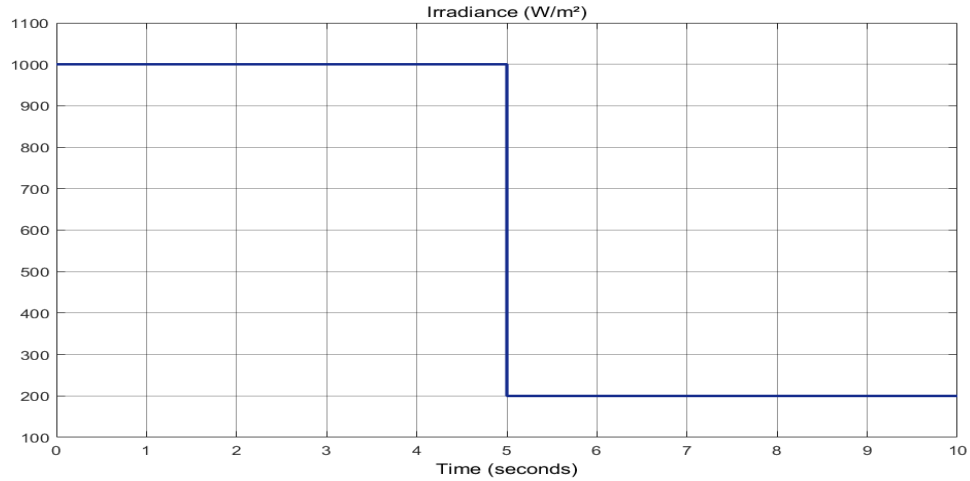

Figure 4.10 : Variation of irradiance

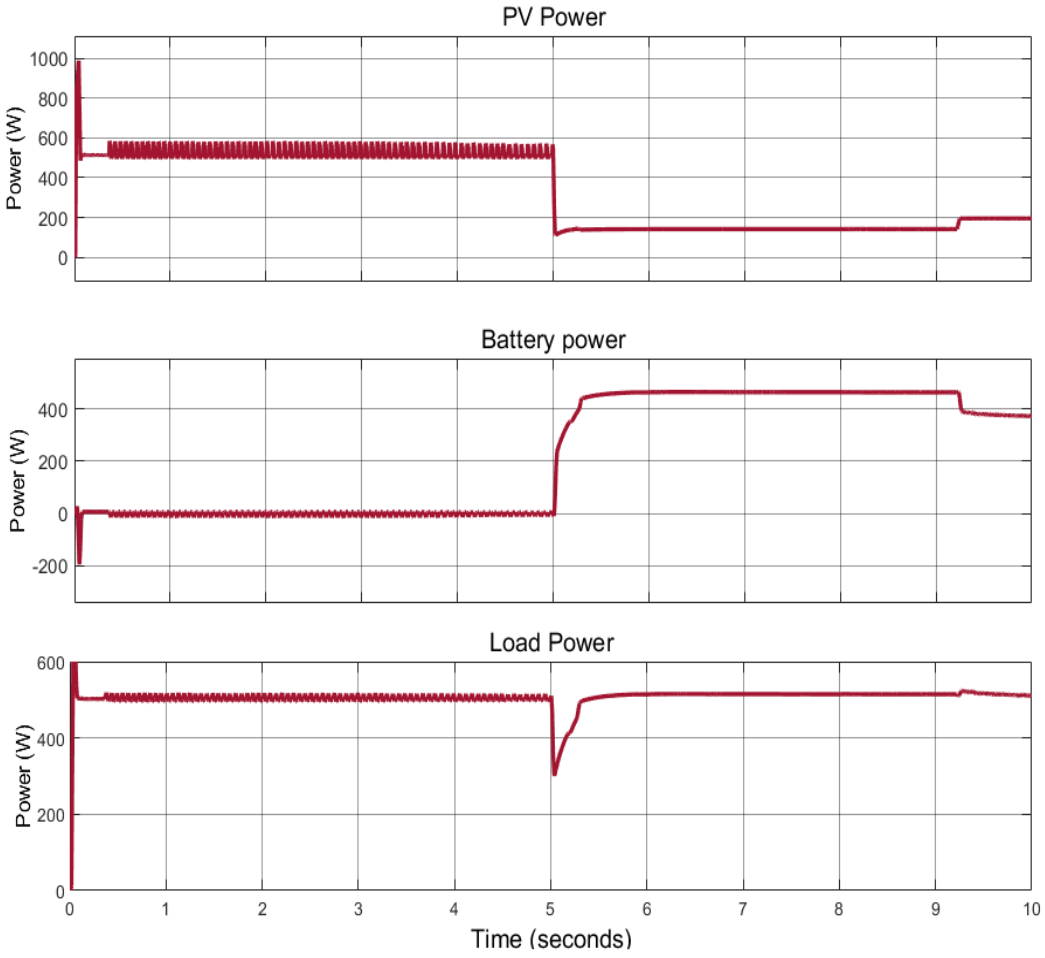

Figure 4.11 : PV power and load power,battery power

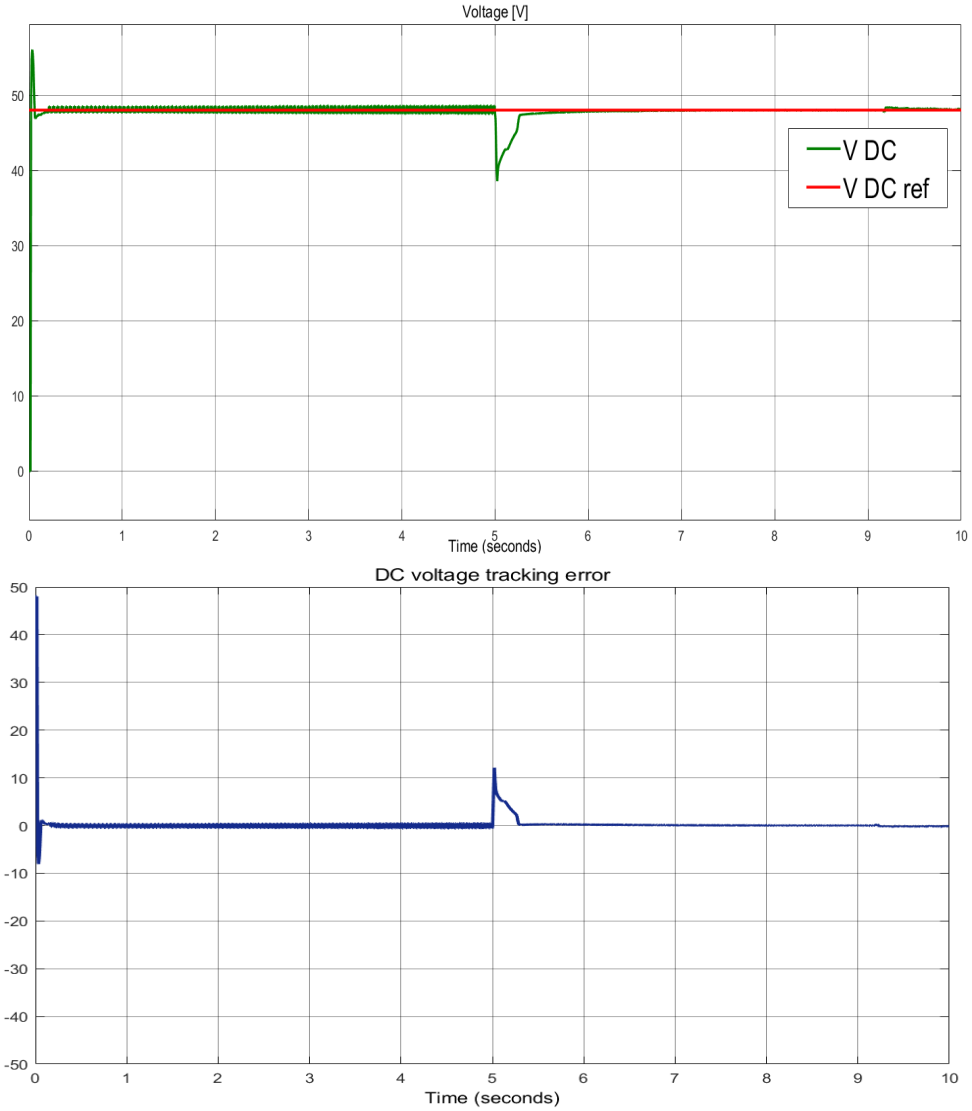

Figure 4.12 : DC bus voltage, Vdc error

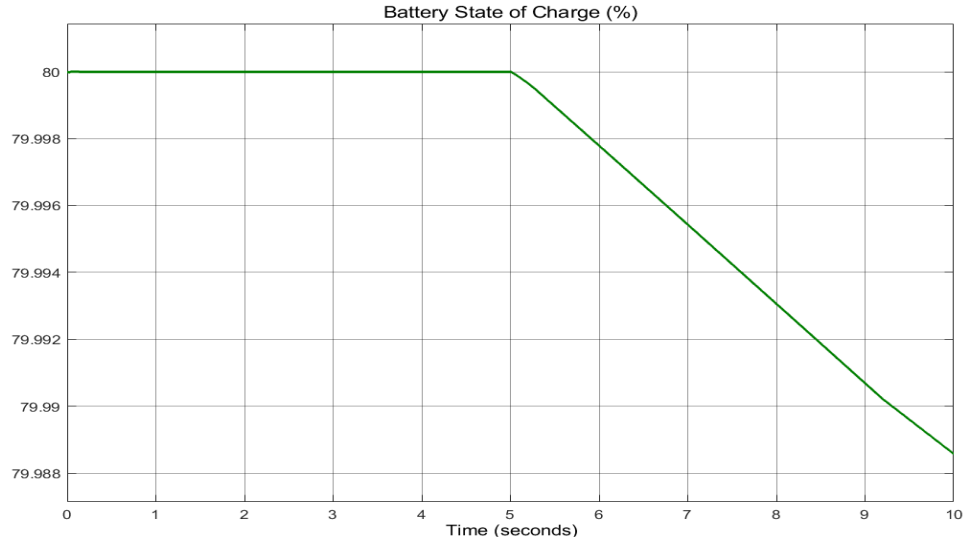

Figure 4.13 : Battery state of charge

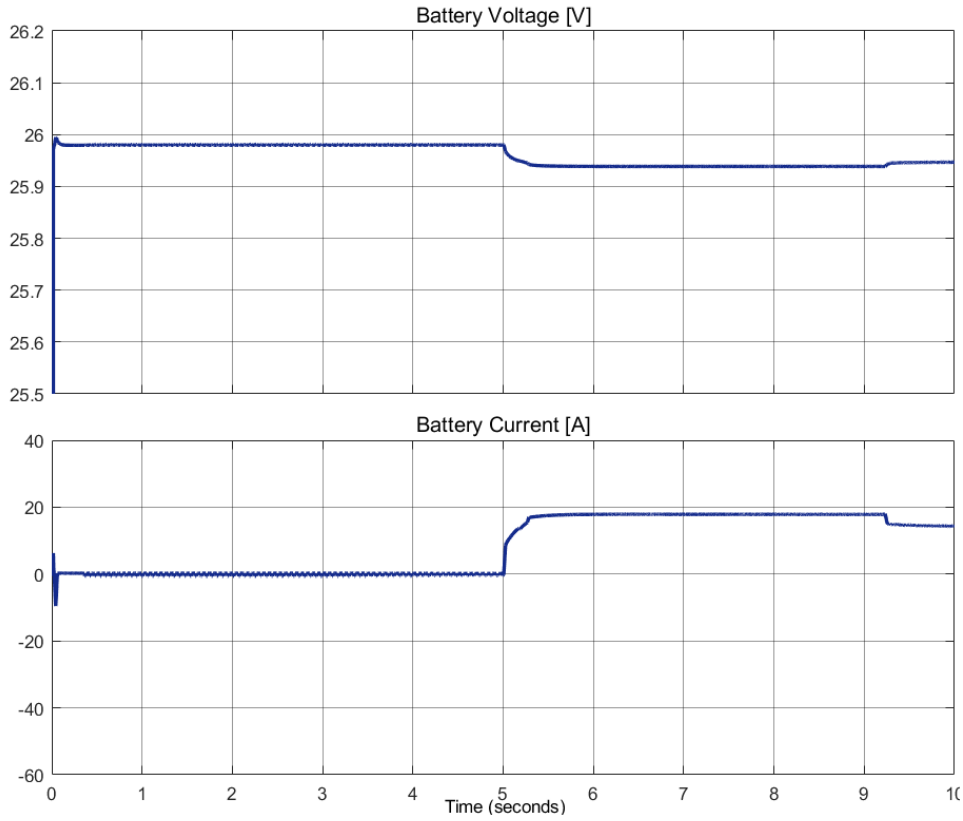

Figure 4.14 : Battery voltage and battery current

- At the beginning, the irradiance was maintained at 1000 W/m^2, so the PV power P_{pv} is greater than the load demand as shown in figure (4.11), the DC bus voltage increased up to the desired DC bus voltage and is maintained as illustrated in Figure (4.12). In this scenario, it's important to note that the battery is fully charged, with a State of Charge (SOC) of 80%. Therefore, we switch the Maximum Power Point Tracking (MPPT) to a Proportional-Integral (PI) regulator. This regulator is configured to deliver precisely the amount of power required by the load, as shown in Figure (4.11). This is the 'limited power' operating mode.

- After 5 seconds, the solar irradiance decreases from 1000 W/m^2 to 200 W/m^2. This decrease in irradiance leads to insufficient power delivered by the photovoltaic power output (P_{pv}).Consequently, the DC bus voltage begins to drop. As a result, the battery begins to discharge in order to bring the DC bus voltage back to its reference value and supply the necessary power to the load, as shown in Figures (4.12) and (4.13). This discharge operation is necessary to maintain the desired DC bus voltage, marking the transition into the 3rd operating mode.

- Overall, we can see that the error between the reference DC voltage and the tracking voltage in Figure (4.12) is negligible. There are only minor perturbations that occur when the irradiance changes.

4.7.3 Case 3 : $SOC_i = 20\% = SOC_{min}$

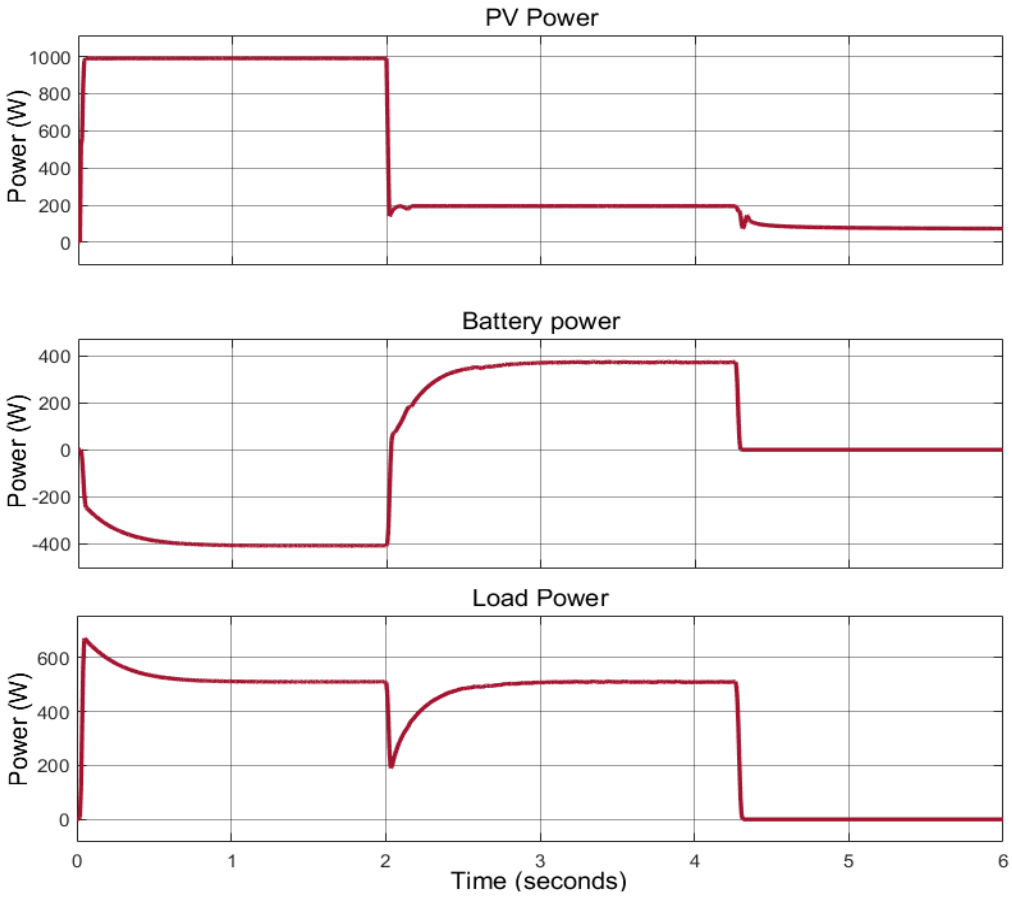

Figure 4.15 : PV output power and load power,battery power

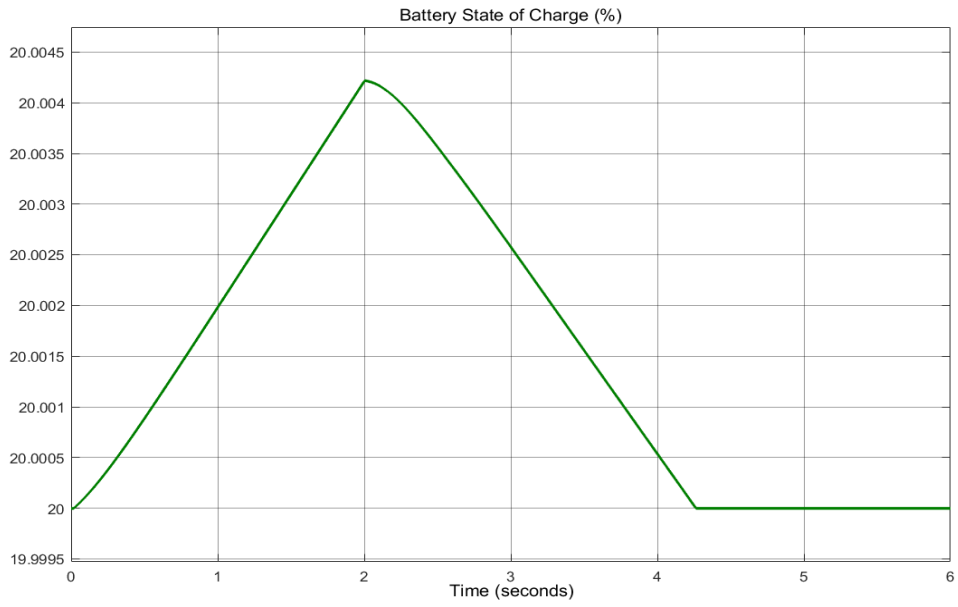

Figure 4.16 : Battery state of charge

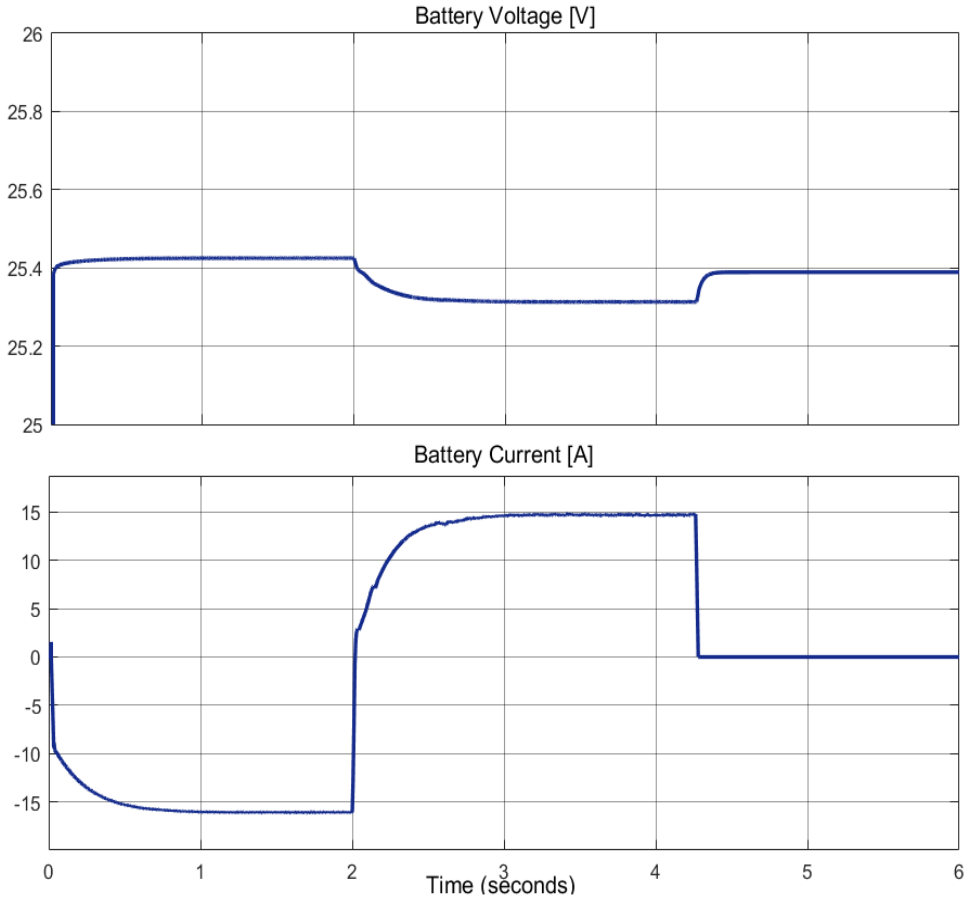

Figure 4.17 : Battery voltage,battery current

- Initially, the irradiance was 1000 W/m^2, ensuring that the photovoltaic power (P_{pv}) is sufficient to meet the load demand, as illustrated in Figure (4.15). During this period, the excess power charges the battery, as shown in Figure (4.16), representing the 1st operating mode.

- Between 2s and 4.2s, the irradiance drops from 1000 W/m^2 to 200 W/m^2. Consequently, the photovoltaic output power (P_{pv}) becomes insufficient to satisfy the load demand. As a result, the battery starts discharging leading to a decrease in the battery's State of Charge (SOC) to its minimum level (SOC = 20% = SOC$_{min}$) at 4.2s. From 4.2s to 6s, the battery power is set to zero, the battery SOC is maintained at 20%, it's no longer charging or discharging. The battery is disconnected to prevent further discharge. The load is also disconnected due to the lack of the necessary power as shown in figure (4.15). In certain scenarios where the load power can be segmented into multiple power requirements, we enter the mode of prioritized load management.

4.8 Conclusion

To increase the efficiency of standalone PV systems, good energy storage and management are required.

In this chapter, we discussed the need for storage in standalone PV systems, as well as how to control battery charging and discharging with a buck-boost converter and a PI controller. This allows us to manage energy more effectively. We also designed and tested an energy management system using simulations. This system optimizes energy consumption, guarantee the battery protection and enhance the system performance.

Chapter 5

Sizing and Control of a Standalone PV System Supplying an AC Load

5.1 Introduction

A stand-alone photovoltaic (PV) system operates based on energy input on the panel surface and energy demand (load). Incident solar radiation contains a random component, making it hard to determine how much energy the system will receive during a certain time period. To create a stand-alone solar system, it's necessary to use a sizing approach to determine the appropriate generator and storage system size for the predicted load [83].

In this chapter, we present a comprehensive case study on the sizing and design of a stand-alone PV system. The sizing of the PV system was performed using PVsyst software, ensuring it meets the specified load requirements and includes the necessary storage capacity. Subsequently, the overall standalone system was designed and simulated using MATLAB/Simulink to evaluate its performance.

5.2 System Sizing with PVsyst

Accurate system sizing is a an important step in designing an efficient photovoltaic (PV) system. It ensures that components are appropriately matched to meet the energy demands of the load while optimizing performance and cost. This section focuses on sizing the PV system to power a laboratory test bench located in the Department of Mechanical Engineering at the National Polytechnic School in El Harrach, Algeria. By considering the specific energy requirements and local environmental conditions, our goal is to create a reliable and cost-effective PV system for this particular use.

5.2.1 Overview on PVsyst Software

PVsyst is a software product created for the solar energy business. PVsyst designs, simulates, and evaluates solar energy systems of various varieties. PVsyst is renowned for its precision and adaptability for two reasons :

- PVsyst lets consumers input particular information about their solar installations. Consider statistics on solar PV modules and inverters.

- PVsyst simulates an energy system's performance under a variety of situations. Examples include the direction of the solar panels, the site's location and temperature, the electrical load and consumption patterns, and so on. Furthermore, PVsyst provides a variety of extensive customization possibilities for PV system design. This includes modeling various panel technologies, taking into account shading and other site-specific characteristics, and optimizing system performance using a variety of criteria.

5.2.2 Initial Setup and Parameters

5.2.2.1 Site Location and Meteorological Data

The National Polytechnic School is located at 36.72° latitude and 3.15° longitude. In PVsyst software, we precisely select the geographical location of the school, as shown in figure (5.1).

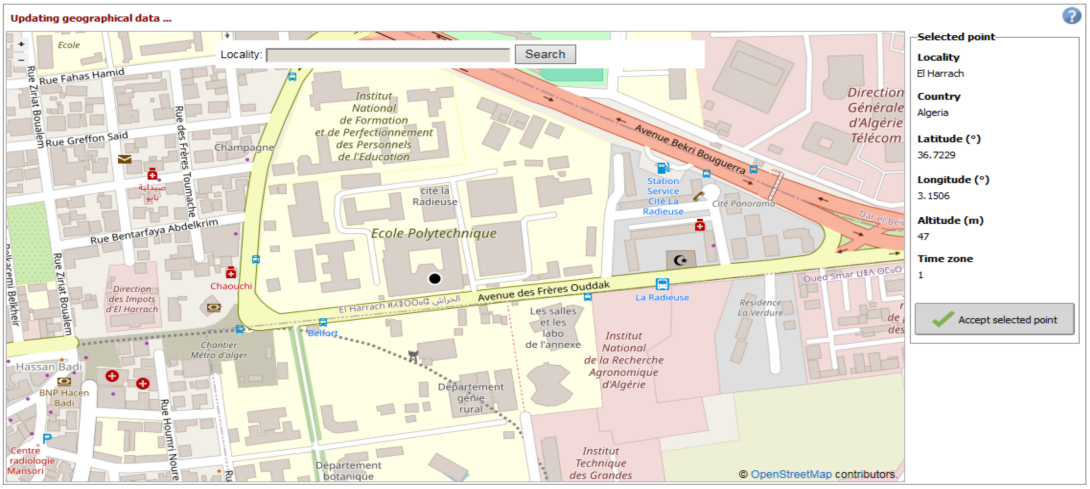

Figure 5.1 : Geographical site of National Polytechnic School

Using PVsyst sowftware, the monthly values of global irradiation, diffused irradiation, temperature and wind speed etc. has been described in table **5.1** :

	Global horizontal irradiation	Horizontal diffuse irradiation	Temperature	Wind Velocity
	kWh/m^2/mth	kWh/m^2/mth	°C	m/s
January	71.4	34.0	10.0	2.60
February	85.3	38.1	10.6	2.80
March	127.6	59.4	13.3	2.90
April	158.3	71.3	15.4	2.99
May	186.7	91.0	18.8	3.00
June	213.7	89.8	22.9	3.09
July	219.3	88.8	26.5	3.20
August	198.5	81.1	26.8	3.00
September	146.9	64.0	23.5	2.80
October	114.5	47.8	20.4	2.39
November	72.7	33.5	14.6	2.59
December	65.3	29.2	11.4	2.40
Year	1660.1	728.0	17.9	2.8

Table 5.1 : Monthly meteorological data for the site of National Polytechnic School

5.2.2.2 Estimated Load Requirements

The primary load is an alternative load which is an **experimental test bench** which operates within the following electrical characteristics : 220-240 V / 3.5-5.5 A
The AC load operates at a nominal power of 770 Watts. The daily and monthly estimated consumption required is detailed in table 5.2 below :

Appliance	Power (W)	Number	Daily use (hour/day)
Lab Equipment	770	1	4
Total daily energy required	3104 Wh/day		
Total Monthly energy required	39.9 kWh/mth		

Table 5.2 : Load energy requirements

5.2.3 PV System Configuration

This section details the configuration of the photovoltaic (PV) system, including the PV modules and energy storage, designed to meet system requirements and ensure adequate energy storage for 4-day autonomy.

5.2.3.1 PV Modules Selection

The PV system consists of three photovoltaic panels, each with the following specifications :

I_{sc}[A]	Short-circuit current	9.47
V_{oc}[V]	Open circuit voltage	46.5
I_{mp}[A]	Current at maximum power point	8.87
V_{mp}[V]	Voltage at maximum power point	38.5
$P_{\max}$[W]	Maximum power	330

Table 5.3 : Characteristics of the PV panel at standard test conditions

These panels are arranged to optimize sun exposure and energy production, ensuring the system can generate sufficient power to meet the load requirements.
The filed structure is a fixed tilted plane of tilt 35° and plane orientation azimuth 0° as shown in figure (5.2). The optimization is done for whole year with respect to optimum loss zero percent.

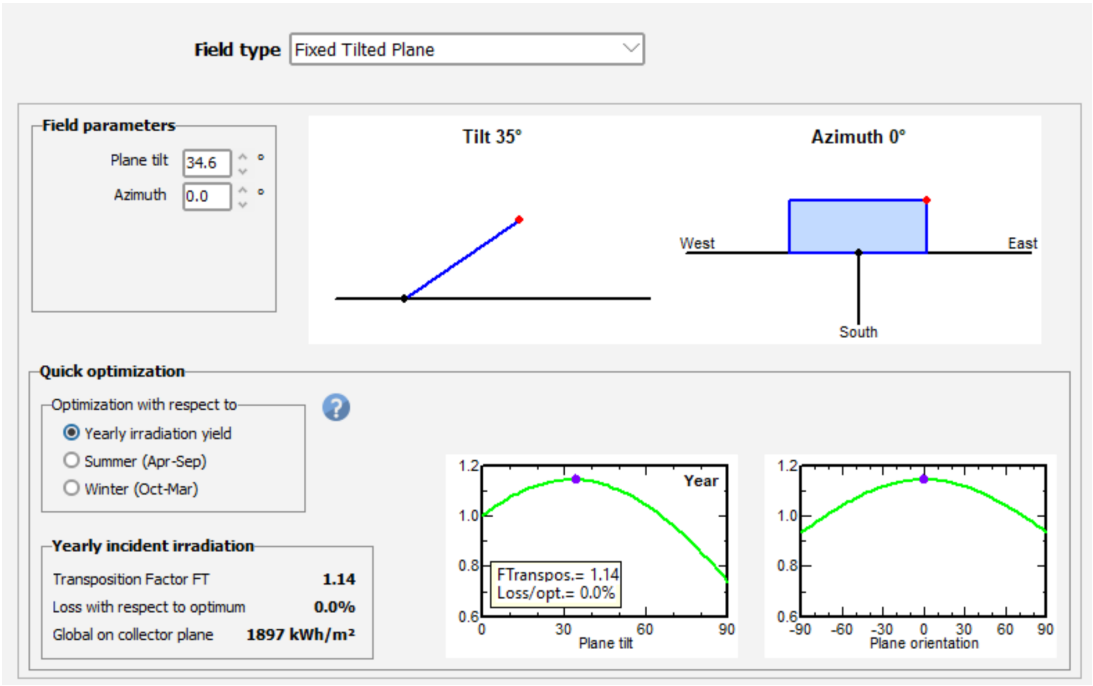

Figure 5.2 : Module orientation and tilt angle

5.2.3.2 Energy Storage

To achieve a 4-day autonomy, the energy storage system must be capable of storing enough energy to supply the load during periods without sunlight.
Based on the system requirements and daily consumption, PVsyst calculated the energy storage needs. The load has a nominal power of 770 Watts, and the desired autonomy is 4 days. PVsyst provided the following battery configuration :

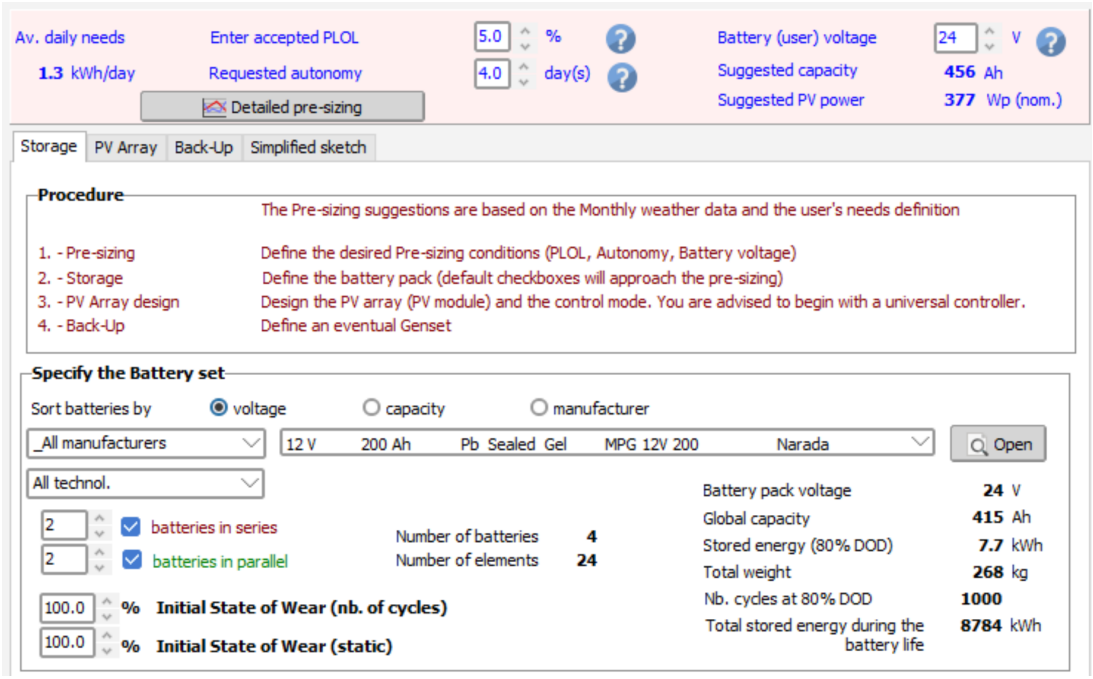

Figure 5.3 : Battery configuration

5.2.4 Simulation Results

5.2.4.1 Summary of the Characteristics of the System Components

Tables **5.4** , **5.5** summarize all the characteristics of the components used in the installation.

PV Module	
Manufacturer	Generic
(Original PVsyst database)	
Unit Nom. Power	330Wp
Number of PV modules	3 units
Nominal (STC)	990Wp
Modules	3 string ×1 In series
At operating cond. (50°C)	
Pmpp	892Wp
U mpp	34 V
I mpp	26 A
Controller Universal controller	
Technology	MPPT converter
Temp coeff.	−5.0mV/°C/ Eler
Converter	
Maxi and EURO efficiencies	97.0/95.0%
Total PV power	
Nominal (STC)	0.990kWp
Total	3 modules

Table 5.4 : Characteristics of the PV array obtained by PVsyst

Battery	
Manufacturer	Generic
Model	MPG 12V 200
Technology	3 Lead-acid
Nb. of units	2 in parallel x 2 in series
Min SOC	20%
Stored energy	7.9 kWh
Battery Pack Characteristics	
Voltage	24 V
Nominal Capacity	400 Ah
Battery Management Control	
Charging.	26.8/25.3 V
Discharging	23.6/24.6 V

Table 5.5 : Characteristics of the battery pack obtained by PVsyst

5.3 Design of Standalone PV System

The standalone PV system is designed to provide a reliable AC power supply to the experimental test bench. This system integrates various components, including a PV generator, boost converter, battery storage system, buck-boost converter, inverter, and transformer, to ensure efficient energy conversion, storage, and delivery. The structure of a standalone PV system is illustrated in figure (5.4) :

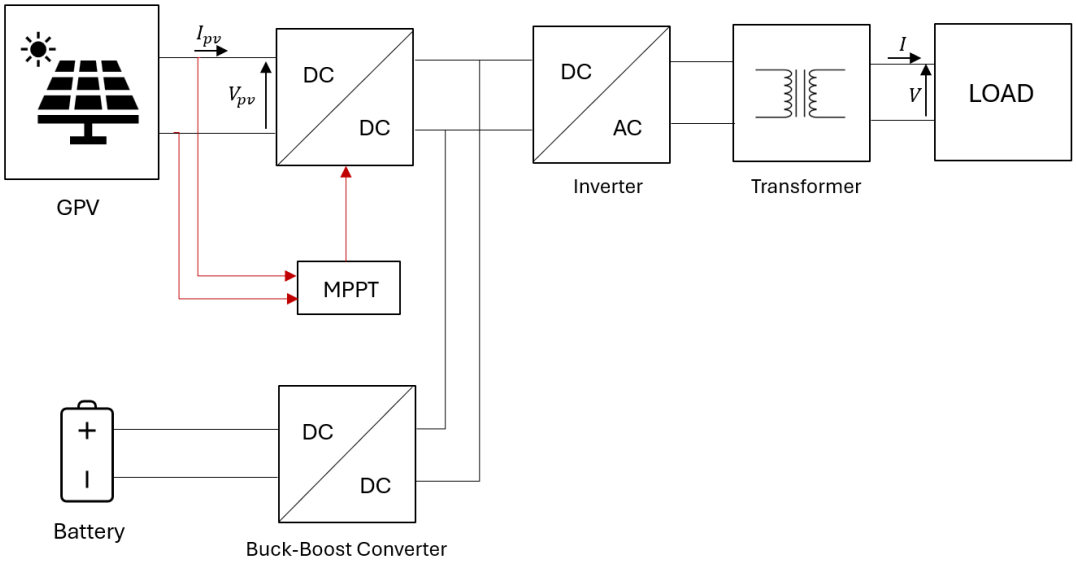

Figure 5.4 : Structure of a standalone PV System supplying an AC load

5.3.1 PV Generator

To supply the required power to our experimental test bench, the configuration of the photovoltaic generator is detailed in section (5.2.3).

The methods for controlling the boost converter to extract maximum power from the photovoltaic panels are comprehensively detailed in Chapter (3).

5.3.2 Battery Storage

The control methods for the battery storage system are detailed in chapter (4). Specifically, the control of the buck-boost converter to manage the battery's charging and discharging cycles is comprehensively discussed. Additionally, this section explains the energy management system (EMS).

Additionally, the specifications of the batteries, including their capacity and voltage, are mentioned (5.2.3) to ensure they align with the system's needs under various operating conditions.

5.3.3 Single Phase Inverter

A single-phase inverter is an electronic device used to convert direct current (DC) power to alternating current (AC) power. There are many types of single-phase inverters, each with their own unique features and purpose. Generally, single-phase inverters are used in applications where only a small amount of power is needed, such as powering small appliances, solar panels, or other electronic devices [84].

Single-phase inverters are classified into two types. Which are : Half bridge inverter and full bridge inverter. In our case, we used a full bridge inverter.

5.3.3.1 Full Bridge Inverter

A full-bridge inverter is a type of H-bridge inverter employed for converting DC power into AC power. The circuit comprises four diodes and four controlled switches, often thyristors. These switches, which can be BJT , IGBT , MOSFET or thyristors , play a crucial role in the inversion process [85].

In Full bridge inverters, a sinusoidal output is achieved by using low-pass filter. Normally the types of filters are L filter, LC filter, LCL filter, and LCL filter. Here the LC filter is used due to simple design. Figure (5.6) shows the circuit of a full inverter with LC filter.

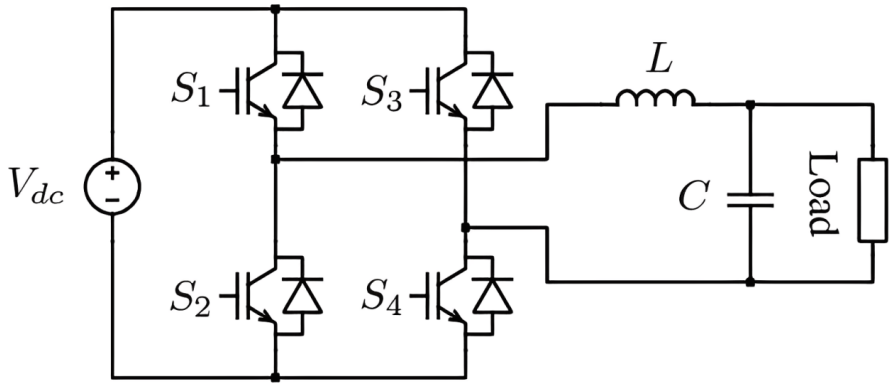

Figure 5.5 : Full bridge inverter with LC filter

5.3.3.2 LC Filter

An LC filter is a low pass filter built with an inductor and capacitor. It is meant to prevent certain high-frequency AC components from passing through the circuit. Here's a typical arrangement of an LC filter [86].

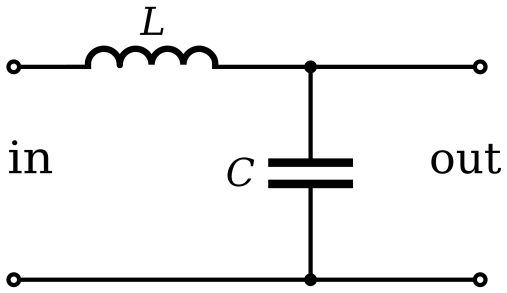

Figure 5.6 : A basic LC low pass filter circuit schematic

It is used to connect the inverter to the load. Since the inverter is based on switching components and pulse-shaped triggering signals, the output current can contain significant harmonic disturbances, which tend to reduce the power quality [86].

The LC filter components can be defined using the following formulas [87], [88] :

- **Inductance L :**

$$L_{\mathrm{i}} = \frac{V_{DC}}{8\Delta \mathrm{I}_{\max} f_{\mathrm{S}}} \tag{5.1}$$

The maximum ripple current was chosen to be 5%-20% (typical value of maximum ripple current is 20% of rated current) [87].
f_s : The inverter switching frequency

- **Filter Capacitance C_f :**

$$C = \frac{1}{(2\pi f_c)^2 L} \tag{5.2}$$

f_c : The cut-off frequency. Generally, the value of f_c is kept below $\frac{1}{10}th$ of the inverter switching frequency [88].

$$f_c \prec \frac{1}{10} f_s \tag{5.3}$$

5.3.3.3 Single Phase Inverter Control

Different control algorithms were developed to control the output of the inverter.

- Authors in [89] employed a current control strategy to mitigate harmonics in the current injected into the grid and regulate the power exchange between the photovoltaic plant and the distribution system. The paper presents a comparative performance evaluation of various current control techniques through simulation and experimental results.

- Authors in [90] proposed a voltage control method for single-phase full-bridge PWM inverters with an output LC filter.

- Authors in [91] addressed control strategies for single-stage photovoltaic (PV) inverters by implementing and experimentally comparing two current controllers: the classical proportional-integral (PI) controller and the novel proportional-resonant (PR) controller.

A bipolar Pulse-Width Modulation (4 pulses) is used here to obtain the gate signals for the switches of the single phase full bridge inverter [92]. The fundamental magnitude of the output voltage from the inverter is controlled to be constant by exercising control within the inverter itself that is no external control circuitry is required [93]. In this scheme the inverter is fed by a fixed input voltage and a controlled ac voltage is obtained by adjusting the on and the off periods of the inverter components. The advantages of the PWM control scheme are [93] :

- The output voltage control can be obtained without addition of any external components.
- PWM minimizes the lower order harmonics, while the higher order harmonics can be eliminated using a filter.

The peak of the fundamental-frequency component in the output voltage is given as [93]:

$$V_{Load} = m_i V_{dc} \tag{5.4}$$

m_i : Modulation index ($m_i \leq 1$)

The input dc voltage was 48 V and the modulation index (m_i) was taken to be 0.9. The switching frequency for the carrier, which is the triangular signal was chosen to be 20 kHz, and the frequency of the reference signal which was internally generated is 60 Hz.

Figure (5.7) shows the simulation setup of the inverter with the LC filter.

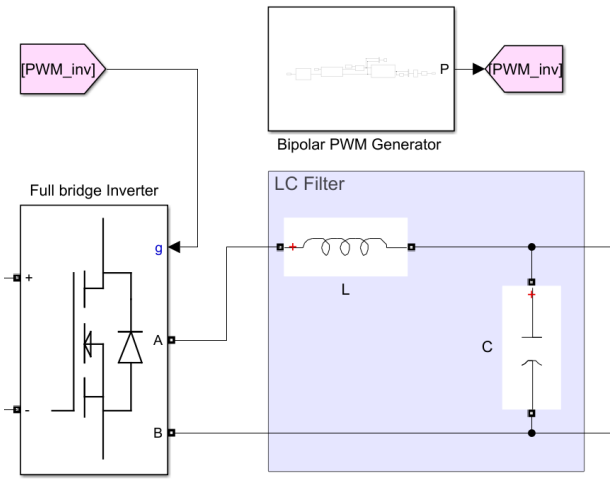

Figure 5.7 : Single phase inverter with LC filter

5.3.4 Single Phase Transformer

A single phase transformer is a type of transformer which operates on single-phase power. A transformer is a passive electrical device that transfers electrical energy from one circuit to another through the process of electromagnetic induction. It is most commonly used to increase (step up) or decrease (step down) voltage levels between circuits. It consists of a magnetic iron core serving as a magnetic transformer part and transformer cooper winding serving as an electrical part [94] as shown in figure (5.8) [94].

A single phase transformer is a high-efficiency piece of electrical equipment, and its losses are very low because there isn't any mechanical friction involved in its operation [94].

Transformers are used in almost all electrical systems, from low voltage up to the highest voltage level. It operates only with alternating current (AC) because direct current (DC) does not create any electromagnetic induction [94].

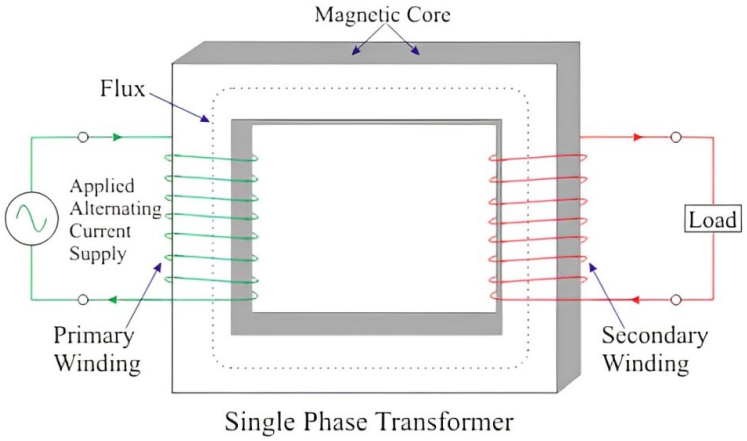

Figure 5.8 : Single phase transformer diagram

The single-phase transformer in our project is used to step up the output voltage of the inverter to the required level for the load. The transformer ensures that the voltage levels are appropriate for efficient power delivery and meets the specifications of the experimental test bench.

The transformation ratio of a transformer is given by the formula (5.5) :

$$m = \frac{N_2}{N_1} = \frac{U_2}{U_1} = \frac{I_1}{I_2} \tag{5.5}$$

N_2 : Number of turns of wire on the secondary windingl
N_1 : Number of turns of wire on the primary windingl
U_2 : Secondary voltage
U_1 : Primary voltage

5.4 Simulation Setup

In this section, we describe the simulation setup for the standalone photovoltaic (PV) system operating at Standard Test Conditions (STC), which include a temperature of 25°C and an irradiance of 1000 W/m². Using MATLAB/Simulink, we modeled the entire system, comprising the PV generator, boost converter, battery storage with buck-boost converter, single-phase inverter, and transformer. Each component is modeled with its specific characteristics and control strategies, as detailed in previous sections. The goal of this simulation is to evaluate the overall system performance, ensuring that all elements work coordinately to meet the power demands of the load.

5.5 Simulation Results

In this section, we present the results of the simulation for the standalone photovoltaic (PV) system. The simulation parameters are configured to ensure accurate representation of real-world conditions. The LC filter, single-phase inverter, and transformer are important for stabilizing the output and efficiently converting power to the resistive load. Below is a summary of the key parameters used in the simulation :

Parameter	Value
LC Filter Capacitance C	7.5 µF
LC Filter Inductance L	0.833 mH
Transformation Ratio m	8
Resistive Load Voltage	220-240 V
Resistive Load Current	3.5-5.5 A

Table 5.6 : Simulation parameters of standalone PV system

The following are the simulation results of our designed system at STC :

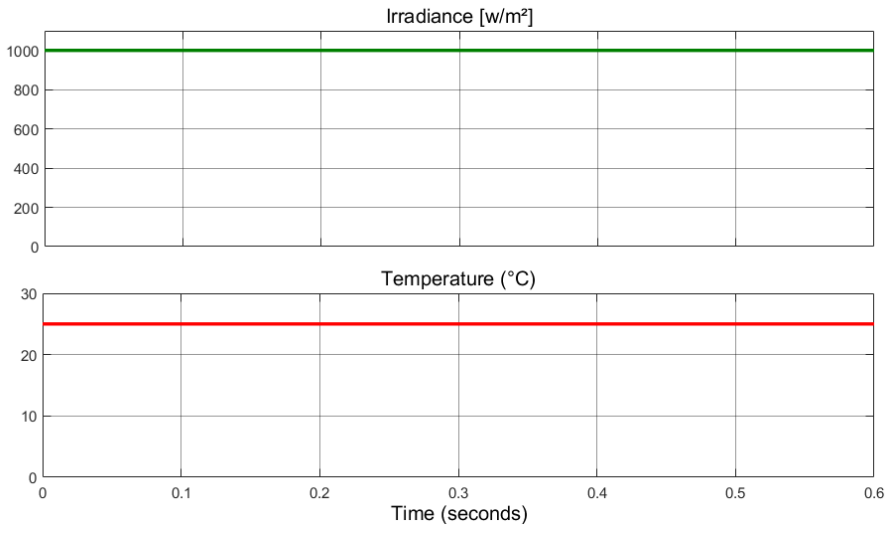

Figure 5.9 : Irradiance and temperature at STC

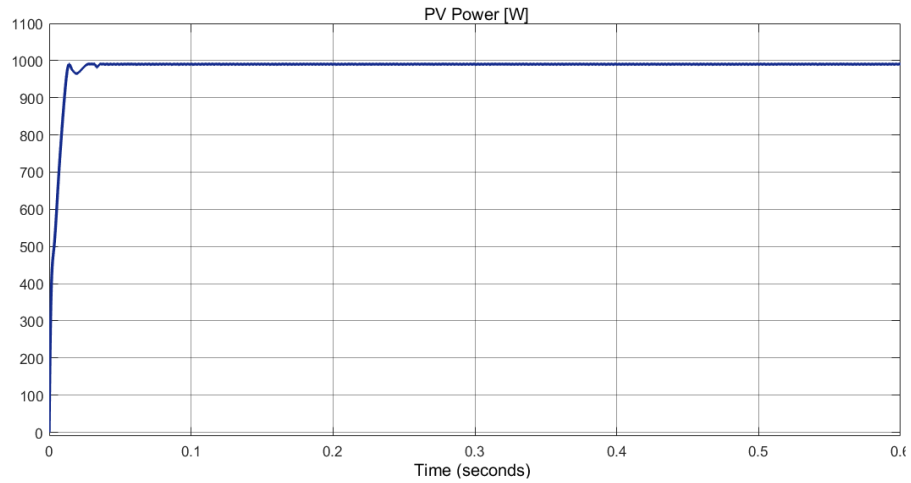

Figure 5.10 : PV output power

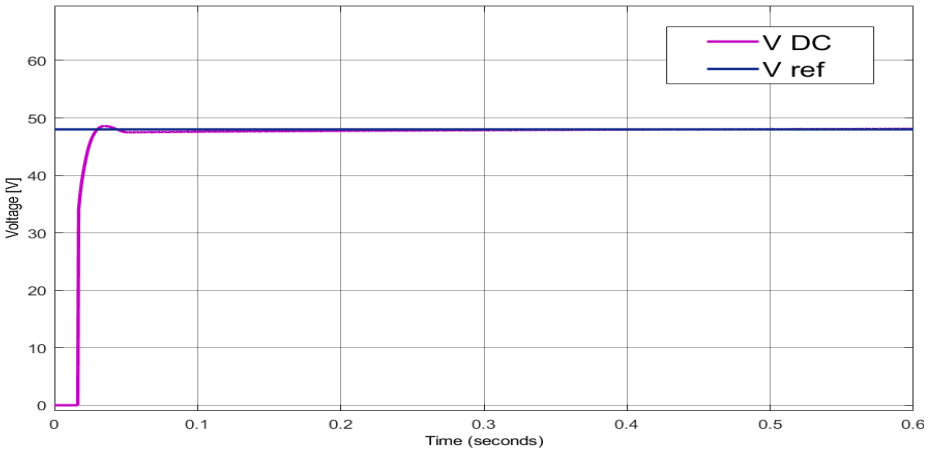

Figure 5.11 : DC bus voltage

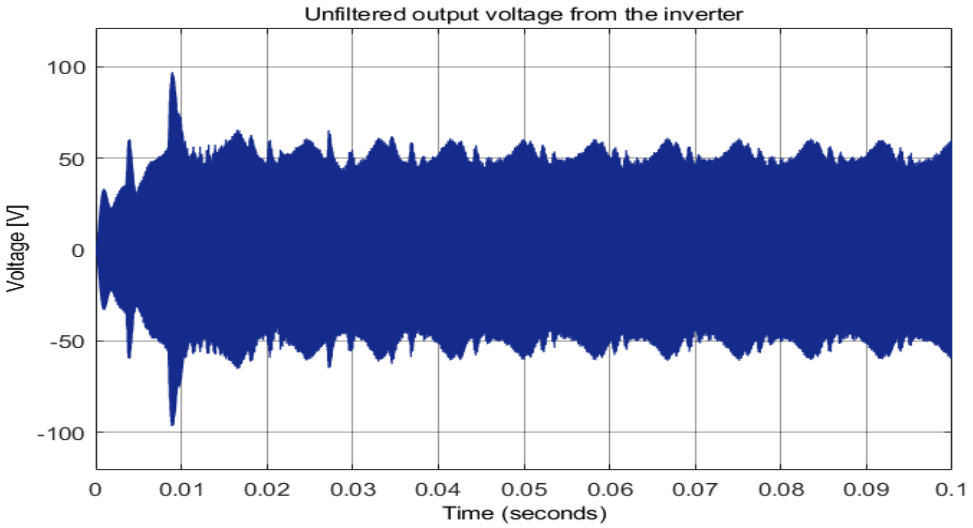

Figure 5.12 : The unfiltered output voltage of the inverter

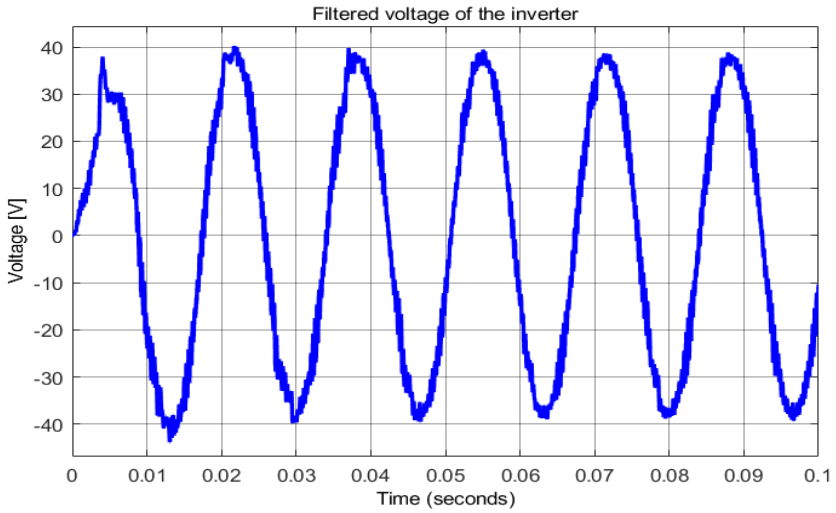

Figure 5.13 : The inverter voltage at the output of the LC filter

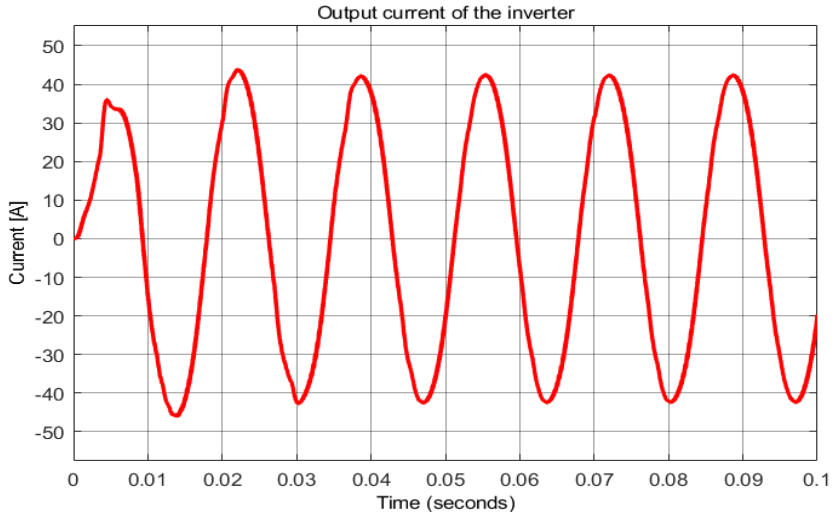

Figure 5.14 : The output current of the inverter

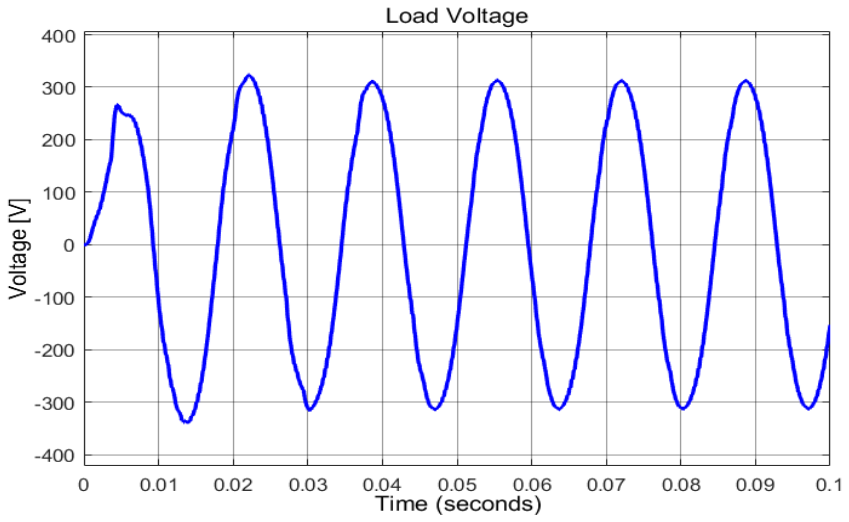

Figure 5.15 : The load voltage

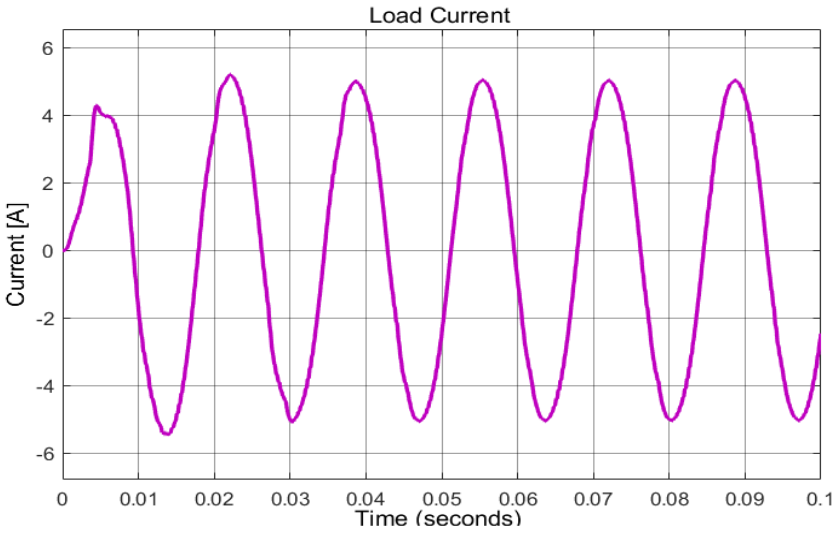

Figure 5.16 : The load current

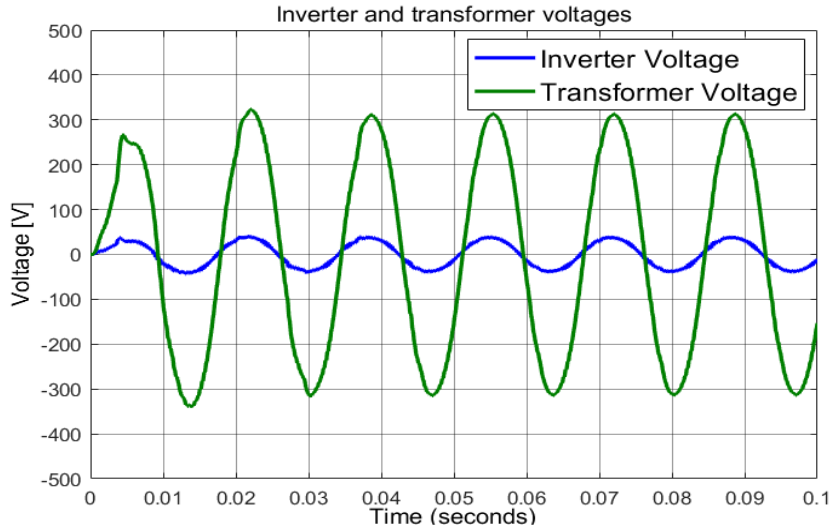

Figure 5.17 : The inverter and transformer output voltage

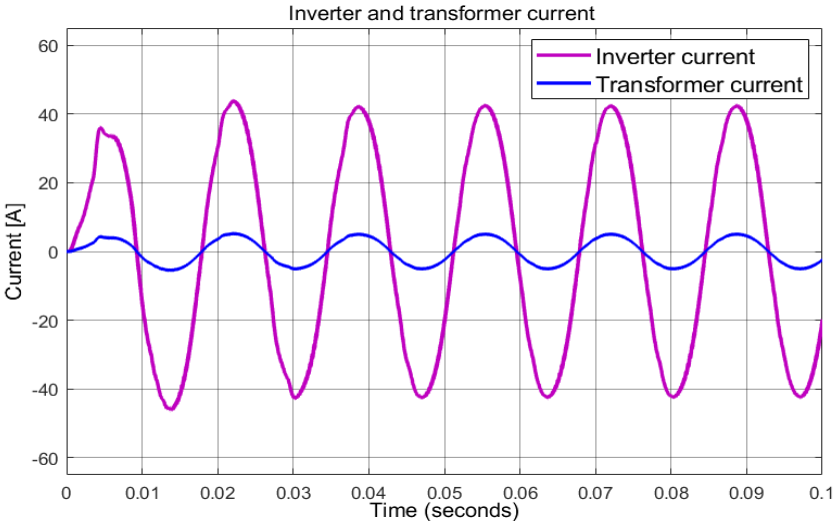

Figure 5.18 : The inverter and transformer output current

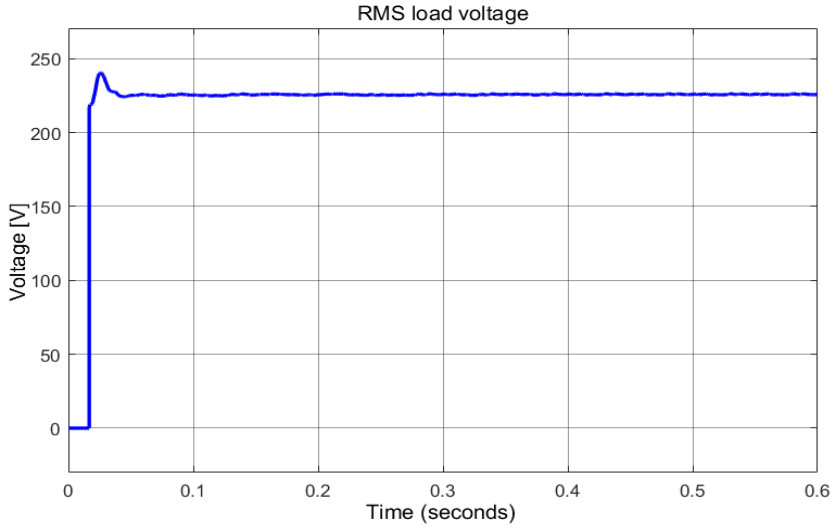

Figure 5.19 : RMS load voltage

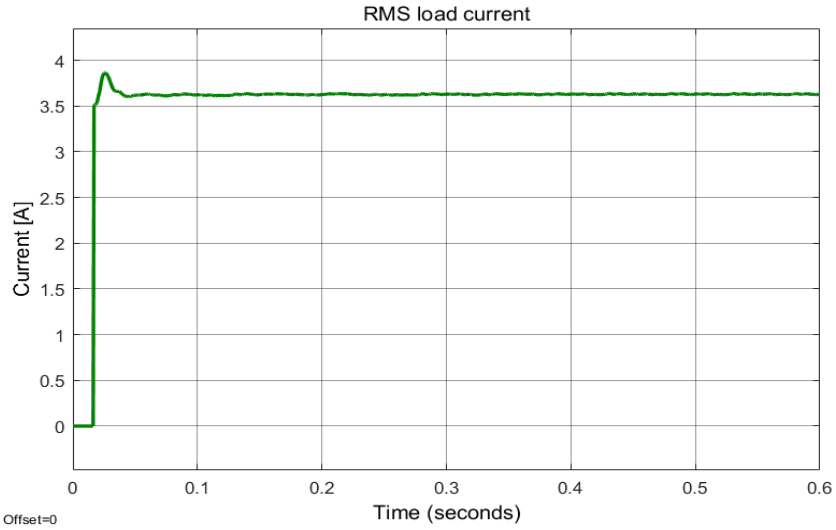

Figure 5.20 : RMS load current

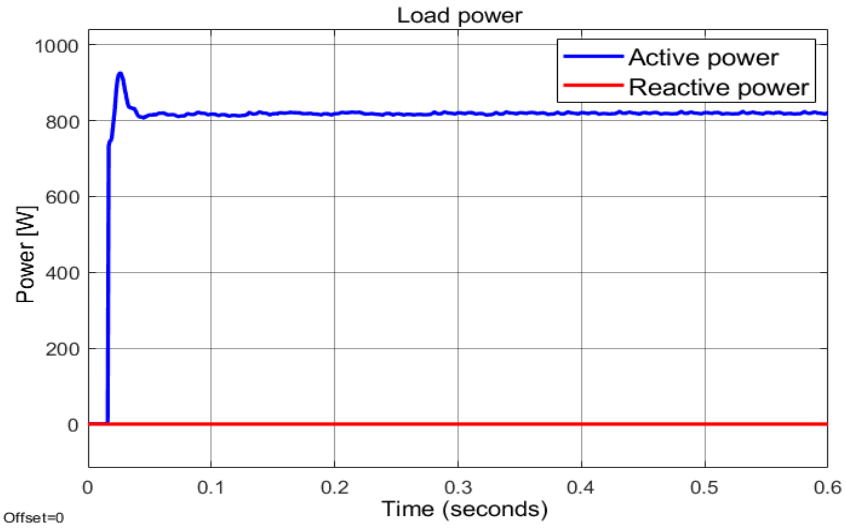

Figure 5.21 : Load power

5.6 Results Analysis

The simulation results of the designed standalone PV system demonstrate several key performance metrics.

- Firstly, the PV generator showed excellent maximum power point tracking (MPPT) with a power around 990 Watts which is equal to the nominal power of the PV array (Table **5.4**. This means the MPPT control mechanism works very well, allowing the PV modules to consistently capture the maximum possible energy. This efficiency in energy extraction is essential for optimizing the overall performance of the PV system.

- The system also showed precise tracking of the DC bus voltage. This reliable voltage regulation ensures stable operation of the entire PV system. It demonstrated the bidirectional DC-DC converter controller's effectiveness in managing the DC bus voltage.

- A notable enhancement was observed when comparing the unfiltered and filtered inverter output voltages. The unfiltered voltage displayed significant improvement after passing through the LC filter, resulting in a nearly sinusoidal output with a frequency of 60 Hz. This indicates that the LC filter is effectively smoothing the voltage waveform, thereby reducing harmonic distortions. Producing a high-quality AC voltage is essential for the proper functioning of AC loads and enhances the overall power quality delivered by the system.

- In addition, the transformer's performance was evaluated, demonstrating its ability to increase output voltage while reducing output current. This conversion ensures that the system responds effectively to load requirements. The transformer demonstrates efficiency in power conversion and delivery when it can vary voltage and current levels without compromising the overall power required by the AC load. Moreover, the results revealed that the transformer, due to the presence of its inductive components, provided superior voltage quality compared to the output observed at the filter stage. The inductors in the transformer contribute to better voltage regulation and reduced harmonic distortion, resulting in a cleaner and more stable voltage output.

- Furthermore, the RMS values of the voltage, current, and power were analyzed. The RMS voltage is about 230 volts, the RMS current approximately 3.6 Amperes, and the active power around 800 watts. The reactive power was zero due to the purely resistive nature of the load. These values align well with the load requirements, indicating that the system is capable of delivering the necessary power efficiently.

Overall, the simulation shows that the standalone PV system works really well. It tracks power accurately, keeps the voltage stable, reduces harmonics, and delivers power efficiently. These results prove that the system can reliably meet the load energy requirements.

5.7 Conclusion

In this chapter, we focused on the technical aspects of sizing a photovoltaic system, especially in standalone setups. Using PVsyst, we conducted a detailed analysis to determine the optimal size of a real-case standalone PV system. This analysis ensured that the system was appropriately dimensioned to meet the energy demands of the load.

After that, we designed the whole standalone system that powers an AC load, using MATLAB/Simulink for the design part. We checked that our design worked well by running detailed simulations, which confirmed that the system functions properly and can meet the energy needs.

Conclusion and Future Work

General Conclusion

Solar energy represents one of the alternatives to fossil fuels, helping to preserve these resources from depleting more quickly and also reducing the emissions of greenhouse gases that cause global warming. The work carried out as part of this final year project allowed us to study and simulate the operation of an energy-autonomous photovoltaic system.

In a first place, a background of solar energy and photovoltaic systems including different components and state of the art in MPPT control techniques, was introduced.

The modeling of photovoltaic generator managed by boost converter has been investigated in our thesis. We designed the PV array using the first diode model then we sized the boost converter to efficiently control the power extraction from the PV array while stepping up the output voltage.

To ensure that a photovoltaic system operates at its maximum power point, MPPT control techniques are often used. These techniques are designed to track the MPP and thus minimise the error between the operating power and the maximum reference power, which varies in function of load demand and climatic conditions. In this thesis, three control techniques have been studied and developed in order to optimise the performance of PV systems under different operating conditions, which are : the conventional P&0 algorithm, Fuzzy logic controller and PSO algorithm. The performance of these three approaches has been evaluated through simulation results.

Additionally, the integration of battery-based storage system, managed by a bidirectional DC/DC converter with PI control, was highlighted to maintain the stability of the DC bus voltage and controlling the power flow within the system components. The integrated EMS optimized overall energy management, resulting in improved system efficiency and longevity.

The accurate sizing of the standalone PV system was achieved using PVsyst software, ensuring that the designed system could meet the energy demands of the load under different conditions. The complete system, including the PV generator, boost DC/DC converters, battery storage, DC/AC inverter, and transformer, was designed and simulated in MATLAB/Simulink. The simulation results confirmed the system's ability to efficiently supply the AC load.

Future Work

The future of standalone photovoltaic (PV) systems looks promising, with several key developments on the horizon :

- Increased adoption of mini-grids : With the advent of batteries with increased capacity and the portability, as seen by the various lithium-based battery technologies, standalone systems are being heavily considered in the application of mini-grids. These systems, essentially large scale standalone systems that operate like a grid, can serve the purpose of providing energy from multiple sources for a community separate from the grid. This is likely to be widely implemented as increasing awareness of the effects of fossil fuels on the environment and increasing costs of electricity puts standalone PV forward as a cheaper alternative.
- Improved battery storage : Advancements in battery technologies, particularly lithium-based systems, are enabling standalone PV systems to have greater storage capacity and portability. This will facilitate the wider implementation of these self-sustaining mini-grid systems.
- Improved hybrid MPPT techniques : There is a growing trend towards combining conventional MPPT methods (like Perturb & Observe, Incremental Conductance) with artificial intelligence (AI) or meta-heuristic optimization algorithms. These hybrid techniques aim to provide faster tracking speed, higher efficiency, and better performance under partial shading conditions.
- Further exploration of ways to improve the efficiency and reliability of stand-alone PV systems by integrating advanced storage solutions, such as batteries, would enable a more robust and continuous response to growing energy demand, while optimizing the use of available renewable resources, presenting a particularly advantageous solution for the Mechanical Department's exprimetal test bench.

The renewable energy industry will see great advances in the next few years with the development of MPPT control techniques and the implementation of battery storage in homes and businesses. Systems capable of off-grid operation will be part of this future.

Bibliography

[1] Carlos Andrés Ramos-Paja, Efraín Pérez, Daniel González Montoya, Carlos E Carrejo, Adan Simon-Muela, and Corinne Alonso. Modeling of full photovoltaic systems applied to advanced control strategies. *Columbia: Universidad Nacional de Columbia*, 2010.

[2] Duberney Murillo-Yarce, José Alarcón-Alarcón, Marco Rivera, Carlos Restrepo, Javier Muñoz, Carlos Baier, and Patrick Wheeler. A review of control techniques in photovoltaic systems. *Sustainability*, 12(24):10598, 2020.

[3] Anca D Hansen, Poul Ejnar Sørensen, Lars H Hansen, and Henrik W Bindner. Models for a stand-alone pv system. 2001.

[4] Vaughn C Nelson. *Introduction to renewable energy*. CRC Press, 2011.

[5] Renewable Capacity Highlights. *International Renewable Energy Agency IRENA*, March 2023.

[6] Renewable energies. https://www.enelgreenpower.com/learning-hub/renewable-energies.

[7] What is renewable energy? https://www.un.org/en/climatechange/what-is-renewable-energy.

[8] Aiouadj Mokhtar. Algeria and the transition to renewable energy: the path to achieving energy security. *Finance, Investment and Sustainable Development*, June 2023.

[9] Zafar Salman. Renewable Energy in Algeria. *Africa, Renewable Energy*, 2017.

[10] Ali OM Maka and Jamal M Alabid. Solar energy technology and its roles in sustainable development. *Clean Energy*, 6(3):476–483, 2022.

[11] Md. Mosaddequr Rahman Atib Mohammad Oni, Abu S.M. Mohsin. A comprehensive evaluation of solar cell technologies, associated loss mechanisms, and efficiency enhancement strategies for photovoltaic cells. *Energy Reports*, 2024.

[12] Photovoltaic effect. https://energyeducation.ca/encyclopedia/Photovoltaic_effect.

[13] Photovoltaic module. https://www.enelgreenpower.com/learning-hub/renewable-energies/solar-energy/photovoltaic-module.

[14] R. Mukund. «wind and solar power systems». *Ph.D Patel, edition CRC PRESS*.

[15] Photovoltaic solar energy operation. https://www.iberdrola.com/sustainability/what-is-photovoltaic-energy.

[16] Mouhoub Birane and Abdelghani Chahmi. Study of photovoltaic systems with differences connecting configuration topologies for applications in renewable energy systems. *Int. J. Energetica*.

[17] Preeti Verma, Afroz Alam, Adil Sarwar, Mohd Tariq, Hani Vahedi, Deeksha Gupta, Shafiq Ahmad, and Adamali Shah Noor Mohamed. Meta-heuristic optimization techniques used for maximum power point tracking in solar pv system. *Electronics*, 10(19):2419, 2021.

[18] How to design a solar photovoltaic powered dc water pump? https://www.electricaltechnology.org/2020/09/design-solar-photovoltaic-powered-dc-water-pump.html.

[19] An introduction to buck, boost, and buck/boost converters.

[20] Manuel Arias, Aitor Vázquez, and Javier Sebastián. An overview of the ac-dc and dc-dc converters for led lighting applications. *automatika*, 53(2):156–172, 2012.

[21] P Manimekalai, R Harikumar, and S Raghavan. An overview of batteries for photovoltaic (pv) systems. *International Journal of Computer Applications*, 82(12), 2013.

[22] PVCASE TEAM. What is an off-grid solar power system ? https://pvcase.com/blog/what-is-an-off-grid-solar-power-system/, 2023.

[23] Achwak Alazrag and L Sbita. Pv system with battery storage using bidirectional dc-dc converter. *International Journal of Electrical Engineering and Computer Science*, 5:11–21, 2023.

[24] 5 solar battery specifications to know about. https://igoyeenergy.com/solar-battery-specifications/, 2023.

[25] Roberto Faranda, Sonia Leva, et al. Energy comparison of mppt techniques for pv systems. *WSEAS transactions on power systems*, 3(6):446–455, 2008.

[26] The function and principle of mppt controller. https://www.ipandee.com/the-function-and-principle-of-mppt-controller.html.

[27] Dmitry Baimel, Saad Tapuchi, Yoash Levron, and Juri Belikov. Improved fractional open circuit voltage mppt methods for pv systems. *Electronics*, 8(3):321, 2019.

[28] Aleck W Leedy, Liping Guo, and Kennedy A Aganah. A constant voltage mppt method for a solar powered boost converter with dc motor load. In *2012 Proceedings of IEEE Southeastcon*, pages 1–6. IEEE, 2012.

[29] Mohammed A Elgendy, Bashar Zahawi, and David J Atkinson. Assessment of the incremental conductance maximum power point tracking algorithm. *IEEE Transactions on sustainable energy*, 4(1):108–117, 2012.

[30] Gregory Joseph Kish, John Jaehwan Lee, and PW Lehn. Modelling and control of photovoltaic panels utilising the incremental conductance method for maximum power point tracking. *IET Renewable Power Generation*, 6(4):259–266, 2012.

[31] C Obe, D Nnadi, L Omeje, and UC Asogwa. Incremental conductance method of maximum power point tracking (mppt) for photovoltaic system. In *2nd International Conference on Electrical Power Engineering (ICEPENG 2021)*, 2021.

[32] Derek Ajesam Asoh, Brice Damien Noumsi, and Edwin Nyuysever Mbinkar. Maximum power point tracking using the incremental conductance algorithm for pv systems operating in rapidly changing environmental conditions. *Smart Grid and Renewable Energy*, 13(5):89–108, 2022.

[33] Abubakari Sadick. Maximum power point tracking simulation for photovoltaic systems using perturb and observe algorithm. 2023.

[34] Ahmed M Atallah, Almoataz Y Abdelaziz, and Raihan S Jumaah. Implementation of perturb and observe mppt of pv system with direct control method using buck and buck-boost converters. *Emerging Trends in Electrical, Electronics & Instrumentation Engineering: An international Journal (EEIEJ)*, 1(1):31–44, 2014.

[35] Ahmed IM Ali, Mahmoud A Sayed, and Essam EM Mohamed. Modified efficient perturb and observe maximum power point tracking technique for grid-tied pv system. *International Journal of Electrical Power & Energy Systems*, 99:192–202, 2018.

[36] Chee Wei Tan, Tim C Green, and Carlos A Hernandez-Aramburo. Analysis of perturb and observe maximum power point tracking algorithm for photovoltaic applications. In *2008 IEEE 2nd International Power and Energy Conference*, pages 237–242. IEEE, 2008.

[37] Sabir Messalti et al. A new neural networks mppt controller for pv systems. In *IREC2015 the sixth international renewable energy congress*, pages 1–6. IEEE, 2015.

[38] Lakshmi PN Jyothy and MR Sindhu. An artificial neural network based mppt algorithm for solar pv system. In *2018 4th International Conference on Electrical Energy Systems (ICEES)*, pages 375–380. IEEE, 2018.

[39] Abdullah M Noman, Khaled E Addoweesh, and Hussein M Mashaly. A fuzzy logic control method for mppt of pv systems. In *IECON 2012-38th Annual Conference on IEEE Industrial Electronics Society*, pages 874–880. IEEE, 2012.

[40] Carlos Robles Algarín, John Taborda Giraldo, and Omar Rodriguez Alvarez. Fuzzy logic based mppt controller for a pv system. *Energies*, 10(12):2036, 2017.

[41] RK Rai and OP Rahi. Fuzzy logic based control technique using mppt for solar pv system. In *2022 First international conference on electrical, electronics, information and communication technologies (ICEEICT)*, pages 01–05. IEEE, 2022.

[42] Fatah Yahiaoui, Ferhat Chabour, Ouahib Guenounou, Mohit Bajaj, Syed Sabir Hussain Bukhari, Muhammad Shahzad Nazir, Mukesh Pushkarna, Daniel Eutyche Mbadjoun Wapet, et al. An experimental testing of optimized fuzzy logic-based

mppt for a standalone pv system using genetic algorithms. *Mathematical Problems in Engineering*, 2023, 2023.

[43] C Larbes, SM Ait Cheikh, T Obeidi, and A Zerguerras. Genetic algorithms optimized fuzzy logic control for the maximum power point tracking in photovoltaic system. *Renewable energy*, 34(10):2093–2100, 2009.

[44] Ammar Al-Gizi, Aurelian Craciunescu, and Sarab Al-Chlaihawi. Improving the performance of pv system using genetically-tuned flc based mppt. In *2017 International Conference on Optimization of Electrical and Electronic Equipment (OPTIM) & 2017 Intl Aegean Conference on Electrical Machines and Power Electronics (ACEMP)*, pages 642–647. IEEE, 2017.

[45] Karima Amara, Arezki Fekik, D Hocine, Mohamed Lamine Bakir, El-Bay Bourennane, Toufik Ali Malek, and Ali Malek. Improved performance of a pv solar panel with adaptive neuro fuzzy inference system anfis based mppt. In *2018 7th international conference on renewable energy research and applications (ICRERA)*, pages 1098–1101. IEEE, 2018.

[46] Farhad Khosrojerdi, Shamsodin Taheri, and Ana-Maria Cretu. An adaptive neuro-fuzzy inference system-based mppt controller for photovoltaic arrays. In *2016 IEEE Electrical Power and Energy Conference (EPEC)*, pages 1–6. IEEE, 2016.

[47] Mahlagha Mahdavi, Li Li, Jianguo Zhu, and Saad Mekhilef. An adaptive neuro-fuzzy controller for maximum power point tracking of photovoltaic systems. In *TENCON 2015-2015 IEEE Region 10 Conference*, pages 1–6. IEEE, 2015.

[48] Karima Amara, Ali Malek, Toufik Bakir, Arezki Fekik, Ahmad Taher Azar, Khaled Mohamad Almustafa, El-Bay Bourennane, and Dallila Hocine. Adaptive neuro-fuzzy inference system based maximum power point tracking for stand-alone photovoltaic system. *International Journal of Modelling, Identification and Control*, 33(4):311–321, 2019.

[49] Khaled Bataineh and Yazan Taamneh. Adaptive neuro-fuzzy inference system-based improvement of perturb and observe maximum power point tracking method for photovoltaic systems. *International Journal of Power Electronics and Drive Systems*, 8(3):1327, 2017.

[50] Luis Avila, Mariano De Paula, Maximiliano Trimboli, and Ignacio Carlucho. Deep reinforcement learning approach for mppt control of partially shaded pv systems in smart grids. *Applied Soft Computing*, 97:106711, 2020.

[51] Luis Avila, Mariano De Paula, Ignacio Carlucho, and Carlos Sanchez Reinoso. Mppt for pv systems using deep reinforcement learning algorithms. *IEEE Latin America Transactions*, 17(12):2020–2027, 2019.

[52] Bao Chau Phan, Ying-Chih Lai, and Chin E Lin. A deep reinforcement learning-based mppt control for pv systems under partial shading condition. *Sensors*, 20(11):3039, 2020.

[53] Slimane Hadji, Jean-Paul Gaubert, and Fateh Krim. Theoretical and experimental analysis of genetic algorithms based mppt for pv systems. *Energy Procedia*, 74:772–787, 2015.

[54] Afef Badis, Mohamed Nejib Mansouri, and Mohamed Habib Boujmil. A genetic algorithm optimized mppt controller for a pv system with dc-dc boost converter. In *2017 International Conference on Engineering & MIS (ICEMIS)*, pages 1–6. IEEE, 2017.

[55] Slimane Hadji, Jean-Paul Gaubert, and Fateh Krim. Experimental analysis of genetic algorithms based mppt for pv systems. In *2014 International Renewable and Sustainable Energy Conference (IRSEC)*, pages 7–12. IEEE, 2014.

[56] Ramdan BA Koad, Ahmed Faheem Zobaa, and Adel El-Shahat. A novel mppt algorithm based on particle swarm optimization for photovoltaic systems. *IEEE Transactions on Sustainable Energy*, 8(2):468–476, 2016.

[57] K Sundareswaran, S Palani, et al. Application of a combined particle swarm optimization and perturb and observe method for mppt in pv systems under partial shading conditions. *Renewable Energy*, 75:308–317, 2015.

[58] Yi-Hwa Liu, Shyh-Ching Huang, Jia-Wei Huang, and Wen-Cheng Liang. A particle swarm optimization-based maximum power point tracking algorithm for pv systems operating under partially shaded conditions. *IEEE transactions on energy conversion*, 27(4):1027–1035, 2012.

[59] Satheesh Krishnan G, Sundareswaran Kinattingal, Sishaj P Simon, and Panugothu Srinivasa Rao Nayak. Mppt in pv systems using ant colony optimisation with dwindling population. *IET Renewable Power Generation*, 14(7):1105–1112, 2020.

[60] Sabrina Titri, Cherif Larbes, Kamal Youcef Toumi, and Karima Benatchba. A new mppt controller based on the ant colony optimization algorithm for photovoltaic systems under partial shading conditions. *Applied Soft Computing*, 58:465–479, 2017.

[61] Rakesh Kumar Phanden, Lalit Sharma, Jatinder Chhabra, and Halil İbrahim Demir. A novel modified ant colony optimization based maximum power point tracking controller for photovoltaic systems. *Materials Today: Proceedings*, 38:89–93, 2021.

[62] Gwinyai J Dzimano. Modeling of photovoltaic systems. Master's thesis, The Ohio State University, 2008.

[63] Shah Arifur Rahman, Rajiv K Varma, and Tim Vanderheide. Generalised model of a photovoltaic panel. *IET Renewable Power Generation*, 8(3):217–229, 2014.

[64] Xuan Hieu Nguyen and Minh Phuong Nguyen. Mathematical modeling of photovoltaic cell/module/arrays with tags in matlab/simulink. *Environmental Systems Research*, 4:1–13, 2015.

[65] Saleh E Babaa, Georges El Murr, Faisal Mohamed, and Srilatha Pamuri. Overview of boost converters for photovoltaic systems. *Journal of Power and Energy Engineering*, 6(4):16–31, 2018.

[66] Boost converter: Basics, working, design operation. *Journal of Power and Energy Engineering*, January 2019.

[67] Robert Keim. Understanding the operation of a boost converter. *All About Circuits*, September 2023.

[68] Unal Yilmaz, Ali Kircay, and Selim Borekci. Pv system fuzzy logic mppt method and pi control as a charge controller. *Renewable and Sustainable Energy Reviews*, 81:994–1001, 2018.

[69] Texas Instruments. Basic calculation of a boost converter's power stage. *Application Report SLVA372C*, 2009.

[70] Yongheng Yang, Katherine A Kim, Frede Blaabjerg, and Ariya Sangwongwanich. *Advances in grid-connected photovoltaic power conversion systems*. Woodhead Publishing, 2018.

[71] Leopoldo Gil-Antonio, Martha Belem Saldivar-Marquez, and Otniel Portillo-Rodriguez. Maximum power point tracking techniques in photovoltaic systems: A brief review. In *2016 13th International Conference on Power Electronics (CIEP)*, pages 317–322. IEEE, 2016.

[72] Boualem Bendib, Hocine Belmili, and Fateh Krim. A survey of the most used mppt methods: Conventional and advanced algorithms applied for photovoltaic systems. *Renewable and Sustainable Energy Reviews*, 45:637–648, 2015.

[73] Ahmed IM Ali, Essam EM Mohamed, and Abdel-Raheem Youssef. Mppt algorithm for grid-connected photovoltaic generation systems via model predictive controller. In *2017 Nineteenth International Middle East Power Systems Conference (MEPCON)*, pages 895–900. IEEE, 2017.

[74] Salman Salman, Xin Ai, and Zhouyang Wu. Design of a p-&-o algorithm based mppt charge controller for a stand-alone 200w pv system. *Protection and control of modern power systems*, 3:1–8, 2018.

[75] Achwak Alazrag and L Sbita. Pv system with battery storage using bidirectional dc-dc converter. *International Journal of Electrical Engineering and Computer Science*, 5:11–21, 2023.

[76] Carlos Robles Algarín, John Taborda Giraldo, and Omar Rodriguez Alvarez. Fuzzy logic based mppt controller for a pv system. *Energies*, 10(12):2036, 2017.

[77] Astitva Kumar, Priyanka Chaudhary, and M Rizwan. Development of fuzzy logic based mppt controller for pv system at varying meteorological parameters. In *2015 annual IEEE India conference (INDICON)*, pages 1–6. IEEE, 2015.

[78] Rajib Baran Roy, Enamul Basher, Rojoba Yasmin, and Md Rokonuzzaman. Fuzzy logic based mppt approach in a grid connected photovoltaic system. In *The 8th International Conference on Software, Knowledge, Information Management and Applications (SKIMA 2014)*, pages 1–6. IEEE, 2014.

[79] Ramdan BA Koad, Ahmed Faheem Zobaa, and Adel El-Shahat. A novel mppt algorithm based on particle swarm optimization for photovoltaic systems. *IEEE Transactions on Sustainable Energy*, 8(2):468–476, 2016.

[80] S Mohsen Mirhassani, Mohsen Razzazan, and Amin Ramezani. An improved pso based mppt approach to cope with partially shaded condition. In *2014 22nd Iranian conference on electrical engineering (ICEE)*, pages 550–555. IEEE, 2014.

[81] Suchandan Das. Bi-directional converter topology for solar-battery charging.

[82] Seema Jadhav, Neha Devdas, Shakila Nisar, and Vaibhav Bajpai. Bidirectional dc-dc converter in solar pv system for battery charging application. In *2018 international conference on smart city and emerging technology (ICSCET)*, pages 1–4. IEEE, 2018.

[83] M Sidrach-de Cardona and Ll Mora Lopez. A simple model for sizing stand alone photovoltaic systems. *Solar Energy Materials and Solar Cells*, 55(3):199–214, 1998.

[84] Single-phase inverter | how it works. https://www.bluettipower.com/blogs/articles/single-phase-inverter-how-it-works.

[85] Single phase inverter. https://www.geeksforgeeks.org/single-phase-inverter/.

[86] Omar BOUCHERIT. Etude et modélisation d'un filtre lcl pour onduleur photovoltaïque connecté au réseau. *Master thesis*, 2019.

[87] Maaspaliza Azri and Nasrudin Abd Rahim. Design analysis of low-pass passive filter in single-phase grid-connected transformerless inverter. In *2011 IEEE Conference on Clean Energy and Technology (CET)*, pages 348–353. IEEE, 2011.

[88] Mojgan Hojabri and Mehrdad Hojabri. Design, application and comparison of passive filters for three-phase grid-connected renewable energy systems. *ARPN Journal of Engineering and Applied Sciences*, 10(22):10691–10697, 2015.

[89] Aditi Chatterjee and Kanungo Barada Mohanty. Current control strategies for single phase grid integrated inverters for photovoltaic applications-a review. *Renewable and Sustainable Energy Reviews*, 92:554–569, 2018.

[90] Pekik Argo Dahono and Een Taryana. A new voltage control method for single-phase pwm inverters. *ITB Journal of Engineering Science*, 43(2):139–152, 2011.

[91] Mihai Ciobotaru, Remus Teodorescu, and Frede Blaabjerg. Control of single-stage single-phase pv inverter. *Epe Journal*, 16(3):20–26, 2006.

[92] Zeynep Bala Duranay and Hanifi Guldemir. Modelling and simulation of a single phase standalone pv system. In *2019 11th International Conference on Electronics, Computers and Artificial Intelligence (ECAI)*, pages 1–6. IEEE, 2019.

[93] Muhammad H. Rashid. Power electronics: Converters, applications, and design. 2011.

[94] Single phase transformer: Diagram, working principle and applications. https://testbook.com/electrical-engineering/single-phase-transformer, 2011.

[95] Mostefa Kermadi, Saad Mekhilef, Zainal Salam, Jubaer Ahmed, and El Madjid Berkouk. Assessment of maximum power point trackers performance using direct and indirect control methods. *International Transactions on Electrical Energy Systems*, 30(10):e12565, 2020.

[96] Carlos Robles Algarín, John Taborda Giraldo, and Omar Rodriguez Alvarez. Fuzzy logic based mppt controller for a pv system. *Energies*, 10(12):2036, 2017.

[97] Rajib Baran Roy, Enamul Basher, Rojoba Yasmin, and Md Rokonuzzaman. Fuzzy logic based mppt approach in a grid connected photovoltaic system. In *The 8th International Conference on Software, Knowledge, Information Management and Applications (SKIMA 2014)*, pages 1–6. IEEE, 2014.

Appendix A

Control algorithms

A.1 P&O Algorithm

Algorithm 1 Perturb and Observe (P&O) MPPT Algorithm

Initialize:
  $D_{\text{old}} \leftarrow 0.35$
  $V_{\text{old}} \leftarrow 17$
  $P_{\text{old}} \leftarrow 120$
  $\Delta D \leftarrow 0.001$
Loop:
  $P_{\text{pv}} \leftarrow V_{\text{pv}} \times I_{\text{pv}}$
if $P_{\text{pv}} - P_{\text{old}} \neq 0$ **then**
  if $P_{\text{pv}} - P_{\text{old}} > 0$ **then**
    if $V_{\text{pv}} - V_{\text{old}} > 0$ **then**
      $D \leftarrow D_{\text{old}} - \Delta D$
    else
      $D \leftarrow D_{\text{old}} + \Delta D$
    end if
  else
    if $V_{\text{pv}} - V_{\text{old}} > 0$ **then**
      $D \leftarrow D_{\text{old}} + \Delta D$
    else
      $D \leftarrow D_{\text{old}} - \Delta D$
    end if
  end if
else
  $D \leftarrow D_{\text{old}}$
end if
Update:
  $D_{\text{old}} \leftarrow D$
  $V_{\text{old}} \leftarrow V_{\text{pv}}$
  $P_{\text{old}} \leftarrow P_{\text{pv}}$

A.2 PSO Algorithm

Algorithm 2 Particle Swarm Optimization (PSO) Algorithm for MPPT

Initialize:
Initialize variables and constants:
  $w = 0.4$, $c1 = 1.2$, $c2 = 1.2$, $R1 = 0.25$, $R2 = 0.25$
  $VarMin = 0.4$, $VarMax = 0.95$
  Initialize arrays for positions, velocities, powers, and best values
  $W = 0$

if First Run **then**
    Initialize counters and persistent variables
else
    Generate random initial positions for each population member
    Calculate initial power outputs and update personal bests
    Determine global best duty cycle and corresponding power
end if
while Iterating **do**
  if Not Initialized **then**
      Execute PSO iterations for each population member
      Update velocities and positions based on PSO equations:

$$v_i^{k+1} = \omega v_i^k + c_1 r_1 (d_{best,i} - d_i^k) + c_2 r_2 (d_{best} - d_i^k) \tag{A.1}$$

$$d_i^{k+1} = d_i^k + v_i^k \tag{A.2}$$

      Evaluate power outputs for current positions
      Update personal bests if improved
      Update global best duty cycle and power if improved
  else
      Select final duty cycle based on global best
  end if
end while
return
  $D1$: Current duty cycle for selected member
  $D2$: Global best duty cycle across all populations

A.3 EMS Algorithm

Algorithm 3 Energy Management Algorithm

Require: P_dif: Power difference (PV power - load power)
Require: SOC: State of Charge of the battery
Ensure: $R1, R2, R3$: Mode indicators (binary flags)

$SOC\_max \leftarrow 80$
$SOC\_min \leftarrow 20$
Mode Determination:
if $P\_dif > 0$ **then**
  if $SOC < SOC\_max$ **then**
    Mode 1: PV power is sufficient to supply the load and charge the batteries
    $R1 \leftarrow 1$, $R2 \leftarrow 1$, $R3 \leftarrow 0$
  else
    Mode 4: PV power is sufficient and batteries are completely charged
    $R1 \leftarrow 1$, $R2 \leftarrow 0$, $R3 \leftarrow 0$
  end if
else
  if $SOC > SOC\_min$ **then**
    Mode 3: No energy from the PV generator, batteries supply the load
    $R1 \leftarrow 1$, $R2 \leftarrow 0$, $R3 \leftarrow 1$
  else
    Mode 2: PV power is insufficient, battery compensates
    $R1 \leftarrow 1$, $R2 \leftarrow 0$, $R3 \leftarrow 0$
  end if
end if
return $R1, R2, R3$

Appendix B

Presentation of PVsyst software for standalone systems

B.1 First contact with PVsyst

Stand-alone systems are always organized around a battery storage. A PV array charges the battery or directly delivers its power to the user. Therefore, the daily profile of the user's needs (consumption) should be well defined (i.e., in hourly values).
On the hour, the simulation performs a balance between the PV production (depending on the irradiance) and the user's needs. The difference should be derived in the battery, either positively (charge) or negatively (discharge).
This energy balance is controlled by a controller. The role of the controller is to handle the energy flow, mainly for the protection of the battery :

- When the battery is full, the PV array should be disconnected.

- When the battery is empty, the user should be disconnected.

Moreover, the controller may manage the starting of an eventual back-up generator (Genset), when the battery is empty, and the solar gain is not sufficient.
In any case, the reconnection will be performed with a specific hysteresis, depending on the state of charge (SOC) of the battery.

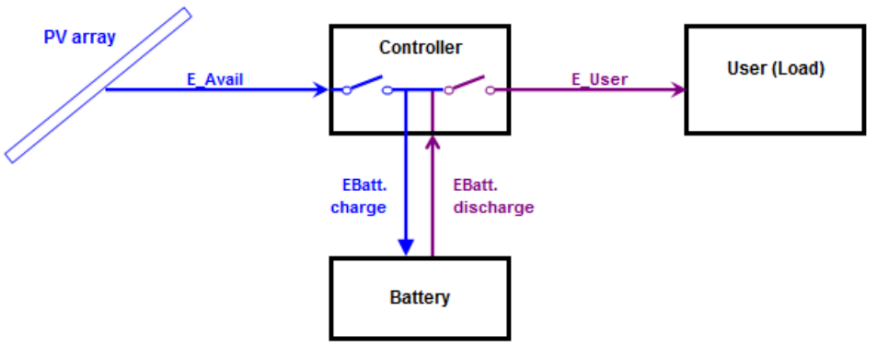

Figure B.1 :A basic standalone system diagram

B.2 Steps to define a standalone system in PVsyst

The PVsyst software start-up window :

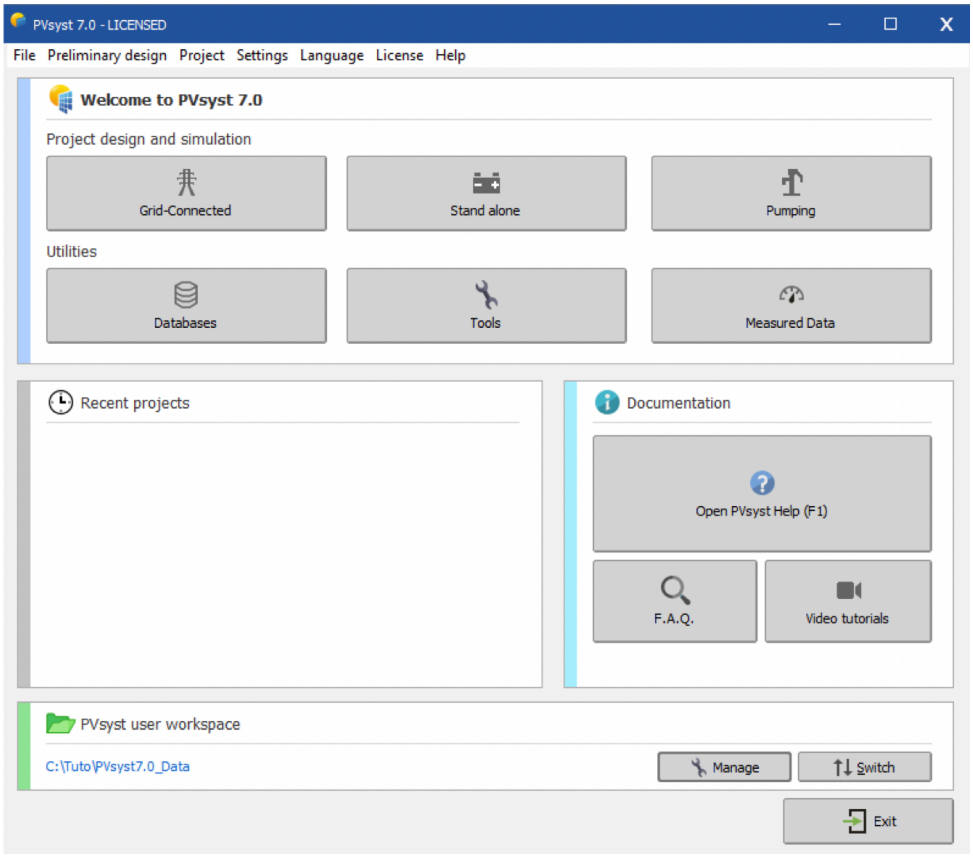

Figure B.2 : Home page of PVsyst software

Step 1: **Specify PV Array Orientation**

- Similarly to any PVsyst system, specify the orientation of the PV array.

Step 2: **Define User's Needs**

- You will be asked to define the user's needs.
- For small systems, a list of domestic appliances and their consumption is proposed (may be seasonal or monthly).
- For industrial or larger systems, define a load profile, potentially including hourly values.

Step 3: **Pre-sizing Tool**

- Use the Pre-sizing tool (on top) to receive advice about the required Battery bank and PV array power.
- Define:
  - The required autonomy (usually around 4 days),
  - The acceptable Probability of Loss of Load (PLOL),
  - The nominal voltage of the battery bank.

- The program will perform a system sizing based on meteorological files and your definitions.
- Use the button for more refined sizing studies for different meteorological distributions or according to the PLOL parameter.

Step 4: **Define Battery Pack**

- Define the battery pack by choosing a battery model on the "Storage" page.
- The program will suggest the number of batteries in series and parallel based on the pre-sizing tool suggestions.
- Define the operating temperature conditions for the batteries according to your system implementation.

Step 5: **Define Array Configuration and Control Strategy**

- Go to the "PV array" page to define array configuration and control strategy.
- Acknowledge the pre-sizing propositions (planned power or available area).
- Choose a PV module model from the database.
- Choose the control strategy (direct coupling, MPPT, or DCDC converter).
- Start with the "Universal controller" for general control conditions.
- The program determines the number of modules in series and parallel based on battery voltage or MPPT conditions and required PV power.

Appendix C

The real-case PV installation

This appendix presents visual documentation of the real case photovoltaic (PV) installation, focusing on the PV array and the experimental test bench used as the load. The section includes detailed photographs of the PV array, showcasing its layout, orientation, and specific characteristics of each solar panel such as power ratings. Additionally, images of the experimental test bench highlight its setup and operational characteristics, including voltage and current ratings.

Figure C.1 : The PV array installation

Figure C.2 : The characteristics of the PV panels

Figure C.3 : The experimental test bench (the AC load)

Figure C.4 : Characteritics of the experimental test bench